

Review

Review and perspectives on TS-1 catalyzed propylene epoxidation

Jimei Yang,¹ Shuling Liu,¹ Yanyan Liu,^{1,2,3} Limin Zhou,^{1,3} Hao Wen,¹ Huijuan Wei,¹ Ruofan Shen,¹ Xianli Wu,¹ Jianchun Jiang,³ and Baojun Li^{1,*}

SUMMARY

Titanium silicate zeolite (TS-1) is widely used in the research on selective oxidations of organic substrates by H₂O₂. Compared with the chlorohydrin process and the hydroperoxidation process, the TS-1 catalyzed hydroperoxide epoxidation of propylene oxide (HPPO) has advantages in terms of by-products and environmental friendliness. This article reviews the latest progress in propylene epoxidation catalyzed by TS-1, including the HPPO process and gas phase epoxidation. The preparation and modification of TS-1 for green and sustainable production are summarized, including the use of low-cost feedstocks, the development of synthetic routes, strategies to enhance mass transfer in TS-1 crystal and the enhancement of catalytic performance after modification. In particular, this article summarizes the catalytic mechanisms and advanced characterization techniques for propylene epoxidation in recent years. Finally, the present situation, development prospect and challenge of propylene epoxidation catalyzed by TS-1 were prospected.

INTRODUCTION

Propylene oxide (PO) is a high value-added commodity chemical as the starting material for the synthesis of polyether polyols and propylene glycols. Polyether polyols and propylene glycols are used in the manufacture of polyurethane foams and polyesters, respectively.^{1–3} PO as the second most important chemical building block after ethylene is widely used in medicine, food, automotive, agriculture and construction.⁴ At present, the annual output of PO in the world (10 million tons) cannot meet the increasing demand.⁵ From 2020 to 2027, PO is projected to experience a compound annual growth rate of 3.9%.⁶ However, traditional methods of producing PO (chloropropane and hydroperoxide processes) have major disadvantages such as the generation of toxic waste, complex multi-step processing and the formation of by-products.^{7–9}

So far, PO production processes such as chloropropane, hydroperoxide (indirect oxidation or by-product), directed oxidation, electrochemical and biochemical processes have been proposed (Figure 1A).^{1,10,11} The chlorohydrin process is the most common process in the PO industry today. Various harmful side products (salt chlorides) are formed in the chlorohydrin process because of the dehydrochlorination of chlorohydrin. The hydroperoxide processes (indirect oxidation or by-products) are environmentally friendly. But a significant number of by-products (styrene, *tert*-butyl alcohol, and dimethyl benzyl alcohol) are produced in hydroperoxide routes. Catalytic epoxidation, photocatalytic epoxidation, electrochemical and biochemical processes had also attracted considerable interest.^{12–19} An excellent turnover frequency (TOF) can be observed in the biological processes.¹² Nevertheless, the toxicity of the product to microorganisms and the stability of the enzyme are the major challenges in the biological process. As far as the direction of oxidation is concerned, the low conversion efficiency of PO is urgently needed to be enhanced before production on an industrial scale. In the alternative process of propylene epoxidation, the hydrogen peroxide-PO (HPPO) route with high selectivity has been concerned because of environmentally friendly.²⁰

Titanium silicalite-1 (TS-1) with the MFI-type framework is composed of tetrahedral titanium atoms and silicon atoms for boosting HPPO.^{21–23} In 1983, the first patent for TS-1 zeolites was filed by Taramasso et al. of Snamprogetti S.p.A.²⁴ The discovery of TS-1 was a milestone in the history of zeolites and heterogeneous catalysis. By using hydrogen peroxide (H₂O₂) as the oxidant, TS-1 revolutionized the green oxidation system because of no by-products.^{25–31} In the epoxidation of propylene, the carbon-carbon double bond of propylene is attacked by the oxygen atom in H₂O₂.^{32,33} Prior to transferring an oxygen atom to react with organic molecules, H₂O₂ is activated on TS-1 by the formation of titanium peroxocomplexes.³⁴ High Atomic utilization efficiency of oxygen and the ability to run “clean” reactions without by-products are achieved by using H₂O₂ as the oxidizing agent. In addition, the direct epoxidation of propylene with H₂ and O₂, as a greener and more sustainable PO production process, has also attracted wide attention from scientific and industrial circles.³⁵

¹College of Chemistry, Zhengzhou University, 100 Science Road, Zhengzhou 450001, P.R. China

²College of Science, Henan Agricultural University, 63 Nongye Road, Zhengzhou 450002, P.R. China

³Institute of Chemical Industry of Forest Products, CAF, National Engineering Lab for Biomass Chemical Utilization, Nanjing 210042, P.R. China

*Correspondence: lbjfc@zzu.edu.cn

<https://doi.org/10.1016/j.isci.2024.109064>



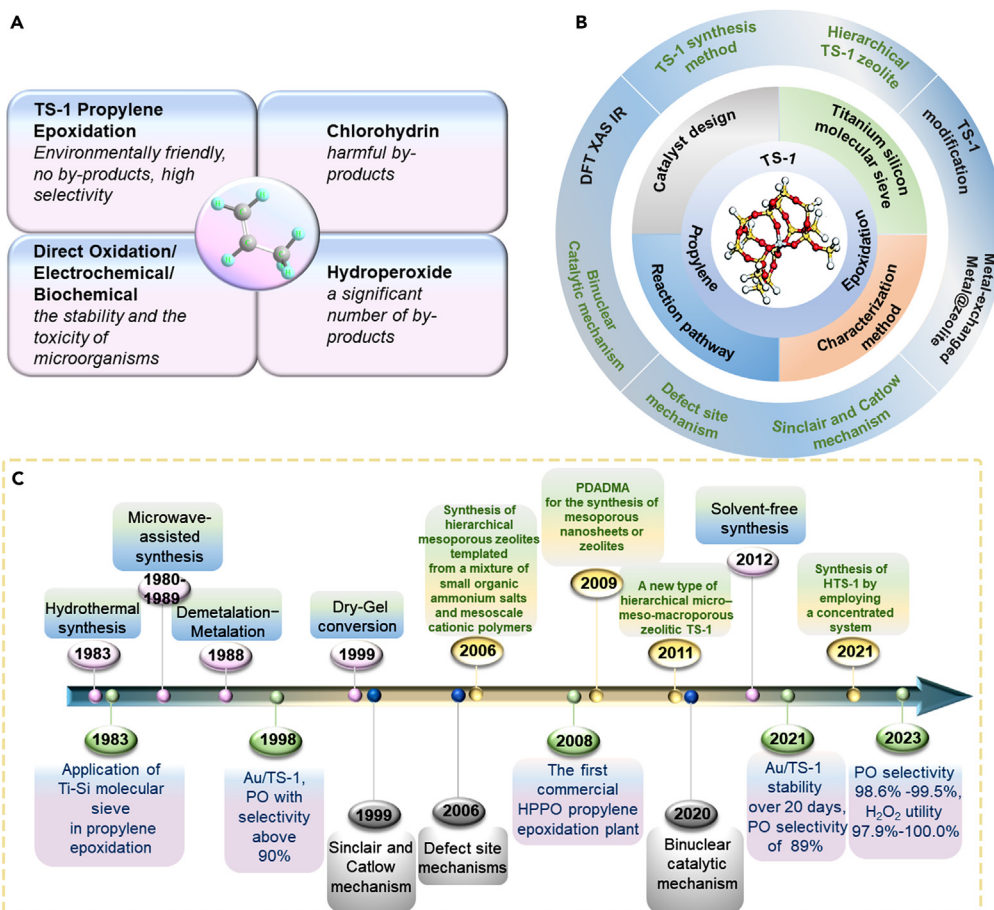


Figure 1. Review of propylene epoxidation catalyzed by TS-1

(A) Various production processes of PO.

(B) Overview of TS-1 catalyzed propylene epoxidation.

(C) Development history of propylene epoxidation catalyzed by TS-1.

In this review, we summarize the progress of TS-1-catalyzed propylene epoxidation from 2015 to 2023, as shown in Figure 1. Special attention was given to the synthesis and modification of TS-1 and the reaction mechanism of propylene epoxidation catalyzed by TS-1. Following a brief introduction (introduction section), advances in strategies for synthesizing zeolite TS-1 are presented (TS-1 zeolite section), followed by catalyst modification and catalytic performance (TS-1 catalyst design for efficient catalytic performance section). In determination of active sites section, we describe the advanced characterization techniques, such as X-ray absorption spectroscopy (XAS), and infrared spectroscopy (IR), of TS-1 at the atomic level. The catalytic mechanism of propylene epoxidation catalyzed by TS-1 and the production process of PO were summarized in reaction pathways section. The final part (conclusions and perspectives section) is the conclusion and outlook. Although there are already some excellent reviews about TS-1 materials for propylene epoxidation, there is presently no review about the synthesis and modification of catalysts, the characterization and confirmation of reaction intermediates and active centers. We believe that a timely review of propylene epoxidation of TS-1 catalysts will be a valuable resource, which is rapidly expanding in terms of both scope and interest from the scientific community. This review will promote the further development and application of HPPO process to meet the growing needs of practical applications.

TS-1 ZEOLITE

Zeolite is a crystalline microporous material formed by tetrahedral units of TO₄ (T = Si, Ge, Al, P, Ti, and so on) and is well known for its various properties including catalytic activities, shape selectivities, solid acids, and ion exchange capacities.³⁶ Zeolite is widely used as a catalyst to achieve high conversion and selectivity in various reactions.³⁷ Specifically, TS-1 is an MFI-type molecular sieve with titanium atoms partially replacing silicon atoms.³⁸ Due to the intrinsic catalytic effect of the transition metals, the resulting zeolites have specific catalytic activity.^{37,39,40} TS-1 as a redox catalyst offers new options for the homogeneous catalysis of several industrial processes.⁴¹ After the discovery of titanosilicate TS-1 (MFI) in 1983,²⁴ a number of other titanosilicate zeolites have been developed, including Ti-MWW (MWW), Ti-Beta (*BEA) and Ti-MOR (MOR). Titanium-containing catalysts have achieved great success in the synthesis of various oxygen-containing chemicals using H₂O₂ as oxidant.⁴²⁻⁴⁸ Next, we will provide a detailed introduction to the preparation methods and advantages and disadvantages of TS-1 and graded TS-1.

Structure design and modulation of TS-1

Recent years have seen a great deal of work on developing strategies for synthesizing TS-1. At present, nanosized, 2D zeolites, and the most effective hierarchical zeolites have been designed to overcome mass transfer resistance and coking limitations.^{49–51} TS-1 synthesized by different methods differs in framework, size, hydrophobicity and surface morphology. Different preparation methods have a great impact on the catalytic properties of the final zeolite. A current challenge in the preparation of metal-containing zeolites is to modulate the position, distribution and coordination state of the framework metal atoms in zeolites to create highly accessible active sites.⁵² A great deal of effort has been devoted to the exploration of new synthesis strategies in response to such challenges. These methods are presented in detail in this section.

Hydrothermal synthesis

Taramasso et al. prepared TS-1 by two different hydrothermal methods in 1983, and were the first to claim the substitution of Si^{4+} by Ti^{4+} in silicalite-1.²⁴ The synthesis gel is typically composed of sources of framework-building units, organic structure directing agents (OSDAs) or inorganic SDAs, crystallization modulation additives and water. The addition of a metal salt or organic metal complex directly to the synthetic gel for crystallization allows the incorporation of metal atoms in the zeolite. The most common method of synthesizing TS-1 is hydrothermal synthesis. The hydrothermal synthesis method can achieve industrialized production of TS-1. Hydrothermal synthesis is commonly used to obtain highly crystalline, multi-topological, small-sized, and hierarchic metal-loaded zeolites.

The titanium source used in zeolite synthesis, tetraethyl titanate (TEOT), has been shown to be easily hydrolyzed in previous studies. Titanium is difficult to incorporate into the TS-1 framework.^{39,53,54} This results in the formation of extra-framework titanium, including octahedrally coordinated titanium and anatase-type titanium dioxide. The anatase TiO_2 can cover the active sites in TS-1 and cause H_2O_2 to decompose inefficiently. The early method of synthesizing TS-1 using TEOT as the Ti source was complicated. Later, in order to simplify the operation, the more stable tetra butyl titanate (TBOT) was chosen as the Ti source in the synthesis of TS-1.^{55,56} Thangaraj et al. synthesized TS-1 with high Ti content by using TBOT as a titanium source and isopropanol complexing the titanium source (to avoid hydrolysis of TBOT).^{39,57}

The increase of the framework Ti content and the inhibition of the generation of extra framework Ti are still challenges. One of the effective ways to do this is through the matching of the crystallization rates of the titanium and silicon sources. Titanium is reported to crystallize at a faster rate than silicon. Slowing down the crystallization rate of titanium or accelerating the crystallization rate of silicon is conducive to the entry of titanium into the framework. For the inhibition of the formation of extra-framework titanium species, numerous types of crystallization mediators were added to the system, such as hydrogen peroxide, ammonium carbonate, ammonium sulfate, calcium carbonate, isopropyl alcohol or starch, etc. (Figure 2A).^{39,53,58–62} Fan et al. developed a new route for the synthesis of TS-1 using $(\text{NH}_4)_2\text{CO}_3$ as a crystallization mediator. In this way, the content of Ti in the framework can be significantly increased without the formation of additional Ti species in the framework. The addition of $(\text{NH}_4)_2\text{CO}_3$ to the synthesized gels greatly reduced the pH, resulting in a slower crystallization rate. The doping rate of titanium in the framework and the crystallization rate were well matched.⁵⁸ Nucleation is greatly accelerated and active Ti sites are enriched by the crystallization modifier. The crystallization time is reduced. Song et al. used L-carnitine and ethanol as crystal growth modifiers and co-solvent, respectively, to modulate the morphology and Ti coordination state of TS-1 zeolite. Synthesized TS-1 molecular sieves were enriched with isolated skeletal titanium species. The anatase titanium dioxide was suppressed.⁶³ Reported crystallization modifiers also include 1,3,5-phenylacetic acid (H_3BTC), L-lysine, polyacrylamide (PAM), etc.^{64–66} The anatase titanium dioxide in the resulting TS-1 sample can also be removed with acid washing.⁶⁷ But the pickling process causes a reduction in titanium content. This post-treatment reduces the activity of the TS-1 catalyst. Environmental pollution will result from the waste of acid.

Open metal centers can be introduced in the zeolite framework. For example, by a combination of an L-lysine-assisted method and a two-step crystallization, anatase-free TS-1 zeolites with tetrahedrally coordinated TiO_4 species and octahedrally coordinated TiO_6 species have been synthesized (Figure 2B).⁶⁸ In this strategy, the two-step crystallization method is beneficial for the removal of anatase titanium dioxide impurities. The L-lysine molecule acts as a stabilizer, trapping the TiO_6 species and assuring the insertion of TiO_6 into the framework-associated positions of the TS-1. The open sites of TiO_6 provide improved conversion and the closed sites of TiO_4 promise a high degree of epoxide selectivity.

A novel polymer containing sources of Si and Ti has been used in the preparation of TS-1 zeolites (Figure 3). The Ti-diol-Si polymer was prepared via a transesterification process. The reactants used were alkyl silicates, alkyl titanates, and alkyl diols. A reticulated polymer compound was formed by transesterifying the alkoxy groups of the alkyl titanate and alkyl silicate with alkyl diols. The hydrolytic rates of the Si and Ti sources for crystallization were well matched owing to the high hydrolytic resistance of the Ti-diol-Si polymer materials. Ti atoms are incorporated into the framework of the MFI zeolite, preventing Ti from being formed outside the framework.⁶⁹

It is reported improving the static crystallization method to rotary crystallization can reduce the formation of anatase.⁷⁰ Rotational crystallization accelerates the rate of titanium doping so that the rate of titanium doping into the skeleton is matched to the rate of silicon doping. The anatase TiO_2 is inhibited. However, this method showed a limited improvement in catalytic activity, resulting in aggregation of the initial nanosized TS-1 and a reduction in the external surface area of TS-1. Using Triton X-100 as a mesoporous template, Zhang et al. synthesized nanosized hierarchical TS-1, under the conditions of rotational crystallisation.⁷¹ In the meantime, it was found that the intermediate crystallized zeolite with a short crystallization time had an abundance of mesopores. There was an abundance of active titanium species and a lack of anatase species.⁷² Lin et al. proposed the reverse oligomerization strategy to match the hydrolysis rates of Ti and Si precursors by simultaneously reversing the oligomerization of the Ti monomer and accelerating the hydrolysis of the Si alkoxide using hydroxyl-free radicals (Figure 4).⁷³ The effect of anatase titanium dioxide on the epoxidation of olefins needs to be further studied. Some studies have shown that under

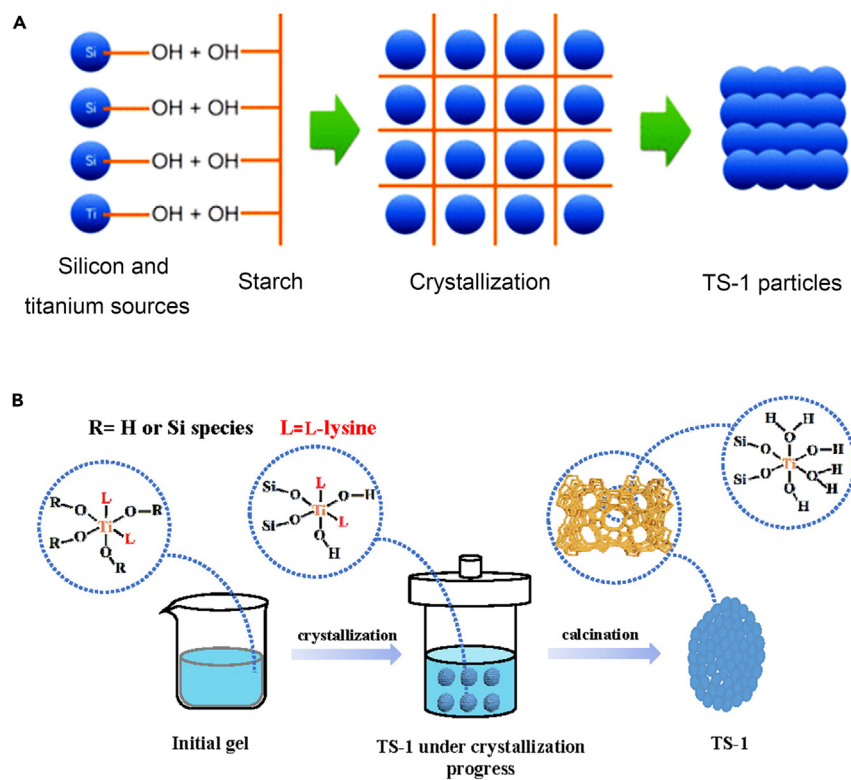


Figure 2. Synthesis of TS-1 by hydrothermal method

(A) TS-1 with little extra framework Ti was hydrothermally synthesized in a tetra propylammonium hydroxide system using starch as the additive.⁵⁹ Copyright 2016, American Chemical Society.

(B) Proposed evolution of the TiO_6 species stabilized by L-lysine in TS-1 zeolites.⁶⁸ Copyright 2022, American Chemical Society.

the synergistic action of anatase titanium dioxide and framework titanium species, the catalytic activity of TS-1 for styrene epoxidation can be improved.⁷⁴ However, the majority of current research indicates that anatase TiO_2 could still have a detrimental effect on the catalytic activity of the catalyst.

Many templates and organic bases are inevitably required to obtain TS-1 with a well-defined structure. However, the expensive tetra-propylammonium hydroxide (TPAOH) templates are usually subjected to the Hofmann elimination reaction in the prolonged hydrothermal process. This leads to decomposition and generation of alkali waste water. Instead of using TPAOH as a template for the synthesis of TS-1, some researchers use relatively inexpensive tetra propylammonium bromide (TPABr)⁷⁵ to reduce the synthesis costs. But the size of the crystals was larger than that of the crystals obtained from the TPAOH-based synthesis. The preparation of TS-1 microcrystals smaller than 1 μm using TPABr as a template is very difficult. Consequently, catalyst activity and PO selectivity are strongly influenced by diffusion restriction. Catalyst activity and PO selectivity are very low. Meanwhile, bromide from the production of TS-1 using TPABr as a template may cause environmental pollution and equipment corrosion during calcination.⁷⁶ Significantly, using the mother liquid of nanosized TS-1 as the seed for crystallization, Zuo et al. synthesized small-crystalline TS-1 in a TPABr-ethylamine system. Using this method, they were able to shorten the catalyst preparation time and obtain small crystals of TS-1 with a size of about 600 nm \times 400 nm \times 250 nm. Small TS-1 crystals precipitate relatively quickly and are easy to separate.⁷⁷ In addition, based on a glycine-assisted strategy in a tetra propylammonium bromide (TPABr)-ethanolamine system, hierarchical anatase-free small crystals of TS-1 have been prepared by hydrothermal route. A 1 μm microporous TS-1 zeolite with all Ti species present as framework Ti was prepared under the synergistic effect of glycine and seed. Glycine reduced TS-1 crystallization rate, while seeds reduced crystal size and enhanced Ti incorporation into a framework.⁷⁸

Hydrothermal synthesis is a convenient and universal method for the preparation of TS-1. Graded TS-1 is usually synthesized by hydrothermal modification.⁷⁹ Different templating agents are added or the synthesis parameters are changed during the synthesis process.⁸⁰⁻⁸³ The synthesized graded TS-1 has different pore sizes thereby increasing the external surface area and diffusion capacity. This helps to improve the propylene epoxidation performance. However, there are still some shortcomings. Ti and Si atoms have different radii and different hydrolysis rates. Metal-containing zeolites synthesized by hydrothermal methods are usually characterized by a long crystallization time, a low concentration of metal atoms, a tendency to form extra framework species, and limited synthesis conditions. The chemical composition of the synthetic gel, the type and nature of the starting source, the uniformity of the gel solution, and the different synthetic conditions are heterogeneous in many aspects. The preparation of metal-containing zeolites by hydrothermal crystallization has always been considered to be a highly complex process. This complicates the screening of synthesis parameters to break the Si/Ti framework constraint and to incorporate noble metals into the zeolite framework. The

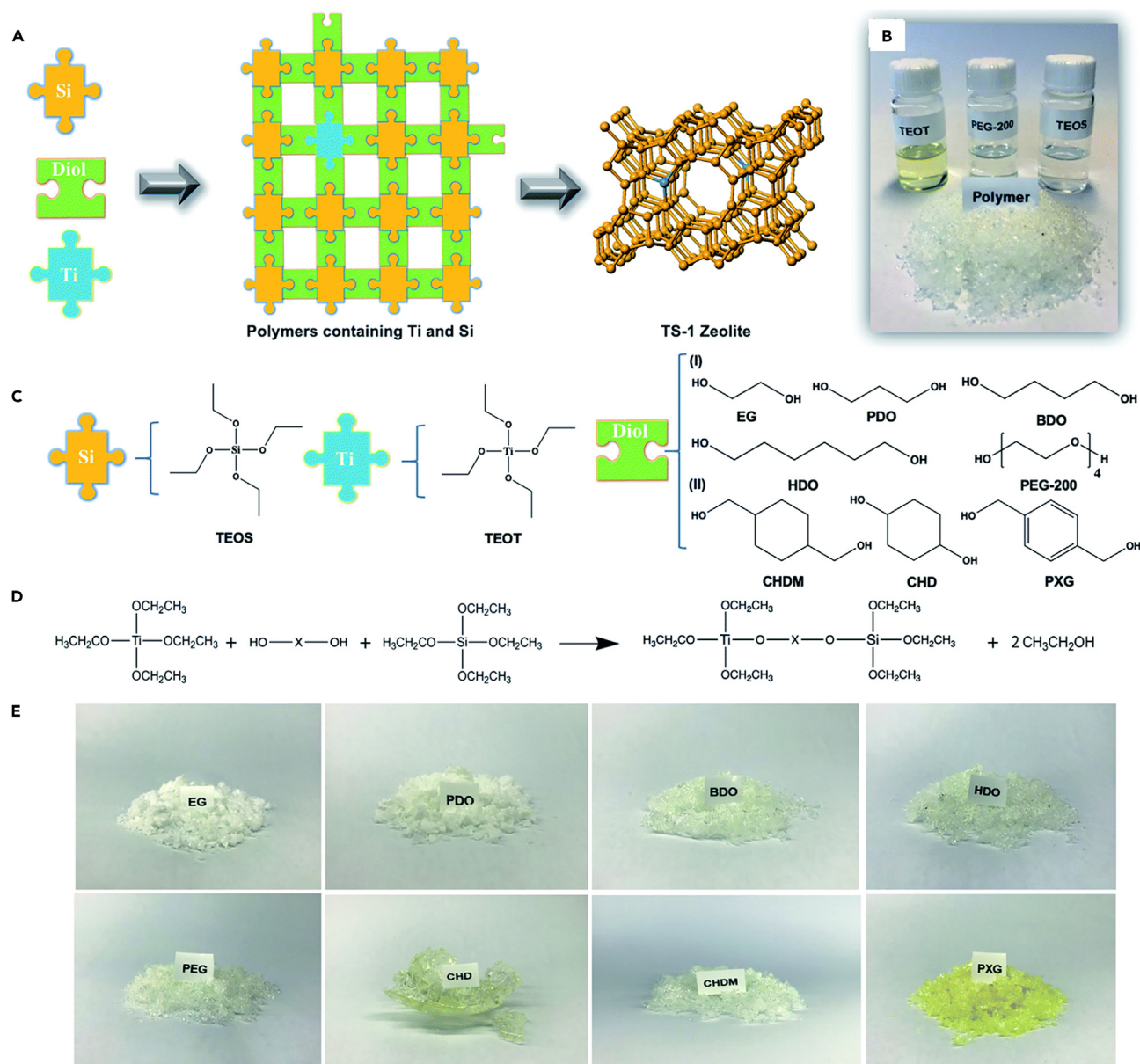


Figure 3. Synthesis of TS-1 by hydrothermal method from Ti-diol-Si polymer

(A) Synthesis of the TS-1 zeolite from Ti-diol-Si polymers.

(B) Photos of the liquid raw materials and solid polymer products.

(C) Types of alkyl titanates, alkyl silicates, and alkyl diols used.

(D) Transesterification reaction.

(E) Photos of the Ti-diol-Si polymers.⁶⁹ Copyright 2021, the Royal Society of Chemistry.

development of advanced synthetic techniques on the basis of hydrothermal synthesis or new systems like hydroxyl radical-assisted synthesis, kinetic regulation and two-step crystallization is desirable to overcome the aforementioned problems.^{84–86}

Demetalation–Metalation

Direct metallization is the so-called “atom-planting” strategy before the introduction of the demetalation-metallization method. Trivalent or tetravalent cations (Al, Ga, and Ti) can be inserted into the framework of zeolites by high temperature, continuous and stable metal chloride evaporation of high silica zeolites. This is called “atom-planting”. In 1988, Kraushaar et al. proposed this approach for the preparation of Ti-containing zeolites by the introduction of TiCl_4 vapor reaction with dealuminated ZSM-5 zeolite at high temperatures.⁸⁷ Vacant sites (i.e., silanol

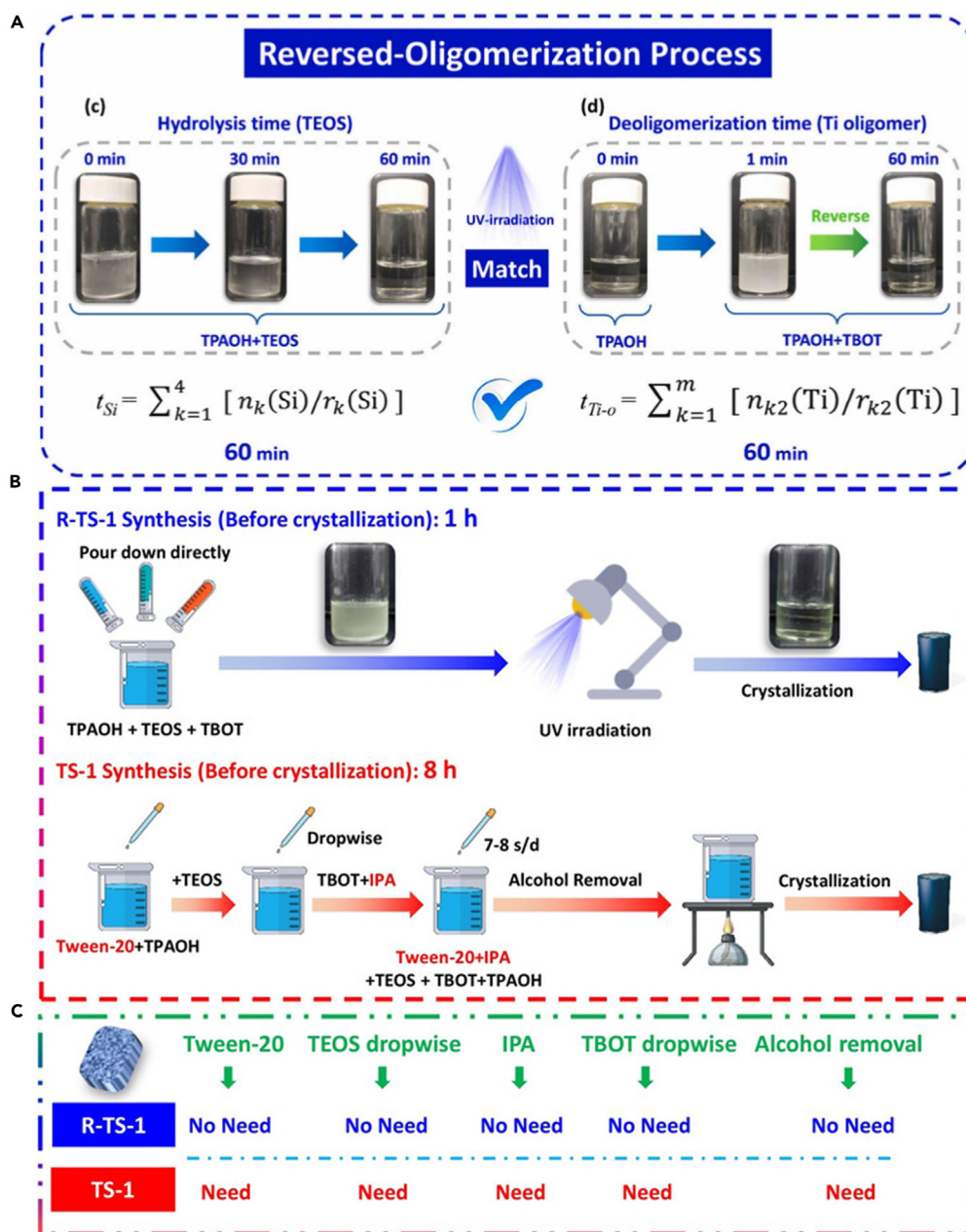


Figure 4. Synthesis of TS-1 by the reversed-oligomerization process

(A) The hydrolysis of Ti and Si species in the reversed-oligomerization process.

(B and C) Schematic representation of the synthetic procedures.⁷³ Copyright 1999–2023, John Wiley & Sons, Inc.

necks) are generated in the zeolite framework during the dealumination or deboronation step. Ti precursors are able to react with these vacancies in the following titanation process to generate tetrahedral titanium sites in the zeolite framework. Catalytic activities are similar to directly synthesized ones.⁸⁸ In the strategy of direct metallization and “atom-planting”, metal incorporation is often followed by the generation of a large number of extra framework species. The demetallization-metallization process has been developed to overcome these shortcomings. It optimizes the conventional metallization process. The metal-doped demetallization-metallization process can be achieved by framework demetallization of synthetic zeolites (e.g., desilicization, dealkalization, deboronization, and degermanization of silicate, aluminosilicate, borosilicate, and germanosilicate zeolites). Subsequently metals are doped into pre-formed lattice voids during gas-phase, liquid-phase and solid-phase metallization processes.^{89,90} Specifically, in the process of alkali (or acid) treatment, the removal of framework silicon (or aluminum) atoms from aluminosilicate molecular sieves will produce lattice vacancies and defects. Metal atoms with a suitable diameter will react with regenerated hydroxyl groups originating from lattice vacancies at high temperatures. The metal will be effectively doped into the zeolite framework.

Dealumination, boron removal and desilication are the most commonly applied method to create lattice vacancies among various demetalization processes. For instance, partial boron atoms were first removed from the framework of B- β zeolite by dilute acid treatment to create lattice vacancies in the framework. The deboronized H-B- β zeolites are then processed in titanium chloride vapor at 300°C in combination with an effective methanolysis treatment. The Ti heteroatoms are inserted at the tetrahedral sites in the framework of the zeolite. The Ti- β molecular sieves synthesized by this method were stable and almost free of non-framework titanium. It showed high activity and selectivity in the alkene epoxidation reaction of hydrogen peroxide.⁹¹ Similarly, commercial H- β zeolite (Si/Al = 13.5) was treated with a concentrated nitric acid solution to remove some of the Al atoms. Vacant Ti containing silanol groups was introduced. In addition, the dry impregnation method was applied by mechanical grinding of Si- β and the organometallic precursor of titanocene dichloride (Cp₂TiCl₂). The physical mixture was further calcined at a temperature of 800°C. Ti species are introduced into the zeolite framework in the form of isolated tetrahedron-coordinated Ti (IV).⁹²

The preparation of precursors such as H-ZSM-5, B-ZSM-5 and Al-ZSM-5 is key to this synthesis method. These precursors are then subjected to a titanation treatment. The catalytic activity of these samples is commonly much poorer than that of the hydrothermally synthesized TS-1.⁹³ This method has recently been applied to the reaction of TiCl₄ with acid-treated de-boronated ERB-1 zeolites at high temperatures. Titanium-containing epoxidation catalysts were prepared.⁹⁴ For instance, by pillaring the ERB-1 precursor with SiO₂ and atom-planting with TiCl₄, a novel titanosilicate MCM-36 with a pillared MWW structure was synthesized.^{95,96}

The demetalization-metallization method has the advantages of a short synthesis cycle, high efficiency, high metal loading, and small crystal size.⁹⁰ Nevertheless, the demetalization-metallization approach still has some drawbacks. (1) Demetalization of unmodified zeolites using acidic or alkaline conditions helps to create framework vacancies for subsequent metal insertion. This process can reduce the yield and crystallinity of zeolite solids and even lead to structural damage of the zeolite. (2) Most of the isomorphous substitution of heteroatoms in the zeolite framework takes place in the steam of metal precursors at high temperatures, seeming complicated, dangerous, and energetically costly. Compared to direct hydrothermal synthesis, the demetalation-metallization process is more complicated and expensive. (3) Extra-framework metal species formation is inevitable. Under the conditions of energy saving and environmental protection, the present demetalization-metallization may not be a generally applicable method for industrial preparation of metal-containing zeolite materials.

Dry-gel conversion

The dry gel conversion (DGC) process was an effective alternative to traditional hydrothermal crystallization of zeolite. DGC involved vapor phase transport (VPT) and steam-assisted conversion (SAC) of the dry gel.^{97,98} The VPT process is a method of incorporating steam recrystallization of the zeolite template. The SAC process uses steam to recrystallize the dry gel containing the zeolite template. The titanium-containing catalysts synthesized by the above methods also have high catalytic activity in macromolecular epoxidation.⁹⁹ Generally, the DGC process includes evaporating water from the aqueous synthetic gel, hand grinding (or mechanical bead grinding) the solid raw materials to obtain a homogeneous dry gel, and then crystallizing in vapor conditions. Under high-temperature vapor, the initial materials and amorphous/crystalline intermediates have optimal aggregation and binding rates because of low mobility. Zeolites with nanosized and/or hierarchical structures are usually formed.¹⁰⁰

Hierarchical TS-1 zeolites were prepared by the SAC strategy. TS-1 precursors, triethanolamine and TPAOH were included in the synthesis gel. UV-vis spectroscopy revealed that most of the Ti species in the hierarchical zeolite sample are tetrahedrally coordinated. But the crystallization time is usually very long.¹⁰¹ The hierarchical TS-1 was prepared by the one-step steam-assisted DGC method with TPAOH as the only template. The results showed that to successfully synthesize TS-1 with a hierarchical structure, a certain amount of TPAOH (such as TPAOH/SiO₂ = 0.08, molar ratio) was required. The crystal size of TS-1 decreases and the mesoporous surface area increases by increasing the amount of TPAOH in the synthesis solution. More extra-framework Ti would be formed in the prepared TS-1 samples if the excess template were used in the synthesis of TS-1.¹⁰² Nanocrystalline mesoporous titanium silicalite-1 (MTS-1) has also been synthesized by DGC using inexpensive triblock copolymers as templates (Figure 5A). Owing to its smaller crystal size (<100 nm) and the presence of mesopores (approximately 3 nm), MTS-1 has a shorter reactant/product diffusion length than TS-1.¹⁰³ Some studies indicate the preparation method, hydrophobic hierarchical porous TS-1 (HTS-1-X) was synthesized by the one-step DGC method with phenolic resin as the hydrophobic reagent. HTS-1-X catalysts prepared by the DGC method are characterized by high specific surface area, multilayer pore structure and high titanium content.¹⁰⁴ Remarkably, TS-1 nano zeolites with rich micro/mesoporous hierarchical structures were synthesized through a simple xerogel steam-assisted crystallization process combined with top-down alkali etching treatment.^{105,106}

For the preparation of metal-containing zeolites, the solution of the hydrolysis rate mismatch between metal and Si precursors is very important. On this basis, highly dispersed TiO₂-SiO₂ composites of Ti species were prepared by the sol-gel method in tetrahydrofuran. It was then used as a precursor for DGC-crystallized TS-1 zeolite. The study showed that the dispersion of species in the initial TiO₂-SiO₂ composite is very important for the preparation of TS-1 zeolites of high framework Ti loading.¹⁰⁸ Subsequent to this work, a new mechanochemical DGC has been designed for the construction of Ti-rich MWW-type zeolite in a vapor environment consisting of a mixture of water and piperidine.¹⁰⁹ By this approach, Ti and SiO₂ can also be processed by planetary ball milling technology to prepare TiO₂-SiO₂ composites with high titanium content. DGC is considered to be an efficient and economical method for the production of metal-containing zeolites. It is also a promising method for the synthesis of zeolite materials with higher framework metal content. New studies show the successful preparation of hierarchical TS-1 single crystals via a steam-assisted crystallization strategy using hierarchical porous titania (Ti-NKM5) as precursor (Figure 5B). Owing to the presence of large mesopores (10–40 nm), the micropore structure directing agent enters the interstitial structure of SiO₂ particles. This induces dissolution and crystallization processes. During the crystallization process, the resulting nanocrystals coalesced into a hierarchical structure. No extra-framework anatase was formed and the titanium was fully incorporated into the zeolite framework.¹⁰⁷

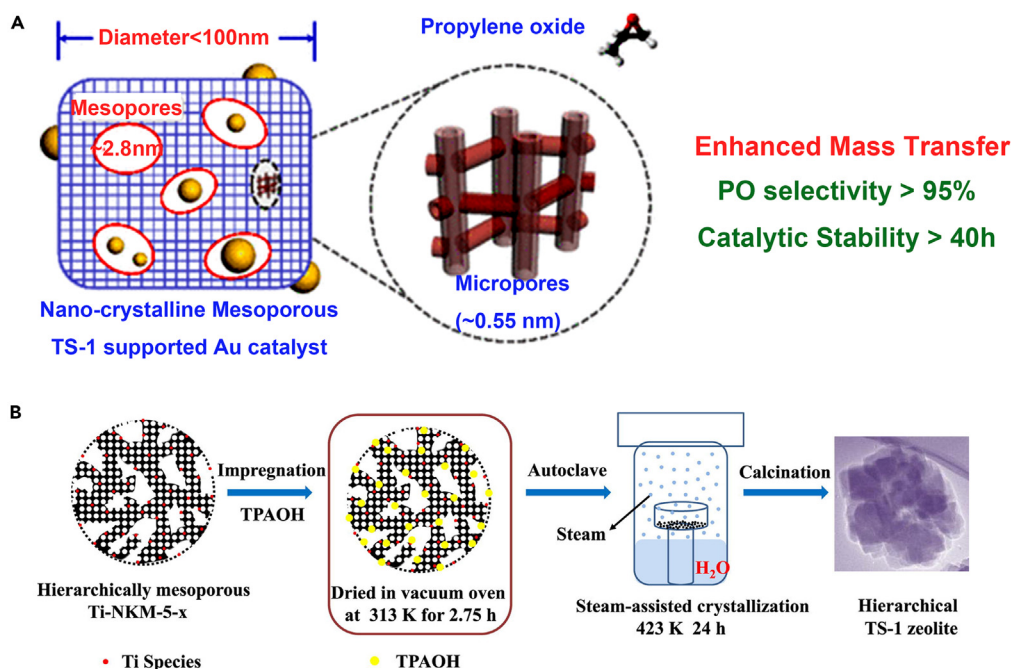


Figure 5. Synthesis of TS-1 by the dry gel conversion process

(A) Synthesis of a nanocrystalline MTS-1 by the dry-gel conversion using cheap triblock copolymers as a template.¹⁰³ Copyright, 2017 American Chemical Society. (B) Schematic illustration of the preparation of hierarchical TS-1 single-crystals.¹⁰⁷ Copyright 2022, Elsevier Inc.

The final morphology of the zeolites should be greatly influenced by the water content and structure of the dry gel. For the synthesis of hierarchical zeolites, the adjustment of the dry gel preparation process, including the water content, etc., is of great importance. It was found that grinding endowed the dry gel precursor with loose morphological features and accelerated the conversion of water vapor. This promoted the crystallization process and the formation of hierarchical structures in the zeolite. During the DGC process, a portion of the dry gel precursor is dissolved by water vapor. The dissolved Si atoms migrate from the surface of the precursor to the interior. The migratory behavior of Si leads to an inhomogeneous distribution of Ti atoms. This leads to the enrichment of Ti species on the surface of the final hierarchical TS-1 zeolite crystals.¹¹⁰ Both mesopore size and particle size could be controlled by variations in the amount of water in a steam-assisted dry gel crystallization.¹¹¹

Owing to their advantages of efficiency, high utilization, high product yield, and less environmental pollution, dry-gel conversion strategies have been greatly expanded in the synthesis of zeolites in recent years. In many studies, direct encapsulation of metal nanoparticles into MFI-type zeolites has been achieved by a steam-assisted dry-gel conversion process.^{112–115}

The DGC method has the significant advantages of less exhaust gas, shorter crystallization time under mild conditions, lower energy and structure-directing agent consumption, smaller reactor volume, higher metal content and higher solid yield. Nano TS-1 and hierarchical TS-1 were synthesized by DGC method. The water vapor treatment during the DGC process causes the xerogel precursors to explode and nucleate, allowing the crystallites to coalesce into zeolite aggregates, resulting in a self-assembled hierarchical structure.¹¹⁶ The synthesized TS-1 has abundant intracrystalline mesopore and high surface area, and importantly maintains the intrinsic hydrophobicity of the microporous TS-1 zeolite. Nevertheless, the DGC method has the following limitations: (1) To obtain a homogeneous metal dispersion and a high degree of crystallinity, the starting material and SDA must be dissolved in water and agitated for several hours. The water is then evaporated at elevated temperatures or frozen to obtain a dry gel. Large-scale production of zeolites is limited by time-consuming and labor-intensive processes. (2) To obtain a homogeneous mixture of dispersed metals, the solid raw material must be used directly and then ground by hand. The DGC method does not function well for transparent solutions with low metal source content in synthetic gels. (3) The DGC method is not applicable to zeolite systems utilizing inorganic cations as SDAs, particularly in the lack of crystalline zeolite seeds. (4) Since both structural units and SDA molecules are immobile during crystal growth. The gas-phase crystallization of the dry gel cannot well tune framework and the location and distribution of metal sites.

Microwave-assisted synthesis

Microwave irradiation has been used as an energy source for the production of zeolites since the first reports by Mobil in the 1980s¹¹⁷ There are advantages to using microwaves to heat chemical reactions. Microwave energy could be directly introduced into the zeolite synthesis system. The heating speed is faster compared to the traditional hydrothermal method.¹¹⁸ Selective and rapid crystallization of zeolites can be achieved in high yields.^{119,120} Microwave energy can also increase the hydrophobicity of zeolites by effectively controlling crystal

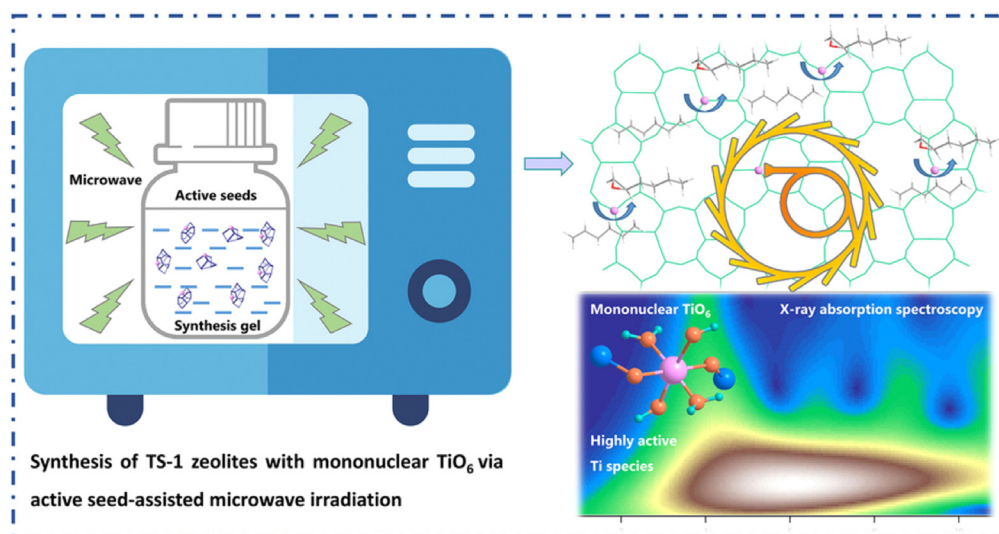


Figure 6. Microwave-assisted synthesis of TS-1

Synthesis of TS-1 (MFI framework type) zeolites with highly catalytically active Ti species via active seed-assisted microwave irradiation.¹²⁸ Copyright 2020, The Royal Society of Chemistry.

morphology and particle size.^{121,122} Typically, these are due to the rapid and even heating caused by microwave radiation and its selective interaction with specific reagents or solvents.

In the synthesis of porous materials, microwave synthesis has been recognized as an effective means of controlling particle size distribution, phase selectivity and macroscopic morphology. It is capable of rapid crystallization. For example, microwave irradiation was used to prepare MFI-type zeolite crystals with a fibrous morphology containing Ti. The type of tetravalent metal ions used determines the degree of self-assembly. The crystals are stacked along the b-direction to form fibers. The self-assembly of the zeolite crystals and the resulting fibrous morphology are only observed in the presence of the substituent metal ions. Fibrous morphology is attributed to the condensation of terminal hydroxyl groups between crystal surfaces, inducing multilayering of planar crystals.¹²³ By microwave-assisted detitanation in H_2O_2 solutions at 353 K for 15 min, Pavel and Schmidt obtained the hierarchical titanosilicate zeolite ETS-10 with native micropores (0.7 nm), newly formed supermicropores (0.85 nm), and intercrystalline mesopores (10 nm). No mesoporosity was induced by the same treatment without microwaves.¹²⁴ Compared to the standard conventional heating, the application of microwave radiation in combination with NaOH solution favored the formation of intercrystalline mesoporosity in the commercial ZSM-5 zeolites. This effect is attributed to the efficient transfer of thermal energy into the synthesized zeolite solute. The result is an increase in the rate of silicon removal. Hierarchical zeolites with a mesoporous surface area of about $230 \text{ m}^2 \text{ g}^{-1}$ and a pore size of about 10 nm can also be prepared in a short period of time (3–5 min). The crystallinity of the parent sample is preserved.¹²⁵ It is noteworthy to apply microwave irradiation in post-synthetic treatment to generate mesoporous structure. TS-1 with unique mesoporous structure were prepared by microwave-assisted H_2O_2 post-treatment. H_2O_2 -coupled microwave radiation produced mesopores in microporous TS-1 crystals. And the catalytic activity of TS-1 was enhanced by generating external Ti species on the TS-1 surface. During the post-synthetic treatment, the oxidation activity of the catalyst was affected by both microwave exposure time and temperature.¹²⁶

Microwave-assisted synthesis of Ti-ZSM-5 (TS-1) showed that even in the presence of fluoride, nucleation takes about 7.5 h and crystallization takes only 1.5 h.¹²⁷ All these results indicate that nucleation is the key step determining the crystallization rate in the microwave-assisted synthesis of MFI zeolites. Crystallization is greatly enhanced in the presence of seeds. By introducing active seeds and irradiating with microwave energy, the one-step rapid preparation of TS-1 zeolite with highly catalytically active Ti species was obtained (Figure 6). The novel octahedral coordinated Ti species (TiO_6) was present in the resulting TS-1 zeolites based on the ultraviolet-visible (UV-Vis) spectroscopy and ultraviolet resonance Raman (UV-Raman) spectra. XAS was also used to determine the mononuclear state of the TiO_6 species. Experimental studies indicate that mononuclear TiO_6 formation can be induced by the addition of active seeds. Meanwhile, the formation of such TiO_6 is enhanced by microwave irradiation. Without the formation of anatase TiO_2 , the mononuclear TiO_6 species in the as-prepared TS-1 remain stable during calcination. TS-1 mononuclear TiO_6 catalyst shows excellent catalytic activity and stability for the epoxidation of 1-hexene.¹²⁸

With microwave synthesis, zeolites can be synthesized in less time, with less energy, more uniformly, in a wider variety, and with better control over particle size distribution and morphologies.¹²⁹ The synthesis of highly active Ti species is facilitated by microwave-assisted heating. The catalytic performance of TS-1 is highly dependent on the intrinsic activity of the Ti species.¹³⁰ There are, however, certain drawbacks to microwave-assisted synthesis. When using microwave heating, great care must be taken. Reactions carried out in closed vessels using low-boiling solvents can build up high pressures. To avoid bursting the container, damage to the microwave, and potential injuries, it is necessary to anticipate and control significant internal pressure variations. Vessels equipped with venting mechanisms are recommended as a safety precaution. On the other hand, because leaked microwave radiation is hazardous to health, care should be taken when modifying the oven.

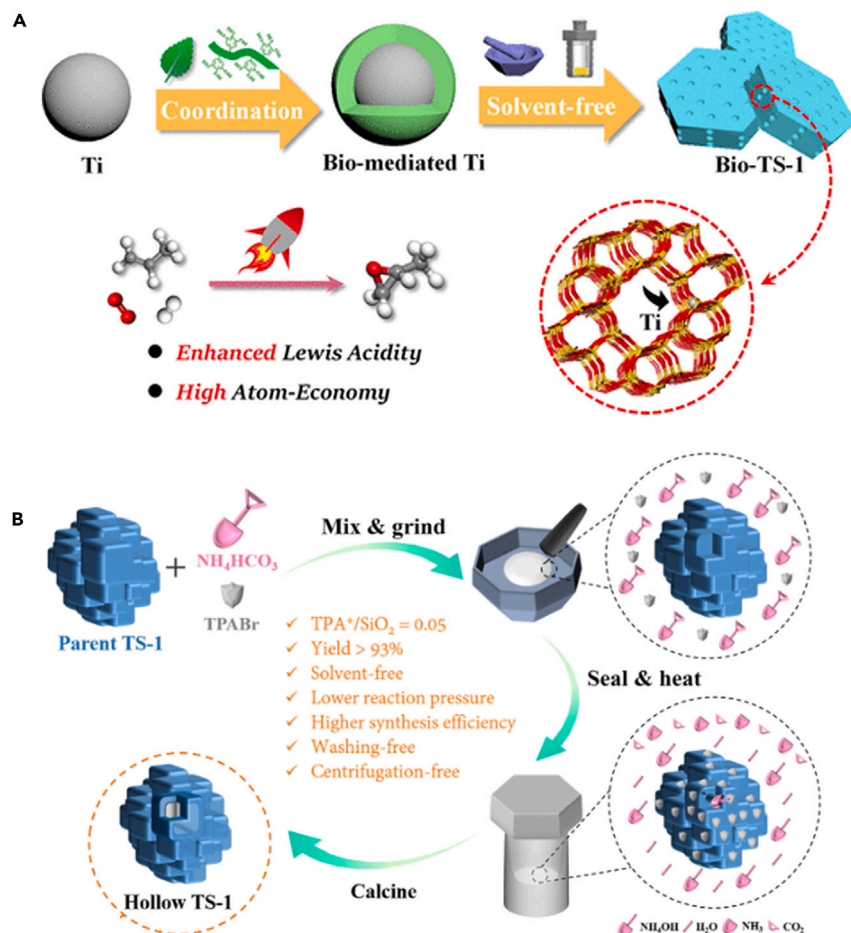


Figure 7. Synthesis of TS-1 by solvent-free method

(A) A biophenol-mediated solvent-free strategy is adopted to synthesize bio-TS-1 with an improvement of acidity character.¹³⁸ Copyright 2020, American Chemical Society.

(B) Schematic representation for the preparation of hollow TS-1 with solvent-free post-synthesis method.¹³⁹ Copyright 2023, Springer Nature.

Solvent-free synthesis

Conventionally, zeolite crystallization is carried out under solvothermal conditions using large amounts of water or organic solvents. The environmental problem caused by contaminated water is unavoidable. The high pressure generated by high-temperature water poses a safety issue for large-scale manufacturing. Ren et al. reported a generalized, solvent-free route to zeolite synthesis by mixing, grinding, and heating solid precursors.¹³¹ For at least 20 zeolites, a solvent-free synthesis involving simple grinding and subsequent heating was successful. Trace amounts of water from anhydrous starting materials, acting as a “catalyst”, were sufficient to crystallize.¹³² F^- ions can act as a catalyst to depolymerize and polymerize in addition to a trace amount of water.^{133,134} Not even trace amounts of water are needed in the specific case of the synthesis of silica-aluminum phosphates. This is because water can be produced as a by-product as a result of the interaction between the raw materials.¹³⁵

The advantages of the solventless process, including significant resource, energy, and cost savings, may be important for future industrial applications of titano-silicate zeolite. The preparation of TS-1 zeolites from pyrogenic silica, titanium sulfate, TPAOH, and zeolitic seeds in a solvent-free environment. The catalytic performance of the zeolites synthesized in this way is almost the same as that of the zeolites synthesized by the conventional hydrothermal process.¹³⁶ It is also possible to dramatically reduce the time required to crystallize the zeolite. In combination with a significantly better utilization of reactor volume, it is possible to significantly improve the space/time yield (S/TY) of zeolites prepared by high-temperature synthesis in absence of water solvent.¹³⁷

A significant increase in yield and reduction in environmental pollution was achieved by synthesizing TS-1 zeolite via a solvent-free method. More importantly, a mediator is needed to further control this synthesizing process. The main objective is to coordinate the hydrolysis of the Ti source in a highly alkaline synthetic environment to match well with the crystal growth. This allows the possibility of Ti substitution at some sites. A solvent-free bio phenol-mediated strategy is used for the synthesis of bio-TS-1 with improved acidic character (Figure 7A). Nowadays, bio phenol, as a mediator, achieves a homogeneous crystallization of Bio-TS-1. It is greatly beneficial to the Ti substitution in the center of the

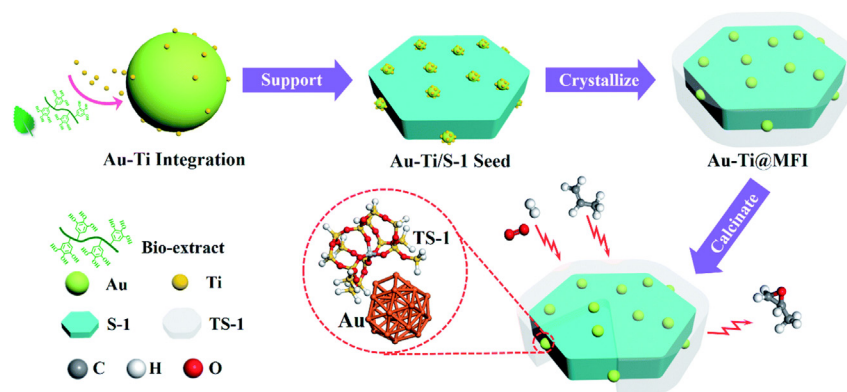


Figure 8. Synthesis of TS-1 by solvent-free method

Schematic illustration of the preparation procedures for the proposed Au–Ti@MFI catalyst (enlargement: a representative model of Au anchored with Ti sites of TS-1, symbolizing the zeolite encapsulated structure).¹⁴⁴ Copyright 2023, Royal Society of Chemistry.

framework, especially in the center of the framework with a single acid. This improvement of acidity enhances the intrinsic catalytic activity of Ti–OOH species and further improves the epoxidation performance of propylene.¹³⁸ Recent work has shown that the formation of the hollow structure can be achieved in solventless conditions using NH_4HCO_3 and TPA^+ for dissolution-recrystallization (Figure 7B). For the preparation of hollow TS-1 by dissolution-recrystallization process, the cheap and readily available ammonium bicarbonate (NH_4HCO_3) and tetra propyl ammonium bromide (TPABr) were applied in place the traditional TPAOH solution. The key to this strategy was the proper combination of the base generating agent NH_4HCO_3 with the crystal surface protecting and recrystallization directing agent tetra propyl ammonium cation (TPA^+). The final product has a rich hollow structure and retains good crystallinity and Ti active sites. The catalytic performance was greatly improved in the epoxidation of 1-hexene. At the same time, liquid waste was completely eliminated. The use of an organic template for the post-synthesis of the hollow zeolite was significantly reduced.¹³⁹

The solvent-free strategy has been applied to the preparation of metal/metal oxide catalysts encapsulated in zeolites. Several encapsulated catalysts have been prepared by using particulate@ SiO_2 as the silicon source (e.g., Au–Pd@S-1, Pd@S-1, and TiO_2 @S-1)^{140–142} or by using particulate zeolite as the crystal seed (e.g., Pd@S-1-OH).¹⁴³ A novel zeolite-encapsulated catalyst (called Au–Ti@MFI) with enhanced Au–Ti synergistic interaction was then prepared (Figure 8). The Ti and Au species were first integrated by means of the bio-extract based on polyphenols. A seed-directed solvent-free synthesis was then performed. The Ti site of TS-1 zeolite anchors the encapsulated Au nanoparticles (NPs).¹⁴⁴

In addition to these features, it has also been possible to combine the solvent-free method with other sustainable strategies for the preparation of zeolites. For instance, the synthesis of *BEA and MFI zeolites without the addition of solvents and organic templates has been successfully achieved by combining solvent-free and organic template routes.¹⁴⁵ In this way, the use of expensive and toxic organic templates and solvents can be avoided. This reduces harmful gas emissions from roasting organic stencils and liquid waste containing organic stencils and silicon-based inorganics. The reduction of costs and environmental problems of zeolite synthesis is the ultimate goal of sustainable and economic zeolite synthesis. The morphology can be adjusted by the addition of surfactants in solvent-free synthesis.¹⁴⁶ The molecules of the surfactant were selectively adsorbed on the surface of the crystal. The result was the prevention of continuous growth of a particular plane. In contrast, in a hydrothermal synthesis system, the surfactant molecules behaved differently and had a tendency to form micelles within the silica matrix. It is worth mentioning that the anatase-free nanosized zeolite TS-1 has been successfully synthesized by the direct introduction of the seed solution by means of a solvent-free synthesis method. The raw seed solution produced by TPAOH and TEOS, silicon and titanium sources were simply mixed, ground and crystallized. By studying the possible mechanism of TS-1 zeolite, it was discovered that the seed solution is the crucial factor in obtaining nanosized TS-1 zeolite. This method opens up new possibilities for the preparation of nanosized TS-1 crystals with the advantages of simple operation and high yield.¹⁴⁷

In comparison with conventional hydrothermal synthesis, the solvent-free production of zeolites is generally sustainable and has the following obvious advantages. (1) High yields are obtained. In traditional hydrothermal synthesis, nutrients (silica and alumina) are dissolved in the mother solution, whereas in solvent-free synthesis, these losses are greatly reduced. This makes the yield of MFI zeolites from the solventless process 93–95%, higher than the hydrothermal process (80–86%). (2) Autoclaves become better utilized. In hydrothermal synthesis, a large amount of water generally occupies most of the autoclave space. In solvent-free synthesis, water has been eliminated. (3) Significantly reduced contaminants. The formation of liquid waste is maximally reduced by avoiding the addition of water in the synthesis. (4) Low pressure needed to crystallize. The absence of solvents in zeolite crystallization effectively reduces the autogenous pressure. This eliminates many safety concerns. (5) Easy to crystallize. (6) The solvent-free strategy can be combined with other strategies to synthesize graded TS-1, thereby improving the epoxidation properties of propylene. The basic process of mixing and heating the raw solids is the most important step in the solvent-free route. However, since most OSDAs are in hydroxide form and crystallization in solid salt form is difficult to control. It remains a challenge to extend the solvent-free strategy to other zeolites.¹⁴⁸

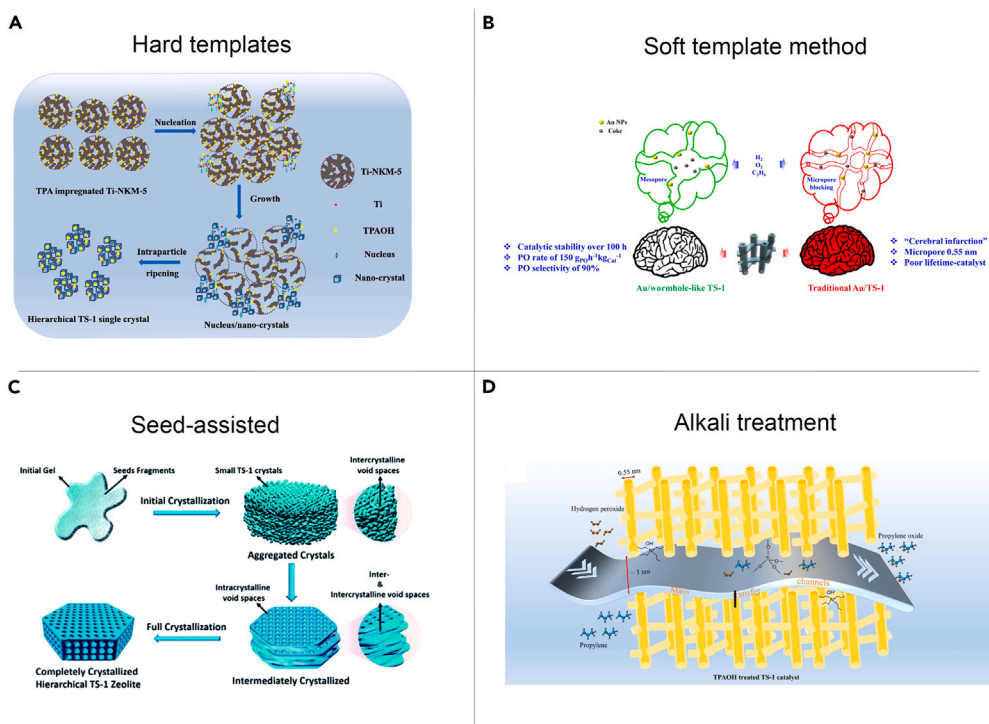


Figure 9. General overview of different porosity introduction strategies

The hard template method of (A) illustrated the formation process of hierarchical TS-1 single-crystal zeolite from an amorphous Ti-NKM-5 sphere.¹⁰⁷ Copyright 2022, Elsevier Inc.

(B) Novel hydrophobic hierarchical TS-1 (HTS-1) with wormhole-like mesopores (ca. 45 nm) and small crystal size (100 nm) is synthesized by a two-step crystallization method using CTAB as a template.¹⁶⁰ Copyright 2018, Elsevier B.V.

(C) The seed-assisted method of synthesis of the intermediately and completely crystallized zeolite catalyst. Insight into the effect of mass transfer channels and intrinsic reactivity in TS-1 catalyst for one-step epoxidation of propylene.⁷² Copyright 2018, The Royal Society of Chemistry.

(D) The alkali treatment of propylene epoxidation in the mass transfer channels derived from the TPAOH modification over the TS-1 catalyst.¹⁶¹ Copyright 2022, Elsevier B.V.

Structure design and modulation of hierarchical TS-1 zeolite

Microporous zeolites have good shape selectivity in catalytic reactions. But the relatively small size of the micropores greatly affects the diffusion of reactants, leading to rapid coking and side reactions. More specifically, fine chemical synthesis typically involves bulky compounds bigger than the pore size of the zeolites. Active sites located on the outer surface of zeolite catalysts achieve catalytic conversion. The lower catalytic activity is caused by the inaccessibility of the active sites inside the zeolites.^{149,150} The configuration diffusion mechanism controlled by the micropore structure is responsible for the diffusion of molecules in the micropores of zeolites.^{151,152} Intercrystalline transport is the rate-determining step in adsorption and catalytic steps on zeolite catalysts. The way to solve these problems is to reduce the mass transfer resistance by reducing the diffusion path length. This includes the design of oversized micropores in zeolite crystals, the introduction of meso and/or macropores in zeolite crystals, and the preparation of hierarchical zeolites.^{153,154}

Secondary porosity (mesopores and/or macropores) is characteristic of hierarchical zeolites. The secondary porosity is in excess of the typical and uniform zeolitic microporosity. They have modulated acid strength and increased external surface area and mesopore volume.^{116,155–157} Hierarchy zeolites have the following characteristics. The main results are as follows: (1) The space limitation of macromolecular conversion is reduced. (2) The intragranular diffusion rate is increased. (3) The deactivation of coke is inhibited. (4) The utilization rate of active sites is improved. (5) And adjusting the selectivity of the product.^{158,159} These characteristics provide hierarchical molecular sieves with better catalytic performance than microporous counterparts, especially for macromolecules involved in catalytic reactions. The wide variety of synthetic strategies used to construct pore hierarchies can be classified into “*in situ*” and “*post-synthetic*” strategies. The *in situ* method prepares hierarchical zeolites by generating microporous and mesoporous products during zeolite synthesis, with or without the use of secondary hard or soft templates. The *post-synthetic* method involves the post-treatment of the prepared zeolites to generate a hierarchical structure in the zeolites. The next sections of this paper will discuss these two preparation methods in detail. Figure 9 provides a general overview of different porosity introduction strategies. Table 1 summarizes the different preparation methods.

Table 1. Preparation method and advantages and disadvantages of graded TS-1

Route	Additional pore type	Advantages	Limitations
Hard templating			
Carbon particles	Mesopores	High zeolitic character,	High production costs
Carbon fibers	Mesopores	Wide Si/Al,	
Carbon nanotubes	Meso- or macropores	Applicable to different zeolites,	
Carbon black	Mesopores	High porosity	
Resin	Meso- or macropores		
Starch	Meso- or macropores		
Sucrose	Meso- or macropores		
Silica gel	Macropores		
CaCO ₃	Macropores		
Silica	Meso- or macropores		
Soft templating			
Surfactants	Mesopores	Tunable mesoporosity, Wide Si/Al,	High production costs,
Nonsurfactants		Applicable to different zeolites,	Low to medium zeolitic character,
Polymers		The high degree of additional porosity, Good pore connectivity	Not industrially available
Non-templating			
Organosilanes	Meso- or macropores	Eco-friendly,	Low to medium zeolitic character,
Seed-assisting		Cost-effective,	Applicable to a few zeolites,
Kineticregulating of crystallization		Medium zeolitic character	Cannot control the additional porosity
Dry gel conversion			
Demetalation			
Acid leaching	Mesopores	High zeolitic character,	Low pore interconnectivity (dealumination),
Alkaline leaching	Mesopores	Applicable to different zeolites,	Dealumination applies to Al-rich zeolites only,
Fluoride leaching	Meso- or macropores	Wide Si/Al,	Expensive when organic templates/acids are involved,
		Cost-effective,	May alter the original Si/Al,
		High pore connectivity,	Cannot control porosity
		Scale-up possible	

In situ approach/bottom-up strategies

Bottom-up approaches are the introduction of secondary porosity during zeolite synthesis by using templates (template approach) or by using reaction conditions alone (non-template approach). Template approaches generally require mesoporous and/or macroporous templates (also known as porogen) to generate extra porosity and a structuring reagent to form the microporous zeolite structure. The mesoporous and/or macroporous templates are first embedded in the slurry of the zeolite precursor. They are then removed following zeolite formation to release extra porosity. These synthesis methods can be categorized into hard and soft template routes based on the rigidity (solid or liquid) of the mesoporous and/or macroporous templates.^{162,163} The non-templated method does not require the templating action of meso- or macroporous templates (in the absence of meso- or macroporosity). Additional porosity can be created in the zeolite material.¹⁵⁹ The non-template method is realized through the aggregation of nanocrystals to form intercrystalline mesopores, or based on the controlled crystallization of amorphous gel into zeolite crystals with intracrystalline mesoporous pores, or by selectively changing the growth direction of zeolite crystals (twins).

The hard template method uses either nonporous or porous solids with relatively rigid structures. During the zeolite crystallization process, these are usually used as sacrificial templates to introduce additional porosity. Carbonaceous materials (e.g., carbon black, carbon nanoparticles, nanotubes, and nanofibers),^{164,165} polymers (e.g., Resin),¹⁰⁴ biological materials (e.g., starch, sucrose),^{59,166} and inorganics (e.g., silica gel, CaCO₃, SiO₂)^{62,107,167–169} as mesoporous or matrices have been extensively used for the construction of hierarchical zeolites.¹⁷⁰ The hard template does not interfere with the creation of the intrinsic structure of the zeolite because it is chemically inert. The method is applicable to the preparation of hierarchical porous zeolites with different zeolite structures.^{116,171} A typical synthesis process involves the preparation of a standard synthesis gel to be mixed with the hard template. The mixture is then treated under hydrothermal conditions to form a microporous

zeolite network around the hard template. The final step is the removal of the hard template by calcining or extraction using acid or base.¹⁵⁰ Zeolites synthesized by the hard template method are characterized by high crystallinity, uniform porosity and regular pore structure. Owing to the specific nature of the titanium species, the hard template route is well suited for the production of hierarchical titanasilicate zeolites under either acid or alkali leach conditions. However, this approach is still expensive because of having to use templates. The formation of mesopores or macropores by this approach is poorly interconnected. The conditions required to remove titanium are harsh. Many defects and internal silanol groups were created in the zeolite crystals under the harsh conditions used to remove the hard template. This caused the acidity and framework stability of the zeolites to decrease.

As an alternative, the soft-templating method, including the utilization of mesoporous such as surfactants (e.g., CTAB, Triton X-100),^{160,172–177} nonsurfactants (e.g., PDADMA),^{178–180} polymers^{181–183} and organosilanes,¹⁸⁴ is one of the most extensively used design approaches in the construction of hierarchical TS-1 zeolite structures. There are generally two ways to make a strategy. One is the primary approach, where all ingredients are added to the synthesis system at the start of a one-step synthesis. The other is a secondary process where all ingredients but the surfactant are added at the beginning. The surfactants are then added in the final step prior to the hydrothermal synthesis.¹⁸⁵ In the primary approach, surfactants help assemble framework units into zeolite crystals with additional intracrystalline or intercrystalline porosity. Most surfactants serve two functions. The first one concerns the hydrophilic part of surfactants. It directs the formation of the zeolite structure and/or “anchors” the surfactant in the zeolite framework. The second one is related to the hydrophobic part of the surfactant. It is intended to initiate the formation of organic domains between the inorganic components, thus allowing the surfactant to act as a mesoporosity or spacer phase during the crystallization process. Either mesoporous zeolite crystals or a layered structure of zeolite nanosheets will eventually form.^{172,173,186,187} The secondary approach uses a two-step synthesis step. The first step is the addition of all components except the surfactant. In the second step, the soft template either supports the assembly of zeolite seeds into hierarchical porous structures or forms microemulsions/reverse micelles for “confinement synthesis”/ “vapor-assisted transformation” of hierarchical porous zeolite.^{160,162} Although the soft templating process is a good method for the preparation of hierarchical zeolites with a high level of mesoporosity and can be used for various zeolite structures. But most templates are not commercial. The production of such templates is very labor-intensive and very expensive. The resulting zeolitic materials are shown to have low zeolitic behavior because of the high level of defects and small micropore volumes.

Surfactants have the following benefits. (1) The use of a lot of hazardous templates for the production of TS-1 is avoided and the costs are lowered. (2) Fractional TS-1 with micropores and mesopores was synthesized. (3) Ensures no extra TiO₂ framework at low TPAOH concentrations. (4) Increases mass transfer and improves catalytic performance and stability. R.B. Khomane et al. report for the first time that it is possible to prepare TS-1 in the presence of a small amount of template using a non-ionic surfactant (tween 20).^{188,189} Ryoo's group reported that a new class of surfactants with multiple ammoniums could be used as mesopore directing agents for the synthesis of mesostructured nanosheets and mesoporous zeolites. To enhance the interaction with growing zeolite crystals, they designed surfactant molecules with functional groups. Finding amphiphilic surfactant molecules containing a hydrolysable methoxy silyl moiety, a zeolite structure-directing group such as quaternary ammonium and a hydrophobic alkyl chain moiety was key to their design concept.¹⁷² Bola form surfactants (BC_{ph-12-6-6}), non-ionic surfactant polyethylene glycol test-octyl-phenyl ether (Triton X-100), and cetyltrimethylammonium bromide (CTAB) can also be used as mesoporous templates.^{190–192} Using cheap cetyltrimethylammonium bromide (CTAB) as a template, Sheng et al. proposed a novel hierarchical TS-1 (HTS-1) zeolite via a two-step crystallization process (Figures 10A–10C).¹⁶⁰ The elimination of anatase TiO₂ impurities in this strategy benefits from the two-step crystallization approach. However, there are obvious drawbacks to these methods. The removal of silicon atoms from the zeolite framework also removes the framework titanium species. The original composition of the TS-1 framework has been changed, and even the framework has been collapsed. Similarly, using a methyl iodide-treated polystyrene-co-4-polyvinylpyridine copolymer as a mesopore-directing template, Xiao et al. showed the preparation of hierarchical ZSM-5 zeolite possessing b-axis-aligned mesopores.¹⁷⁵ In another study, using a commercial polymer, poly diallyl dimethylammonium chloride (PDADMA), as a dual-functional template, monocrystalline zeolite beta with interconnected mesopores was synthesized.^{178,179} Similar to the dual-function templates based on surfactants, the abundant quaternary ammonium groups located on the polymer are used as a structure directing agent (SDA) for the zeolite. Unlike surfactants, due to the lack of hydrophobic segments, PDADMA does not self-assemble into regular micelles or ordered structures. PDADMA simply acts as a “porogen” rather than a true mesoscale SDA, resulting in disordered mesopores. Polyquaternium-7 (M550) could be used as a “porogen” for the synthesis of hierarchical TS-1 at the nanoscale and to avoid the formation of anatase species.¹⁸⁶ But the nanosized particles make them difficult to separate from the mother liquor. Using the non-surfactant cationic polymer PDADMAC as a mesopore-directing template, Du et al. reported a simple hydrothermal route for the preparation of hierarchical TS-1 zeolites (Figures 10E and 10F). Optimization of the synthesis conditions allows the preparation of TS-1 zeolite with regular hexagonal morphology, high crystallinity, and abundant and uniform intercrystalline mesopores (~ 10 nm).¹⁸⁰

Templating approaches are effective for preparing hierarchical TS-1 with highly interconnected mesopores. Owing to the mismatch in the incorporation rate of Ti and Si, the mesoporous templates usually result in the formation of anatase TiO₂ species. In particular, efficient mesoporous templates generally have high synthesis costs, complicated preparation processes, and inert properties. This has made TS-1 zeolites very difficult to synthesize at scale.

Non-templating approaches, including seed-assisting,⁷² kinetic regulating of crystallization,^{78,193} and DGC,^{106,111} have been developed as efficient synthetic alternatives to mesoporous approaches to zeolite construction.^{61,194} Seed-assisted processing aims to increase crystallization rate, eliminate impurities, control morphology and particle size, and reduce synthesis costs. Hierarchical zeolite structures can also be

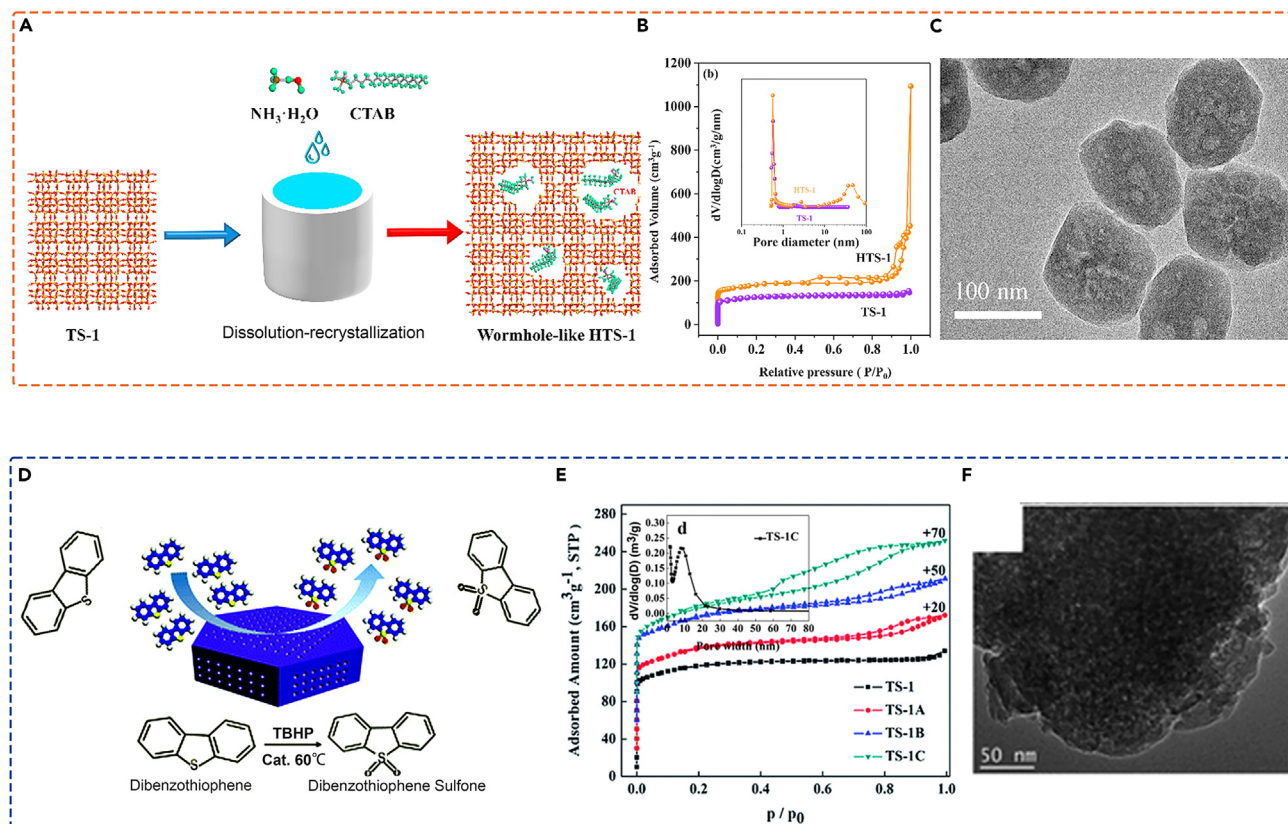


Figure 10. Synthesis method of hierarchical TS-1

(A) Synthesis of the HTS-1 zeolite.

(B) N_2 adsorption–desorption isotherms of HTS-1 and TS-1. The inset shows the pore size distributions of HTS-1 and TS-1.

(C) TEM images of HTS-1.¹⁶⁰ Copyright 2018, Elsevier B.V.

(D) Hydrothermal route to synthesize hierarchical TS-1 zeolites with abundant mesopores (5–40 nm) inside the zeolite crystals by using poly diallyl dimethyl ammonium chloride (PDADMAC) as a mesopore-directing template.

(E) N_2 adsorption–desorption isotherms of conventional microporous TS-1 and hierarchically porous TS-1 zeolites. The inset shows the pore size distributions of TS-1C.

(F) TEM images of TS-1C.¹⁸⁰ Copyright 2017, The Royal Society of Chemistry.

created using the seed-assisted method.^{72,195} For the construction of a hierarchical structure aggregated by zeolite nanocrystals, the DGC method with a highly concentrated zeolite precursor to the promotion of nucleation was a viable approach.^{106,111} In order to achieve good developed mesopores in microporous zeolite, additives like growth inhibiting agents, nucleating agents and growth modifying agents have been used in most cases to control the crystallization process.^{78,193} Recently, the introduction of crystallization modifiers has been shown to be a viable strategy for the modulation of the TS-1 crystallization process. Wang et al. developed a novel one-step aromatic compound-mediated synthesis for the preparation of hierarchical TS-1 molecular sieves without anatase. Aromatic compounds with good structural stability of functional groups are used as multifunctional media. It guides the formation of inter-crystalline mesopores, regulates the distribution of Ti species, and eliminates the generation of anatase during crystallization.¹⁹⁶ However, the synthesis of hierarchical zeolites with tunable mesopore sizes and comprehension of the mesopore generation mechanism are still challenging.

Post-synthesis/top-down

Additional porosity within zeolites can also be obtained by post-synthesis treatment of zeolite crystals, as opposed to the synthesis strategies discussed above.^{197,198} In general, the post-synthetic treatment of preformed zeolites consists of demetallation (extraction of framework atoms) or delamination using steam, acids, bases, or fluorides, or more refined approaches (swell, exfoliation, or interlayer pillaring with amorphous silica).^{199–204}

The most widely used method to create hierarchical structures is demetallation. It involves the elimination of framework atoms (e.g., Si, Al, Ti, etc.) from the microporous crystalline zeolites. Unfortunately, this method of destruction inevitably results in a loss of zeolite mass, which changes the elemental ratio of the zeolite framework.²⁰³ TPAOH,^{161,193–207} NaOH,¹⁰⁶ SO_4^{2-} ⁶² and fluoride^{208,209} are commonly used etchants for the synthesis of hierarchical TS-1 zeolites, especially with hollow morphology.

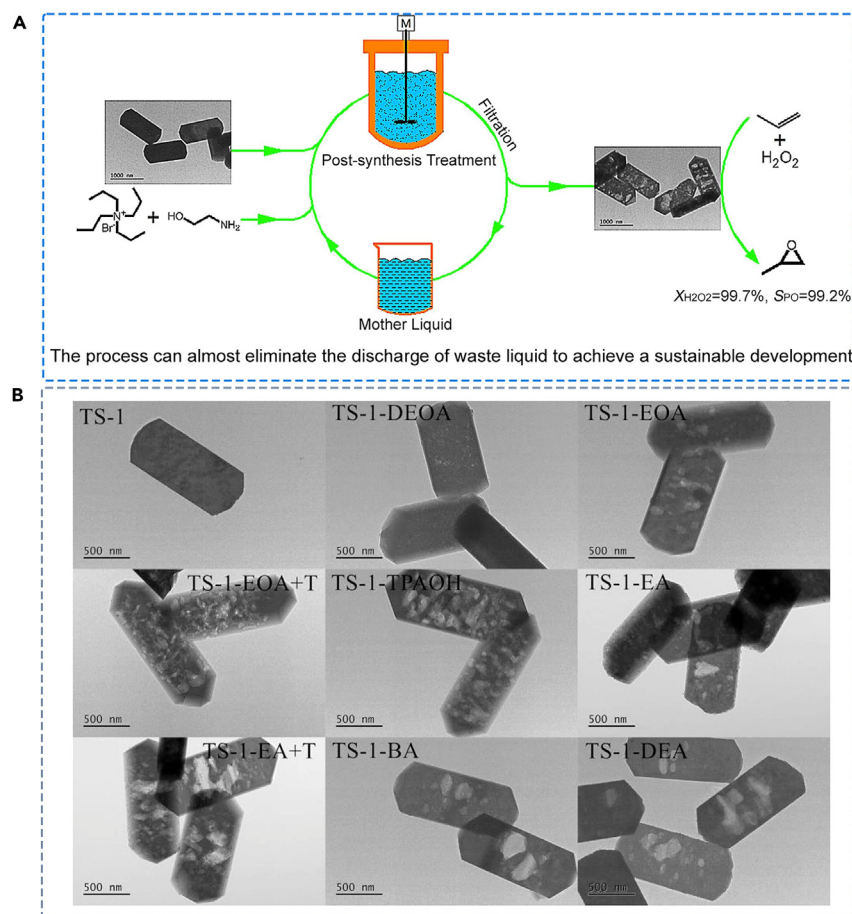


Figure 11. Synthesis of hierarchical TS-1 by post-processing method

(A) Schematic representation.

(B) TEM images of TS-1 treated with different bases: diethanolamine (TS-1-DEOA), ethanolamine (TS-1-EOA), ethanolamine + TPABr (TS-1-EOA+T), TPAOH (TS-1-TPAOH), ethylamine (TS-1-EA), ethylamine + TPABr (TS-1-EA+T), butylamine (TS-1-BA), and diethylamine (TS-1-DEA).²¹¹ Copyright 2017, Elsevier B.V. All rights reserved.

The main function of inorganic alkali is to desilicate and create mesoporous. But the excessive alkalinity of inorganic bases can easily cause excessive desilication, leading to the disintegration of the framework structure and the loss of framework Ti. In contrast to strong inorganic bases, moderate amounts of organic bases (TPAOH) can dissolve the silicon framework and also act as a template to guide recrystallization. The dissolution and recrystallization of non-skeletal Ti species offer the possibility for the return of extra-skeletal Ti to the skeletal lattice. Large-radius TPA^+ ions cannot diffuse into the channel interior. Adding ammonia and NaOH can facilitate the dissolution-recrystallization process by promoting the diffusion and dissolution of OH^- in the pores. Non-framework Ti is still present in the modified samples.²¹⁰ Liu et al. prepared green and efficient hollow TS-1 by post-synthesis treatment using recycled mother liquor (Figure 11A).²¹¹ The TS-1 was hydrothermally treated with different bases. Due to controlled desilication of the framework, hollows appear in the crystals (Figure 11B). In the presence of tetra propylammonium (TPA^+), more hollows are produced and a higher titanium concentration in the crystal is obtained. This is because the removed silica recrystallizes along the Si-OH on the outer surface. When samples are prepared with ethanolamine and TPABr as desilylating media, the mother liquor obtained can be reused in the next synthesis treatment. In the recycling process, the amount of ethanolamine and TPABr added was only 50% and 25% of the amount added in the first post-synthesis treatment. Even though the mother liquor was recycled eight times, the catalytic activity of the obtained hollow TS-1 in the propylene epoxidation reaction was similar to that of the sample prepared with TPAOH as the desilication medium.

Simplicity and low cost are the main advantages of the post-synthetic approach. This method is widely used in industry. It produces catalysts and adsorbents with excellent properties, high stability, designable compositions and desired acidic sites.²¹² Disadvantages of this method are that it requires harsher conditions, which leads to environmental pollution, zeolite flaws, partial disintegration of zeolite structure, and poor control over selective and precise extraction.

TS-1 CATALYST DESIGN FOR EFFICIENT CATALYTIC PERFORMANCE

At the forefront of green oxidation research is the direct synthesis of epoxides from H_2O_2 and olefins using TS-1 as a catalyst.²¹³ Studies have shown that framework titanium species can act as an active center in TS-1.^{214,215} Non-framework Ti species (anatase or amorphous

Table 2. Comparison of catalytic performance of catalysts prepared by different modification methods

Catalyst	Preparation method	C ₃ H ₆ conversion (%)	PO selectivity (%)	PO formation rate (g _{POH} ⁻¹ kg _{Cat} ⁻¹)	Stability (h)	Reference
Au/TS-1-CTES 0.084% wt. Au	Silane-assisted hydrothermal strategy	13.3	92.7	117	24	Liu et al., ⁸¹
Au/uncalcined TS-1	Silanization treatment, DPU, Hydrothermal method	11	88	356	–	Wang et al., ²²¹
ML-TS-1	Alkali treatment, Hydrothermal method	ca. 25.2	98.6–99.5	–	250	Wang et al., ²²²
NaOH–TPABr-RT	Alkali treatment, Hydrothermal method	12.6	96.3	–	–	Miao et al., ²²³
Hollow TS-1	Alkali treatment, Hydrothermal method	–	99.2	–	–	Liu et al., ²¹¹
HTS-1	Salt treatment, DGC	–	97.6	–	120	Li et al., ²²⁴
Hollow TS-1	Templating approach, Hydrothermal method	–	96–99	–	>6000	Lin et al., ²⁰⁵
Au/HTS-1 0.10% wt. Au	Non-templating approach, DP, Hydrothermal method	–	85	125	24	Yuan et al., ¹⁹⁴
Au/TS-1/S-1 0.10% wt. Au	DP, Hydrothermal method	4.51	87.2	126	100	Song et al., ²²⁵
Au/TS-1-B 0.08% wt. Au	DPU, Hydrothermal method	–	91.0	1102	–	Zhang et al., ²²⁶
Au/TS-1-B 0.12% wt. Au	DPU, Hydrothermal method	–	ca. 83	126	30	Feng et al., ²²⁷
Au/TS-1-SG 0.10% wt. Au	SG, Hydrothermal method	7.4	85.0	119	21	Huang et al., ²²⁸
Au/HTS-1(NIMG) 0.10% wt. Au	NIMG, Hydrothermal method	6	91.2	150	25	Sheng et al., ²²⁹
Au/TS-1-B 0.03% wt. Au	IWI, Hydrothermal method	–	95.0	88	42	Zhang et al., ²²⁶
Au/TS-1 0.12% wt. Au	miWI, Hydrothermal method	5.1	ca.92	240	not stable	Lu et al., ²³⁰
Au/TS-1 _{PT} 0.10% wt. Au	Non-thermal plasma chnique	1.3	89	22.5	>480	Kapil et al., ⁵

Ti) are inevitably produced in the traditional TS-1 synthesis. As a result, the decomposition efficiency of hydrogen peroxide is low and the side reaction is increased.^{216,217} The microporous channel structure of TS-1 causes the reactants and the product to diffuse slowly, decreasing the yield and selectivity of the product. TS-1 catalytic performance is highly influenced by substrate and oxidizing agent molecular size, solvent type, crystal size, pore structure, and hydrophobicity.^{31,218–220} Improvements in catalytic performance can focus on (1) generating more active sites and reducing the formation of non-framework Ti. (2) Introducing intragranular mesopores, reducing diffusion resistance, reducing molecular sieve grain size, and making reactants more easily accessible to the active site. (3) Introduction of transition metals in zeolites has been a powerful method for improving catalytic activity and catalyst stability. At present, effective strategies to improve catalytic activity include post-treatment methods and the introduction of transition metals. These two methods will be discussed in detail in the next section. Table 2 summarizes the catalytic performance of catalysts obtained by different modification methods.

TS-1 modification

The catalytic performance of Ti zeolites can be greatly improved by changing the coordination state, porosity (for example, mesopore), morphology and hydrophobicity of TS-1 zeolites.^{107,231,232} Modification of the TS-1 zeolite by post-treatment methods, including silanization reaction, acid treatment,²³³ alkali treatment,²³⁴ and salt treatment, is one of the simplest and most effective strategies.^{235,236}

Acid treatment

It has been found that extra-framework Ti in TS-1 can be washed away using acid solutions, including hydrochloric acid,^{62,191,237} phosphoric acids,²³⁸ hydrofluoric acids,²⁰⁸ sulfuric acids, nitric acid, etc.^{239,240} Acid treatment can form mesopore or macropore in micropore TS-1 and remove titanium except for skeleton. The layered TS-1 without extra-skeleton titanium can be obtained. For instance, For example, Tatsumi et al. treated TS-1 zeolite with H₂SO₄ and later with an aqueous K₂CO₃ solution. K-modified TS-1 showed improved catalytic activity for oxidizing 2-penten-1-ol.²⁴¹ Acid treatment is beneficial for removing non-skeletal titanium species and they can be almost removed.^{67,191,242} Acid extraction and UV irradiation were used in sequence to remove C₂₂₋₆₋₆ surfactant not only between the MFI layers but also in the zeolite micropores.²³⁷

The reduced number of acid sites is the main disadvantage of acid leaching. This results in increased acid strength.²⁴³ The formation of pores during acid leaching is always followed by changes in the number and strength of acid centers. It is difficult to study mesopores on catalytic performance separately.^{201,244,245} This post-treatment, owing to the reduction of the Ti content in the acid wash, will reduce the activity of the TS-1 catalyst. And environmental pollution caused by waste acid.

Alkali treatment

Another approach is to post-treatment the final TS-1 with organic alkalis.^{106,207,246-251} Alkalis dissolve the zeolite and remove the Si matrix from the framework, resulting in the formation of micro- and mesoporous composite layers. Recently, TPAOH has been applied as a hot spot etchant to create hierarchical TS-1 zeolites by desilication.^{206,252} The conversion rate can be improved by alkali-treated TS-1 zeolites with enlarged pores. But the product selectivity will remain the same or may even decrease to a varying degree.^{253,254} The process necessarily involves the removal of Ti atoms from the framework and the conversion of framework Ti into non-framework Ti. Before treating the TS-1 molecular sieve with an alkali, it is necessary to increase the number and stability of active species.

Hollow crystals with large intracrystalline voids can easily be achieved from a traditional TS-1 by post-synthesis modification of the calcined zeolite with highly alkaline TPAOH solutions.¹⁹³ As the concentration of TPAOH increases, the number of hollow crystals increases (Figures 12A-12F).²⁵⁵ The Ti atom state, morphology, and distribution of TS-1 zeolite change significantly with increasing basicity.²³¹ Lin et al. prepared the hollow TS-1 zeolite via a post-synthesis approach in the presence of TPAOH solution at high temperatures (Figures 12G and 12H). The hollow TS-1 zeolite catalyst exhibited high catalytic activity and high selectivity for PO in the HPPO process (Figure 12I). The hierarchical structure of hollow zeolites and isolated tetrahedral Ti species are introduced into the framework matrix of MFI molecular sieves to become effective Lewis acid catalysts.²⁰⁵ Different TPAOH treatment temperatures significantly affected TS-1 dissolution and recrystallization behavior, changing composition and microstructure regarding pore volume and size, surface properties, and active sites.¹⁶¹

An effective method to adjust the local environment of the Ti center of the TS-1 framework is a hydrothermal modification with NaOH in the presence of TPABr. The original framework Ti-sites have been transformed to "open Ti-sites", and the adjacent silicon-hydroxyl-sites have titanium-hydroxyl-sites and sodium-ion counterions. A characteristic IR absorption between 960 and 980 cm⁻¹ was observed at the specific Ti sites. Appropriately modified catalysts used with this method could dramatically improve the gas phase epoxidation of propylene and H₂O₂, while hindering the decomposing of H₂O₂. Surprisingly, the presence of a large number of sodium ions in the TS-1 has been demonstrated in this study. This is the main reason for the deteriorated performance of the liquid phase epoxidation of propylene.²²³ In some studies, TPABr and ethanolamine mixed solution were used for post-treatment to prepare hollow TS-1.²⁴⁸

It is worth noting the rate of Au clusters on alkaline-treated TS-1 has been greatly improved. The pre-treatment of the TS-1 supports with aqueous alkaline metal hydroxides prior to Au deposition is crucial for the preparation of Au clusters smaller than 2.0 nm by solid-state grinding and thus for the achievement of high catalytic performance.²²⁸ Some recent studies showed that the graded TS-1 obtained after alkali etching has higher catalytic activity for propylene epoxidation, and the turnover frequency is as high as 1650h⁻¹.²⁵⁶

After alkaline desilication, the connectivity among hierarchical pore systems is still high. Compared with dealumination, desilication has less effect on acid content.²⁵⁷ Due to its low cost and ease of scale-up, framework removal is highly applicable.²⁵⁸ However, during the alkaline desilication process, it is difficult to control the Si/Ti ratio and porosity of zeolites.²⁵⁹

Salt treatment

Fluorination of zeolites has already been used for the modulation of their acidity and thus their catalytic activity.²⁶⁰⁻²⁶³ The addition of highly electronegative fluorine ions to the zeolite lattice polarizes the structure, significantly increasing the acidity of the surface.²³² Compared to their HF counterparts, the NH₄F-HF treated materials show significantly better catalytic activity. NH₄F is a strong electrolytic agent. In the case of NH₄F - HF, the presence of NH₄F inhibits the dissociation of HF and reduces the concentration of H⁺, favoring the formation of many HF²⁻. Consequently, silicon extraction is increased and preferential extraction of Al does not occur, unlike dilute HF solutions.^{203,208} Remarkably, treating with NH₄HF₂ does not change the surface acidity (neither Lewis nor Brønsted), and no residual fluorine remains after treatment.²⁰³ Treating TS-1 with NH₄HF₂ causes Ti site speciation to change and non-selective H₂O₂ decomposition is found to be drastically reduced.²⁶⁴ More recently, a new post-synthesis treatment based on etching zeolites with an aqueous NH₄F solution has been proposed by Valtchev et al.^{265,266} Because HF₂ is produced by the hydrolysis of NH₄F, Si and Al can be leached from the zeolite framework in an unbiased manner, preferentially attacking structural defect zones in the zeolite crystals. This etching process was proposed as a promising approach. It enables to decrease the effect on the overall zeolite acidity during hierarchization. Pure ammonium fluoride (NH₄F) solution has been used for post-modification in some studies. Uniform intracrystalline mesoporosity was introduced and hydrophobicity was increased by this strategy. Molecular diffusion can be improved by reducing the TS-1 grain size and creating a hierarchical porous architecture. Thus, mass transport problems are solved and catalytic performance

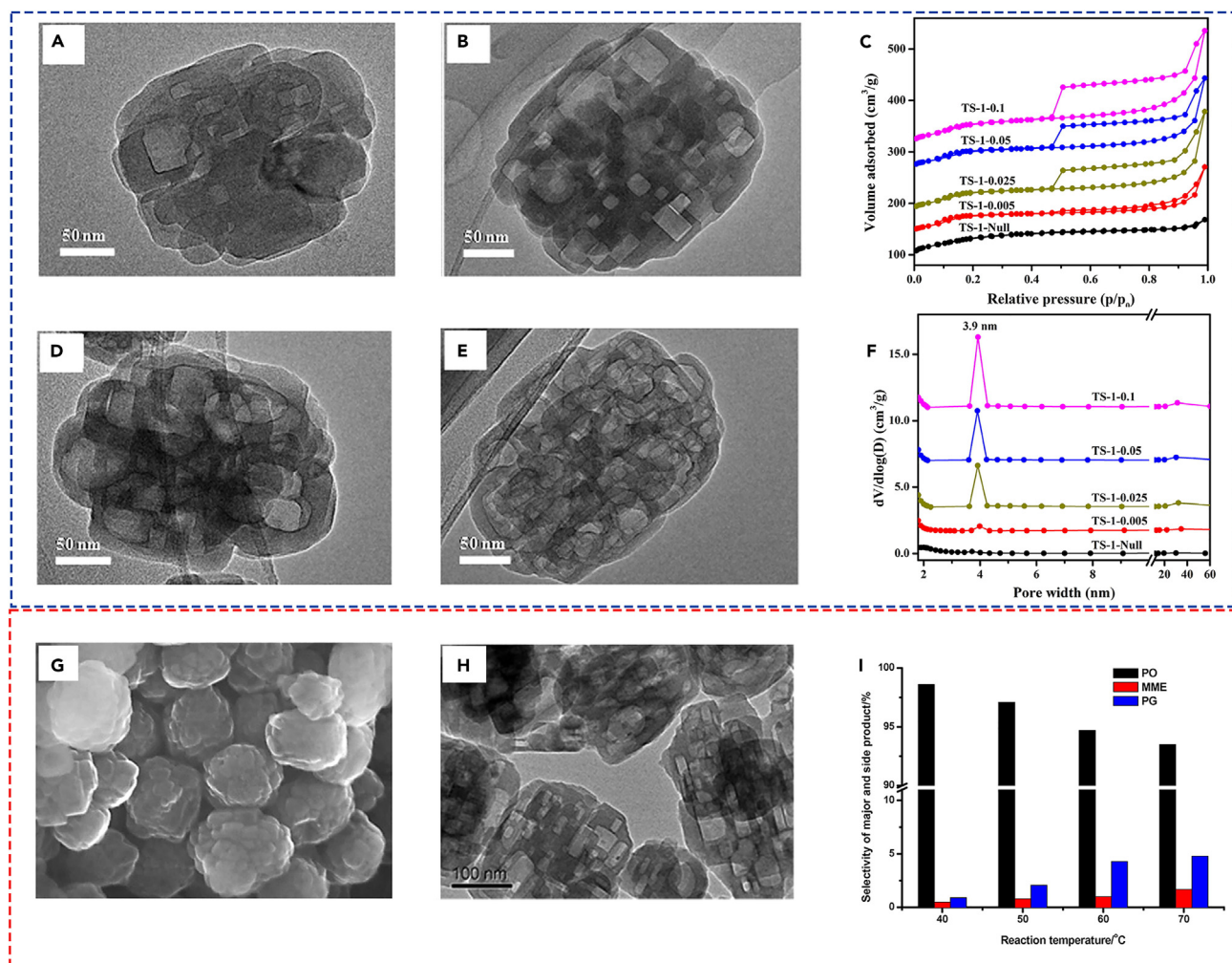


Figure 12. Synthesis of hierarchical TS-1 by alkali treatment

TEM images of catalyst samples: (A) TS-1-0.005, (B) TS-1-0.025, (D) TS-1-0.05, (E) TS-1-0.1.

(C) Nitrogen physisorption curves of TS-1-Null and TS-1 treated with TPAOH solutions.

(F) Pore size distribution curves of the TS-1-Null and modified TS-1 catalysts.²⁵⁵ Copyright 2017, Elsevier B.V. Multiple characterization results of hollow TS-1 zeolite catalyst: (G) SEM image; (H) TEM image.

(I) The selectivity distribution of products in propylene epoxidation reaction. Reaction conditions: $p = 1.5$ MPa, WHSV of H_2O_2 molecules is $1.1\ h^{-1}$, $n_{CH_3OH} = n_{H_2O_2}$ is 6, $n_{Propylene} = n_{H_2O_2}$ is 2.5.²⁰⁵ Copyright 2016, Elsevier B.V.

is enhanced. Propylene epoxidation was performed with this catalyst. Hydrogen peroxide conversion and PO selectivity reached 98.4% and 97.6%, respectively.²²⁴

The prepared TS-1 zeolite was hydrothermally modified with a mixed solution of ammonia, TPABr and potassium chloride. Its excellent catalytic activity was primarily attributed to enhanced mass transport capability and accessibility to active Ti species. Its improved epoxidation selectivity was primarily related to the K^+ introduction. Both the coordination environment of the Ti species and the polarity of the zeolite can be effectively modulated by K^+ . The traditional TS-1 molecular sieve can form mesoporous and eliminate unfavorable hydroxyl groups at the same time by simple hydrothermal treatment in the mixed solution of alkali and salt. Cyclopentene epoxidation catalysts with high activity and selectivity were obtained.²⁶⁷

He et al.²⁶⁸ showed that the hydrothermal treatment of TS-1 with small organic amines (ethylamine and n-propylamine) favored the formation of defective $Ti(OSi)_3OH$ species through the selective dissolving of Si species surrounding the non-defective $Ti(OSi)_4$ species. These results indicate that ammonia solution may favor the generation of defective $Ti(OSi)_3OH$ species in TS-1-B. Ammonia may react with $HAuCl_4$ to produce a positively charged Au compound $(Au(NH_3)_2(H_2O)_{2-x}(OH)_x)^{(3-x)+}$ at high pH (>10).^{269,270} This positively charged gold cation compound is capable of strong adsorption on the negatively charged SiO_2 surface, thus resulting in high gold uptake efficiency. The simultaneous immobilization of small particles of Au (ca. 1.6 nm) on an unroasted TS-1 (i.e., TS-1-B) and the promotion of

the formation of defective Ti^{4+} species were obtained by a modified deposition-precipitation (DP) approach using ammonia solution as a precipitant. The PO formation rate of the as-precipitated catalyst is significantly enhanced.²⁷¹

This non-selective saline treatment has significant advantages in producing hierarchical materials with added porosity. The method is universal and does not depend on the parent zeolite composition or structure. Unlike the steam, acid, or alkaline leaching routes, the obtained hierarchical zeolites are similar in composition to their parents. Post-synthesis treatments can now be used to more rationally modify zeolite catalysts and adsorbents.

Silanization treatment

The hydrophilic Ti and Si hydroxides on the surface of TS-1 may reduce its hydrophobicity and lead to negative catalytic activity.^{272,273} An efficient way to decrease the occurrence of side reactions between the products and water is to improve the hydrophobic performance of the catalyst. Hydrophobic TS-1 can reduce the damage of water molecules and hydrophilic solvents to the active sites of titanium in the catalyst. Hydrophobic molecular sieves improve hydrogen peroxide conversion and PO selectivity during propylene epoxidation reactions.²⁷⁴ The organosilane method is the most commonly used modification route to produce hydrophobic TS-1 zeolites. During silylation, a silanol group of the support reacts with the alkyl silyl group of the silylating agent, making the material more hydrophobic. The organosilane method is effective in reducing the acidity of the TS-1 surface.²⁷⁵ Nevertheless, the silyl group on the surface of the alkylated TS-1s was susceptible to decomposition at high temperatures, resulting in a reduction in the size of the TS-1 and a reduction in the life of the TS-1.²⁷⁶ In order to synthesize hydrophobic TS-1 molecular sieves, a suitable material with good stability and hydrophobicity needs to be found.²⁷⁷

As a post-treatment process, silanization has been proved to be useful in improving the performance of catalysts.^{278–284} The silylation process involves the exposure of the catalyst to a silylating agent. Surface hydroxyls are replaced by R_3Si groups by the silylating agent. Typical silanization reagents include hexamethyldisilazane (HMDS)^{279,282} trimethylchlorosilane (TMCS),^{285,286} triethoxyfluorosilane (TEFS),²⁸⁷ (trimethylsilyl) trifluoroacetamide (MSTFA),²⁸⁴ methoxy trimethyl silane (MTMS)^{284,288,289} and tetramethyldisilazane (TMDS).²⁸² Silanization is usually accompanied by an increase in surface hydrophobicity. Increased hydrophobicity is the underlying cause of altered catalytic activity. The hydrophobic surface facilitates the desorption of polar products and prevents further reaction with the formation of by-products. Other factors besides hydrophobicity may play a role in the enhancement of catalytic activity. For example, the contents of Au and Ti were found to be largely responsible for the magnitude of the improvement in the catalytic activity during the silylation.²⁸⁹ The use of different silylation agents and procedures may have different effects on the catalyst properties and thus on the resulting catalytic performance. At the same time, silylation time has been identified as an important parameter.²⁹⁰ Recently, hexamethyl disiloxane (HMDSO) was used as a silylating agent to modify catalysts. The surface silanization of HMDSO can consume hydroxyl groups, thereby weakening PO adsorption and promoting PO activity. It also changes the electronic properties of the active site and inhibits the formation of by-products, thereby improving PO selectivity and H_2 efficiency.²²¹

Propene hydrogenation is suppressed by silylation. This is a significant disadvantage of the process. In addition, because the silyl group on the surface of alkylated TS-1 was readily decomposed at high temperatures, the size and lifetime of TS-1 were reduced.

Additional metal modification

Metal-exchange zeolite and metal@zeolite materials exploit the synergistic effect between active metal species with different coordination states and the confinement effect in the zeolite matrix microenvironment. A range of new heterogeneous catalysts have been developed for use in many key catalytic reactions. The catalytic performance will also be affected by loading different active metal species. Effective synthetic approaches for both metal-exchanged and metal@zeolite catalysts are of great importance in order to improve the catalytic performance for a given catalytic reaction. After collection and review of recent literature, the main synthesis methods for the confinement of external framework metal single sites, clusters and metal nanoparticles within zeolites include post-synthesis and *in situ* synthesis approaches. We will discuss in detail the impact of different supported active metal species on catalytic performance and the preparation methods of supported catalysts and introduce their advantages and disadvantages.

Type of metal

Au nanoparticles have been the focus of much attention for their potential catalytic applications in a wide range of reactions. Highly dispersed (<5nm) gold nanoparticles were loaded onto amorphous or crystalline oxides containing Ti to catalyze the epoxidation of olefins with O_2 as an oxidant.^{229,291} Au nanoparticles adsorb H_2/O_2 to produce hydrogen peroxide and migrate to nearby isolated tetrahedral Ti^{4+} sites to form $Ti-OOH$ for propylene epoxidation.²⁹² Hayashi et al. first reported in 1998 that gold (Au) nanoparticles (NPs, 2.0–5.0 nm) coated onto anatase TiO_2 catalyzed the gaseous epoxidation of propene (C_3H_6) with a mixture of O_2 and H_2 to produce PO with a selectivity of over 90%.²⁰ Since then, the design of efficient Au catalysts has been the focus of extensive studies. Among the reported Au/Ti-based catalysts (for example, Au/TS-1, Au/Ti-TUD, Au/Ti-HMS, Au/three-dimensional mesoporous titanosilicate, and Au/ $TiSiO_2$), hydrophobic TS-1- supported Au catalysts showed excellent activity and stability.^{293–296} Unfortunately, even the Au/TS-1 catalyst remains subject to severe deactivation, with a loss of approximately 30% activity in as little as 20 h.²²⁷ The inactivation of Au/TS-1 is mainly because the reactants cannot contact the active center of Au-Ti well. And the diffusion limitation of molecules in the narrow 0.55nm of TS-1 blocks the diffusion path. Microporosity blockage due to carbonaceous deposits formed by initial PO adsorption on the catalyst surface and subsequent oligomerizing, rearranging, bonding, and so on^{228,297} renders microporous Au clusters unavailable to reactants.²⁸⁷ From the study of the deactivation mechanism, the concept of using shortened diffusion paths of the products inside the zeolite to improve the mass transfer seems to be a promising solution to this problem.²⁹⁸

Particle size is a strong determinant of the catalytic performance of Au-based materials. High reactivity is only achieved with particles smaller than 5 nm. However, Au particles are susceptible to aggregation upon thermal treatment. This leads to a loss of activity. The addition of a second metal is thought to overcome the aggregation of mono-metal and help activate oxygen.^{299,300} The physicochemical properties of bimetallic catalysts vary greatly because of their composition and particle size, showing complementary advantages and synergistic effects. Au-containing bimetallic catalysts (such as Au-Cu, Au-Ag, Au-Pd, and Au-Pt) may show excellent catalytic performance in many reactions.^{301–303} Lu et al. suggested that alkaline metals (such as K and Cs) and alkaline earth metals (such as Mg, Ca, Sr, and Ba) could increase the trapping efficiency and dispersion of Au, thereby increasing the catalytic activity.³⁰⁴ It was reported that more tiny Au clusters (~0.5 nm) could be located in the microporous channels of TS-1 because of the facilitating effect of Cs.³⁰⁵ The smaller Au clusters are more active in the process of PO formation, resulting in a significant increase in activity. These gold clusters can result in rapid deactivation because of severe microporous plugging phenomena. The design of a highly active and stable Au-based catalyst remains a challenge.

Feng et al. found that Au and Ag synergistically enhanced catalytic performance by reducing Au nanoparticles and increasing oxygen adsorb ability and electron transfer from Au to oxygen.³⁰⁴ As shown in Figures 13A–13F, the Au₁₀-Ag₁/TS-1-B catalyst (i.e., ~2.7 nm) has a smaller average metal particle size than the Au/TS-1-B catalyst (i.e., ~3.2 nm). This shows that the introduction of Ag is conducive to the dispersion of Au on the surface of the TS-1-B catalyst. Ag atoms of high mobility can easily migrate to the Au particles to form Au-Ag bimetallic nanoparticles. The Au agglomeration caused by chloride ions in the catalytic reduction process is avoided.^{306,307} It is clear from Figures 13G–13J that O₂ adsorption on Au-Ag bimetallic nanoparticle surfaces is stronger than on pure Au nanoparticle surfaces.

The epoxidation process of H₂O₂ on Ti-based molecular sieves involves the first dissociation and activation of H₂O₂ on Ti⁴⁺. The reactive oxygen species is then transferred to the double bond of the olefin.³⁰⁸ When searching for active metal species, it is useful to think about whether or not they will aid the epoxidation reaction. The uniquely high oxygen vacancies in ceria can serve as a surface oxygen species transfer medium, effectively trapping reactive oxygen species, reducing the diffusion resistance of reactive oxygen species, and facilitating the epoxidation reaction.²⁰⁷

Preparation methods

In general, post-synthesis approaches are mainly used for the preparation of zeolite-supported metal catalysts. The development of post-synthesis methods has been much more recent.³⁰⁹ It was easy and simple to synthesize by post-synthesis methods. It was suitable for scaling up to produce commercial catalysts. Conventional ion exchange and impregnation methods can only introduce metal into the large pore (>0.7 nm) zeolites but are ineffective on microporous zeolites. Metal particles tend to be located at the outer surface of the zeolite. The use of incipient wetness impregnation and ion exchange approaches tends to result in the formation of large, unevenly distributed metal particles.¹¹² During high-temperature calcining, reducing, and catalyzing of supported metal catalysts, metal species migrate and aggregate and metal species drop out during recovery, thereby reducing catalyst activity. Using these conventional synthesis methods, zeolite-supported metal catalysts (commonly referred to as metal/zeolite) have been synthesized with low stability and dissatisfactory catalytic activity. Various synthetic strategies for *in situ* synthesis of precious metal particles in molecular sieves have been developed to overcome these drawbacks. A new structure, commonly known as metal@zeolite, was eventually formed. On the basis of the chemical bond anchoring effect of the ligands and the space confinement effect, the hydrothermal and solvothermal approaches are the most commonly applied methods for the synthesis of catalysts with a metal@zeolite structure. Chemical bond anchoring generally refers to the noble metal precursor interacting with the functional groups on the support by forming chemical bonds. The noble metal nanoparticles can be anchored to the carrier, thereby preventing movement and aggregation of the nanoparticles. To date, several ligands including ethylenediamine (EN), acetylacetonate (ACAC), polyvinylpyrrolidone (PVP), (3-mercaptopropyl) trimethoxy silane (MPTS), etc. were used for the stabilization of noble metal species in hydrothermal synthesis systems.^{310–314} Hydrothermal and solvothermal synthesis systems require the use of expensive organic ligands and large amounts of solvent. In contrast, spatial confinement of precursor/crystal or precursor/seed intermediates is often used to confine metal particles in synthesis approaches involving inter-zeolite transformation, recrystallization, and seed-direct (or seed-epitaxial) growth routes.^{315,316} The introduction of expensive organic ligands is avoided with these methods. However, during the crystallization process, the encapsulated metal nanoparticles always grow.³¹⁷ The development of a simple approach to encapsulate metal nanoparticles in zeolites is still challenging.

Deposition-precipitation is one of the most widely used methods for preparing well-dispersed Au nanoparticles used in Au catalysis. When the pH of the solution is higher than the isoelectric point of the silicon site, [AuCl_x(OH)_{4-x}]⁻ can be deposited selectively close to the active titanium site instead of the inactive silicon site.³¹⁸ Several investigations have shown that, at similar Au particle size and in the absence of any promoter, the PO formation rate of Au/TS-1 prepared by the DP process (160 g_{PO}·h⁻¹·kg_{Cat}⁻¹) is much higher than that of Au/TS-1 prepared by the SG and SI processes (11 and 25 g_{PO}·h⁻¹·kg_{Cat}⁻¹, respectively).²²⁷ The Au nanoparticles prepared by the DP approach were reported to have a hemispherical shape by Haruta et al. For the epoxidation reaction of propylene, the hemispherical shape of Au nanoparticles results in a long distance between the peripheral interface and the carrier. Another reason for the greater activity of the Au/TS-1-B catalyst is possibly this particular Au catalyst structure. The addition of promoters (such as ionic liquid or NH₄NO₃) could further enhance the activity of the Au/TS-1-B catalyst.¹⁰³ To suppress the deactivation of pore blocking, a strategy was proposed to selectively deposit Au nanoparticles on the outer surfaces of the TS-1 support by Feng et al. (Figure 14A). This was obtained by the use of unroasted TS-1 (TS-1-B) with blocked holes as a substrate, as the TS-1-B had prefilled micropores and similar structural properties to the calcined open pores of TS-1 (TS-1-O). The results showed that the long-term stability was greatly improved.²²⁷ Then, the group first developed a new route to synthesize an efficient Au catalyst using the low-temperature DP process. The catalytic performance of Au/TS-1 catalysts prepared at different temperatures is shown in Figures 14B and 14C. A low temperature of 5°C is shown to retard the Au complex

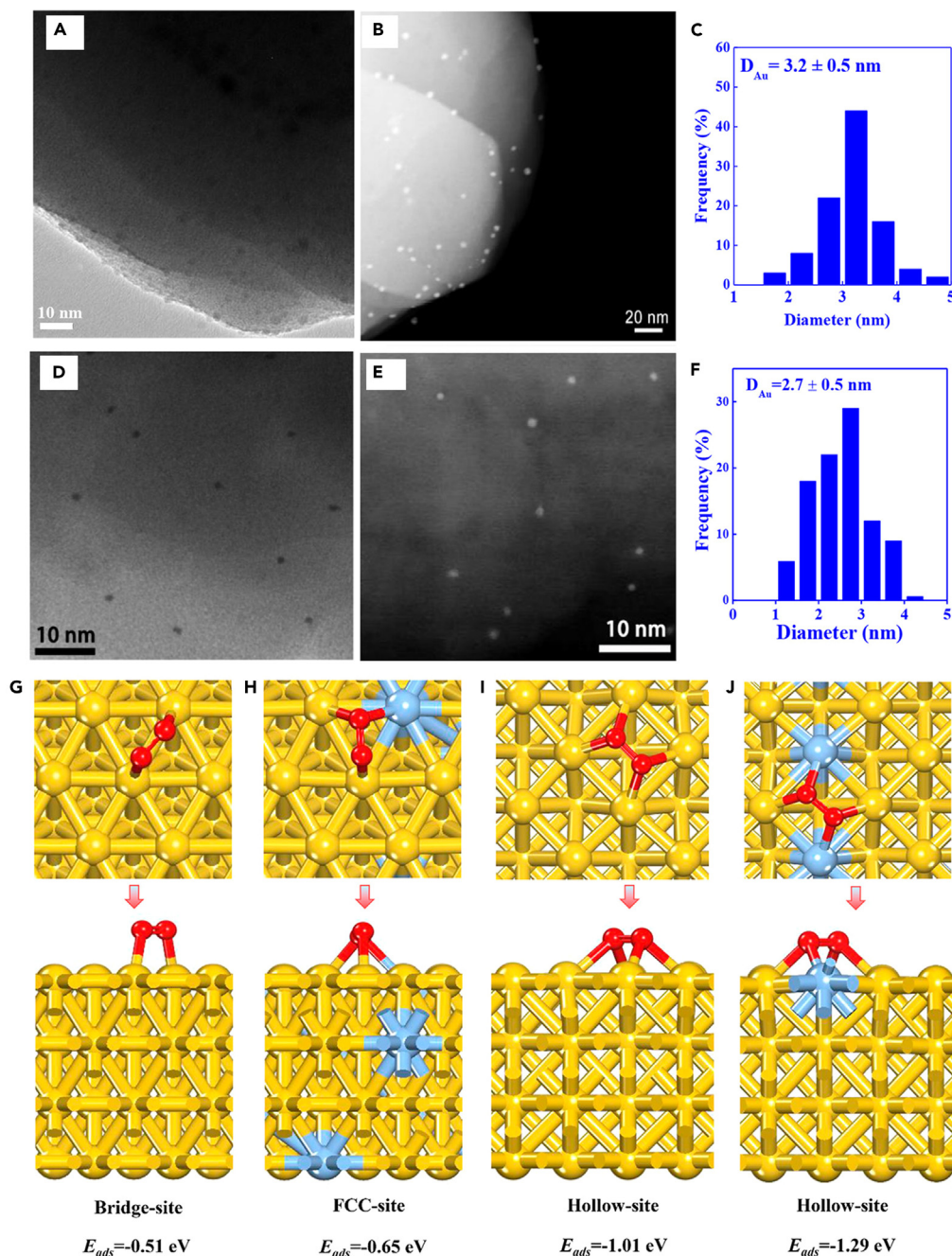


Figure 13. Design of catalysts

Representative HRTEM and HAADF-STEM images and particle size distributions of (A–C) Au/TS-1-B, and (D–F) Au₁₀–Ag₁/TS-1-B catalysts. Stable O₂ adsorption configurations and adsorption energy for (G) Au (111), (H) Au–Ag (111), (I) Au (100), and (J) Au–Ag (100).³⁰⁴ Copyright 2018, American Chemical Society.

hydrolysis rate and Au crystal growth rate on the outer surface of TS-1, resulting in more Au clusters entering the support micropores. Thus, the as-prepared Au/TS-1 catalyst shows significantly improved initial PO formation rate and stable PO formation rate.³¹⁸ Although the DP method is very effective for the preparation of highly active Au/TS-1 for the epoxidation of C₃H₆ with a mixture of O₂ and H₂, the capture rate of Au was never very high owing to the hydrophobic nature of TS-1. Despite the pre-treatment of the TS-1 support with aqueous NH₄NO₃ before DP or the addition of a certain amount of alkaline earth nitrate to the suspension of TS-1 in HAuCl₄ solution during DP, the Au deposition efficiency still remained below 20%.²²⁸ When TS-1 molecular sieves with the above hierarchical structure were used as carriers, Au nanoparticles prepared by the DP method tended to deposit on the hydrophilic outer surfaces of the carriers, thereby clogging the pore mouths.²²⁹

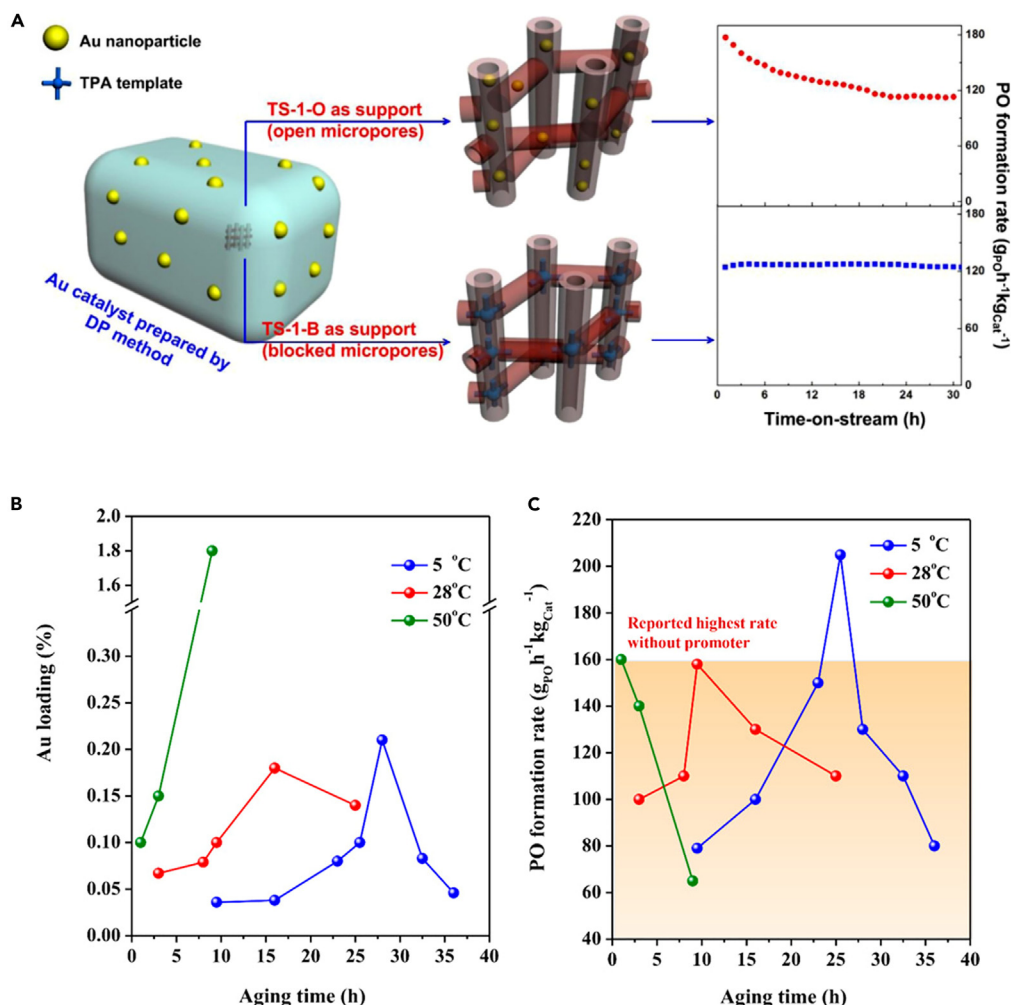


Figure 14. Design of catalysts

(A) Schematic diagram of Au locations of Au/TS-1-O and Au/TS-1-B catalysts.²⁹⁴ Copyright 2013, Elsevier B.V.

(B) Au loading and (C) PO formation rate of Au/TS-1 catalysts prepared at different temperatures as a function of aging time.²²⁷ Copyright 2018, American Chemical Society.

The Au nanoparticles loaded by the traditional impregnation process are spherical and the diameter is larger than that of 10nm. It leads to the combustion reaction of propylene to form CO_2 . Finally, the selectivity of PO is poor.³¹⁹ The spatial position of Au nanoparticles loaded by the conventional impregnation process is relatively random. It is difficult to load Au nanoparticles around the active center of Ti. First, the size of Au nanoparticles generated by the conventional impregnation process is very big. This is because Au complexes, mostly in the form of $[\text{AuCl}_4]^-$ and $[\text{AuCl}_3(\text{OH})]^-$, exist in the $\text{HAuCl}_4 \cdot 4\text{H}_2\text{O}$ impregnation solution at $\text{pH} = 1-3$. These complexes with high Cl-content finally result in larger Au clusters.³¹⁸ Second, the Au precursor solution was not able to load directionally around Ti sites with isoelectric point = 7 under the acidic conditions of the $\text{HAuCl}_4 \cdot 4\text{H}_2\text{O}$ impregnation solution. By adjusting the pH of the impregnation solution to $\text{pH} = 7-8$, Sheng et al. proposed the new modified isometric impregnation (NIMG) method to keep the Au nanoparticles less than 3.0 nm. As the pH of the impregnating solution is increased, the hydrolysis of the Au precursor is further increased. The Cl^- in the Au complex is gradually substituted by OH^- , resulting in a reduction in the size of the Au cluster. The Au precursor tends to be loaded near the Ti sites according to the isoelectric point principle by adjusting the impregnating solution to $\text{pH} = 7-8$. This new method combines the advantage of capillarity of the impregnation method with the advantage of directed loading of small Au nanoparticles near the Ti of the DP method. Figures 15A–15D shows that instead of being densely distributed on the external surface of Au/HTS-1(NIMG), many of the visible Au nanoparticles with an average size of about 2.6 nm were observed to be uniformly distributed within the pores. The Au/HTS-1(NIMG) catalyst shows a good PO formation rate ($150.3 \text{ g}_{\text{PO}} \cdot \text{h}^{-1} \cdot \text{kg}_{\text{cat}}^{-1}$), H_2 efficiency (29.1%), and PO selectivity (91.2%) (Figures 15E and 15F). This shows that the capillary effect of the novel impregnation method can prevent Au nanoparticles from accumulating on the Au/HTS-1(NIMG) catalyst surface.^{229,320} Lei et al. developed a modified incipient wetness impregnation (Miwi) method for the immobilization of Au NPs on TS-1 through hydrolysis (at a Ph of ca. 12.4) of AuCl_4^- to $\text{Au}(\text{OH})_4^-$ free of chloride prior to impregnation.²³⁰ These figures show that an efficient strategy for the synthesis of highly active

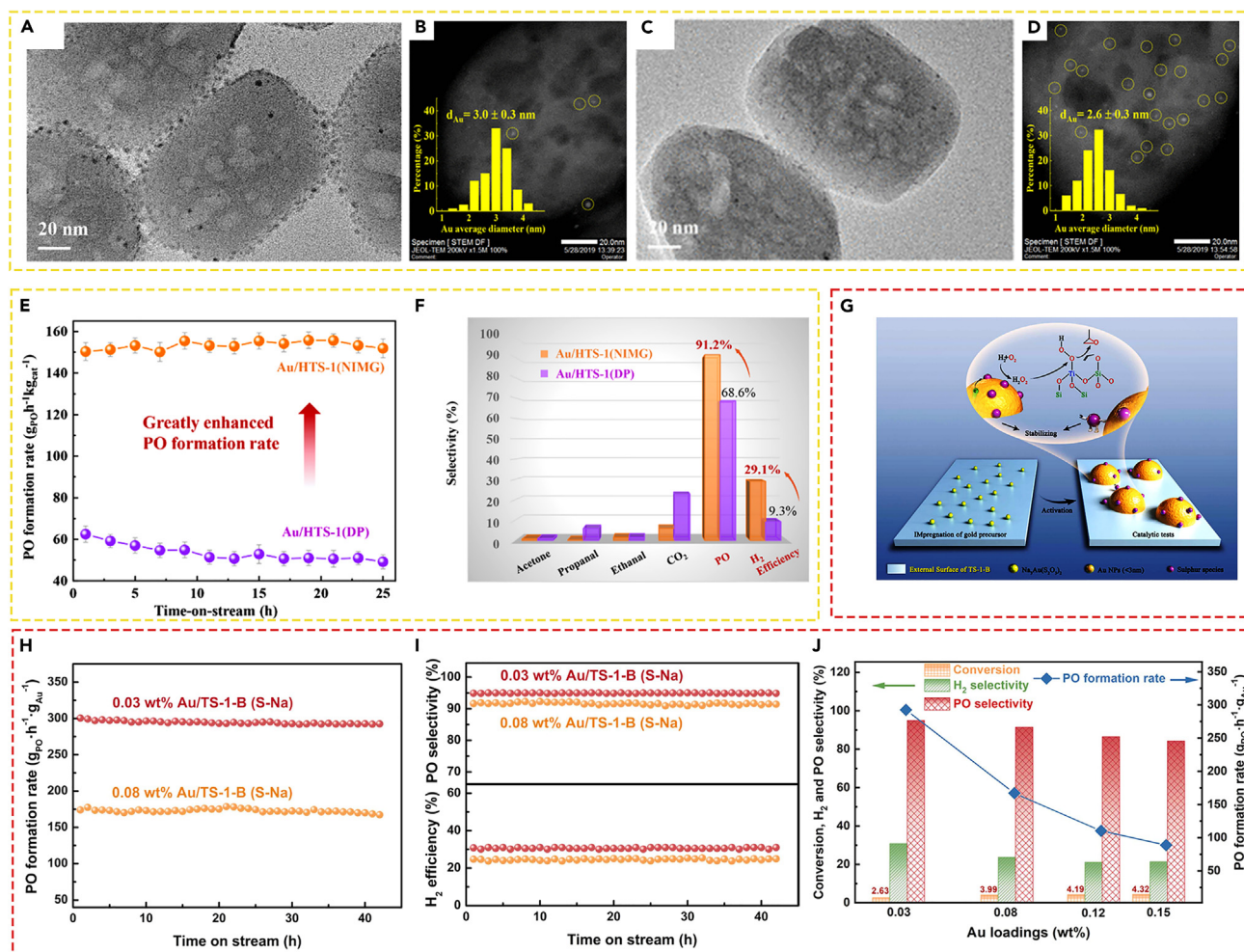


Figure 15. Design and catalytic performance of catalysts

HRTEM and aberration-corrected HAADF-STEM images of (A, B) Au/HTS-1(DP) and (C, D) Au/HTS-1(NIMG). The insets show the Au size distributions of the catalysts.

(E) PO formation rate, PO selectivity, and H₂ efficiency reaction for (F) 1h of Au/HTS-1(NIMG) and Au/HTS-1(DP) catalysts.²²⁹ Copyright 2022, American Chemical Society.

(G) Possible pathway for the immobilization of Au NPs on the TS-1-B via IWI method.

(H) PO formation rate.

(I) PO selectivity and hydrogen efficiency over 0.03 wt % Au/TS-1-B (S-Na) and 0.08 wt % Au/TS-1-B (S-Na) catalysts as a function of time on stream.

(J) Comparison of catalytic performance of Au/TS-1-B (S-Na) catalysts varying Au loading.²²⁶ Copyright 2022, Elsevier B.V.

Au-Ti bifunctional catalysts is to select Au precursors with lower chloride content in combination with appropriate Ti-containing materials. But Zhang et al. proposed an efficient Au/TS-1-B (S-Na) preparation in chloride-free gold precursors. A sulfur-containing Au precursor, sodium dithiosulfatoaurate, was used as an efficient method for the impregnation of Au species onto uncalcined TS-1 (Figure 15G). The Au/TS-1-B (S-Na) catalyst with a very low gold loading of about 0.03 wt % shows a PO formation rate up to $297 \text{ g}_{\text{PO}} \cdot \text{h}^{-1} \cdot \text{g}_{\text{Au}}^{-1}$ with a PO selectivity of about 95%, as shown in Figures 15H–15J.²²⁶

The Haruta group reports that small Au NPs and/or clusters can be deposited on organic polymers, carbon and non-precious metal oxides with very high Au capture rates (86–100%) by milling the carrier material with dimethyl Au (III) acetylacetonate.³²¹ The group then deposited Au on alkali-treated TS-1 using the SG method with a very high Au deposition efficiency of about 100%. A simple and effective method for preparing stable Au clusters has been suggested: roughening the support surfaces prior to Au deposition to increase the number of surface defects, as in Figure 16A.²²⁸ The Au/TS-1 catalysts prepared by solid grinding and sol-gel immobilization have good stability. However, owing to the non-selective deposition of Au nanoparticles, some Au NPs are deposited far from the center of the active Ti, resulting in low catalytic efficiency of Au.²²⁷

In the past few years, DGC methods have been widely used in the preparation of zeolites because of the advantages of efficiency, high utilization, high product yield, and low environmental impact. H. J. Cho et al. reported a direct cationic polymer-assisted vapor

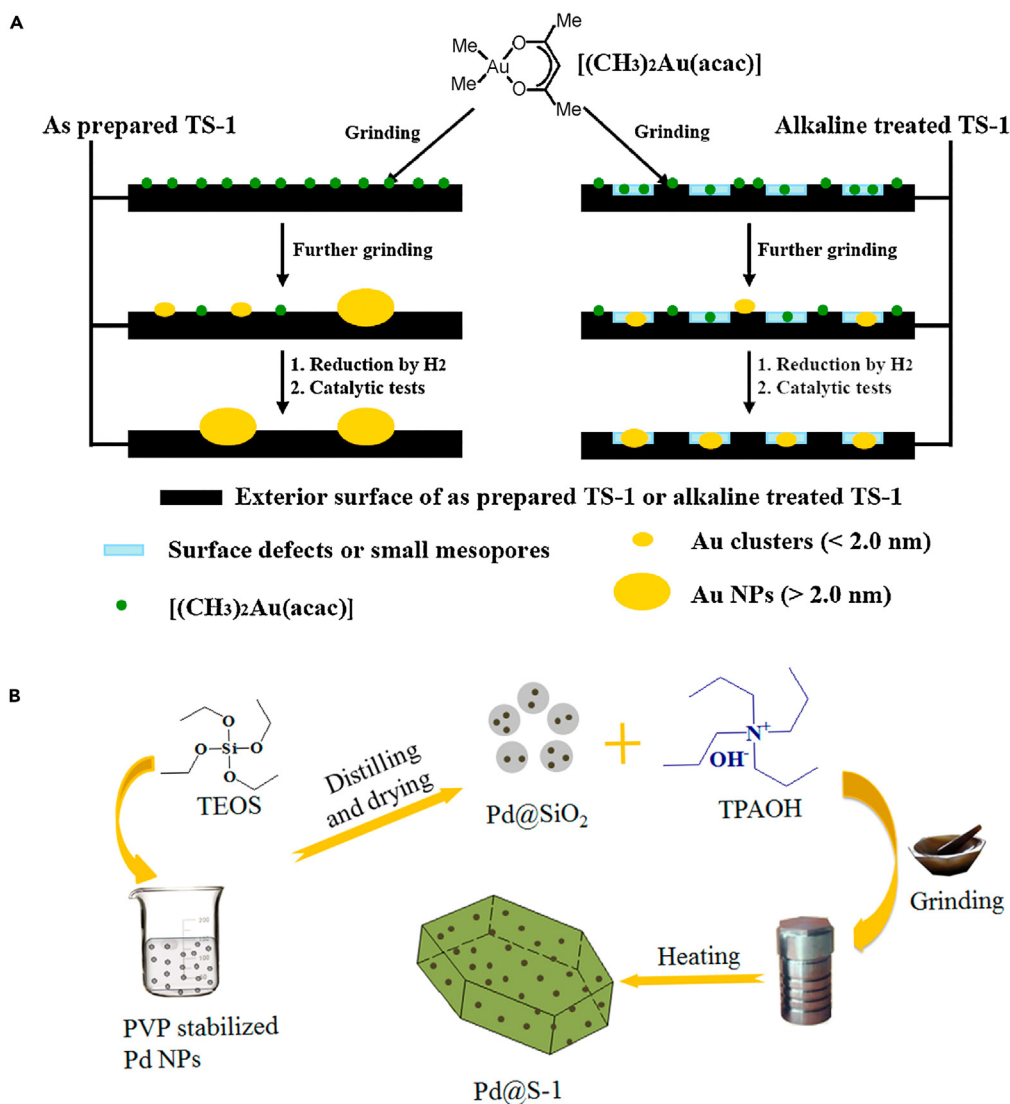


Figure 16. Design of catalysts

(A) Possible pathways for the formation of Au NPs or clusters by solid grinding of $[(\text{CH}_3)_2\text{Au}(\text{acac})]$ with TS-1 or alkaline-treated TS-1.²²⁸ Copyright 2010, Elsevier B.V. All rights reserved.

(B) Synthesis of Pd@S-1 catalyst.¹⁴⁰ Copyright 2016, American Chemical Society.

crystallization strategy to encapsulate Pt NPs in MFI zeolite.^{113,115} Although the high degree of encapsulation of the Pt NPs in the prepared catalysts is more than 90%, the size of the Pt NPs encapsulated in the zeolites is about 5–6 nm. J. Gu et al. managed to encapsulate 3 nm Pt NPs into the crystal structure of MFI via a crystal epitaxial growth route using a DGC process.³²² The key to this approach is the preconstruction of mesopores in the zeolite where the metal species are deposited. Mesopores are covered with a synthetic gel of Silicalite-1. Then the dry gel is recrystallized by a vapor-phase treatment. Using the seed-assisted DGC method, X. Yang et al. were able to synthesize a highly dispersed Pt@MFI catalyst (Pt NPs are about 1–2 nm). Pt precursors were reported to be tightly bound via imine groups in the Schiff-SiO₂ support, and Pt precursors can be retained during crystallization. This approach involved a multi-step process. The MFI seeds were necessary to facilitate the transformation. As mentioned above, the present synthesis method using DGC strategies has been rather complicated, and noble metal particle size is usually large. Subsequently, a simple process to directly encapsulate Pt nanoparticles into MFI-type molecular sieves was reported. First, taking benefit of the stabilizing role of the sulfhydryl (-SH) group, a Pt precursor was anchored to the external surfaces of SiO₂ spheres. Then a SAC crystallization process was used to structurally transform the Pt-containing silicon source into a Pt-encapsulated MFI zeolite. A high degree of encapsulation (>84%) was achieved. The average size of the encapsulated Pt NPs ranged from 1.54 to 2.34 nm. The encapsulated Pt NPs are characterized by exceptional thermal stability and high activity.¹¹²

Typically, hydrothermal conditions are used to synthesize zeolites that encapsulate metal nanoparticles. The metal recovery is relatively low (approximately 34%) and contaminated water is generated.^{309,323} A solvent-free strategy for the preparation of different zeolites has been reported lately. This approach is considered a green process because the absence of solvent avoids the production of polluted water. Some studies have shown that S-1 zeolite crystals encapsulating bimetallic gold-palladium nanoparticles ($\text{Au}_{0.4}\text{Pd}_{0.6}\text{@S-1}$) have been successfully synthesized using a solvent-free strategy. The solvent-free approach enables the efficient utilization of precious metals and significantly reduces the amount of polluted water generated during synthesis compared to the conventional hydrothermal route.¹⁴¹ Wang et al. successfully synthesized the core-shell structure through solvent-free crystallization Pd@S-1 Catalysts (Figure 16B).¹⁴⁰ The advantages of encapsulated metal nanoparticles are summarized below. (1) The dramatically improved stability and recyclability of encapsulated metal nanoparticles in catalysis is one of the most significant advantages. Encapsulation of metal nanoparticles in inorganic nanoshells or nanopores has been shown to significantly suppress their migration and coalescence by spatial confinement. (2) Another advantage of encapsulated metal nanoparticles is the improvement of catalytic selectivity. Controlled porosity allows the encapsulated material to act as a molecular sieve. (3) Another important feature of the encapsulated metal nanoparticles is the strong interaction between the metal nanoparticles and the encapsulating materials. Encapsulation ensures that the metal nanoparticles are in close contact with the encapsulant material with the maximum interface, especially in a core-shell configuration. (4) The size of encapsulated metal particles is controllable.

Significantly, Kapil et al. reported a simple one-pot approach for the preparation of very stable sub-nanometer Au clusters (approximately 0.8 nm core size) using triphenylphosphine as a stabilizing ligand.⁵ A rapid nonthermal O_2 plasma removal technique has been developed to eliminate approximately 74% of the phosphine ligands, resulting in a strongly stabilized catalyst. Figure 17A shows a schematic of the O_2 plasma removal process for Au/TS-1 materials. The Au/TS-1 powder is put into a vacuum chamber and exposed to the plasma for 30 min. The triphenylphosphine ligands are removed under vacuum by the energetic O_2 plasma species. Figure 17B shows the TEM image of Au/TS-1PT. An average particle size of 1.5 nm is confirmed by the corresponding particle size distribution (Figure 17C). Catalysts synthesized by this method showed improved catalytic performance in the indirect gas-phase epoxidation of propylene. PO selectivity was about 89% and stability was more than 20 days (Figure 17E). Triphenylphosphine, as a sacrificial ligand, plays an essential role in preventing nanoparticle agglomeration. It also maintains a small particle size (less than 5 nm) and enhances catalytic activity. Another factor that helps to improve the stability of Au nanoparticles in the process of epoxidation is the existence of Ti defect sites. Ti defects act as nucleation sites for Au nanoparticles. This prevents Au nanoparticle oxidation and improves the stability of Au/TS-1.

DETERMINATION OF ACTIVE SITES

Knowledge of the structure-property relationships of metal-zeolite catalysts is of great importance for the efficient design of high-performance catalysts for heterogeneous catalysis and industrial applications. For the characterization of the metal species and the zeolite matrix, some conventional methods like X-ray diffraction (XRD), X-ray photoelectron spectroscopy, transmission electron microscopy (TEM), N_2/Ar adsorption measurements and hydrogen temperature programmed reduction (H_2 -TPR) were used.^{324,325} These characterizations can only give a few basic information including phase identity, textural characteristics, metal valences, particle size, and so on. Powerful characterization techniques are required to characterize active metal sites on zeolites. Information about structure and dynamics can be obtained at the atomic level using these techniques. In the last few years, scientists have seen a fast development of several characterization techniques, like solid-state NMR, probed infrared spectroscopic techniques, Cs-corrected scanning TEM, and X-ray absorption spectroscopic techniques. This is helpful to understand the structure-property relationship with the increasing complexity of the structure and composition of metal-supported zeolite catalysts.^{326–328} Each approach has distinct advantages and limitations because of the unique operating principles of the novel techniques and the different characterization objectives. A more comprehensive understanding of metal in zeolite catalysts is possible through the combination of the above spectroscopy and microscopy measurements. *In situ* characterization methods are advantageous for knowledge of the development of the coordination environment of active metal sites over the course of the catalytic process. This section highlights recent developments over the past few years.

Characterization of Ti in TS-1 zeolite

Catalytic activity and product selectivity can be enhanced through knowledge of the coordination states and location of Ti in the framework. Advanced structural characterization techniques, like UV-vis spectrophotometry, X-ray diffraction, Raman spectroscopies, Fourier transform infrared (FTIR), UV-resonant Raman spectroscopies, X-ray absorption near edge structure (XANES), extended X-ray absorption fine structure (EXAFS), nuclear magnetic resonance (NMR), and electron microscopy (EM), and electron spin resonant (ESR) spectroscopic techniques have been widely used in the characterization of TS-1 zeolites to gain a deep understanding of the properties of Ti in the zeolite framework.³²⁹

The vibrational band at 960 cm^{-1} is considered to be the characteristic vibrational band of framework Ti species in FTIR and Raman spectra. The peak intensity of this band is believed to have a positive correlation with the Ti content. For the evaluation of the Ti content in TS-1 frameworks, the intensity ratio between the vibrating bands at 960 and 550 or 800 cm^{-1} is the characteristic band of the MFI structure. There is also evidence that the degree of hydration and crystal size of the zeolites can have an effect on the intensity of this band. The exact determination of framework Ti species in TS-1 is still an important issue.^{218,330}

Synchrotron-based XAS is a powerful characterization technique to obtain atomic-scale information on the structure, coordination settings, and electronic properties of metal species bound to zeolites. The XAS spectra typically show two regions, the extended X-ray absorption fine structure and the X-ray absorption near edge structure. The analysis of white line intensities, absorption edge shifts, and pre-edge and post-edge features allows XANES to determine the electronic properties and positional symmetries of metal species.^{331–333} To provide

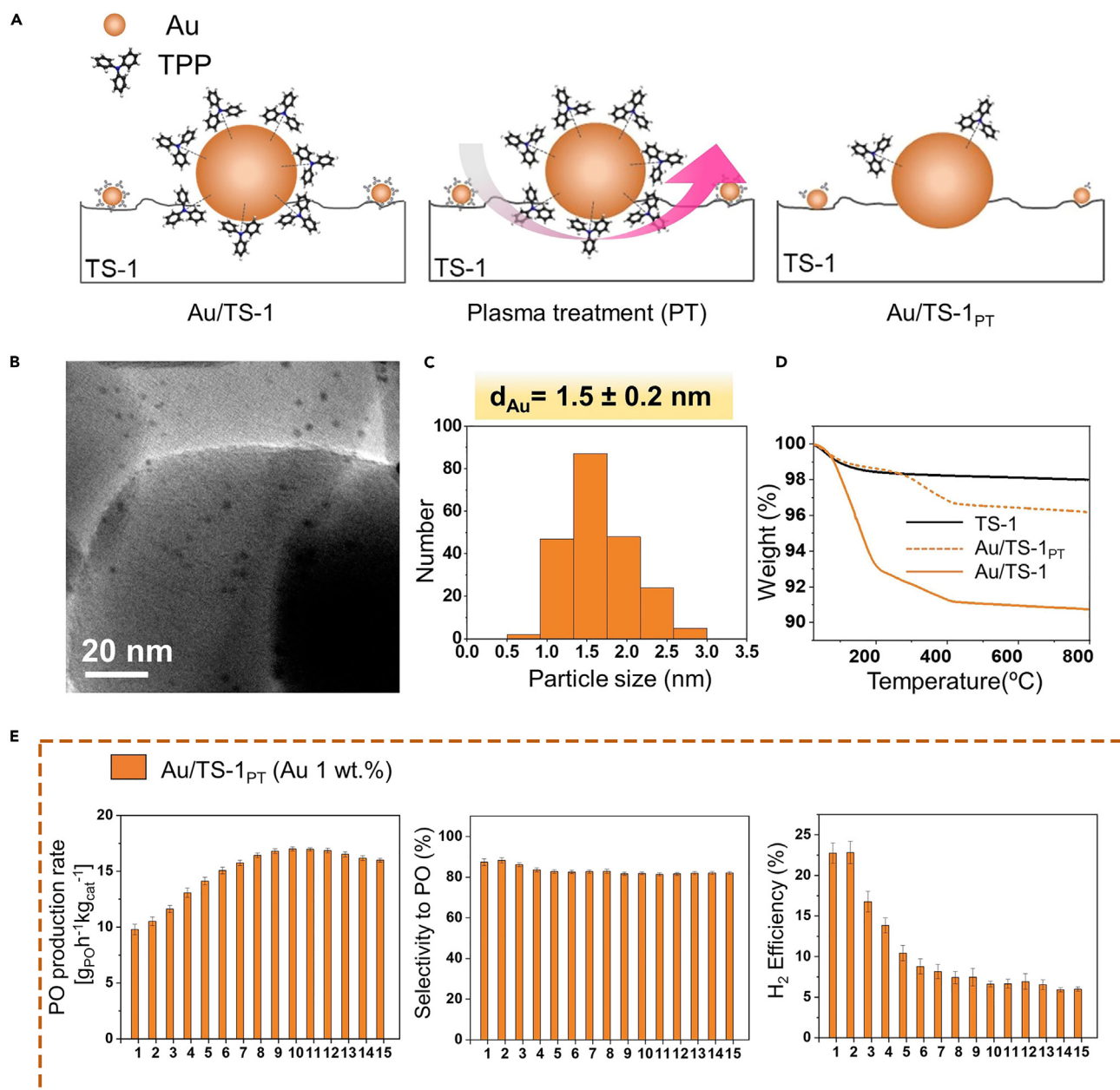


Figure 17. Design and catalytic performance of catalysts

(A) Schematic illustration of nonthermal oxygen plasma treatment on Au/TS-1.

(B) TEM of Au/TS-1 PT.

(C) Corresponding Au particle size distribution histogram.

(D) Thermogravimetric analysis (TGA) of TS-1, Au/TS-1 and Au/TS-1 PT.

(E) Stability test for Au/TS-1_{PT} catalyst. The order is the production rate of PO, PO selectivity and Hydrogen efficiency.⁵ Copyright 1999–2023, John Wiley & Sons, Inc.

detailed information about the coordination environments and bonding distances of single atomic sites, EXAFS and related techniques are powerful. The XAS method is based on spectral fitting to give information about the coordination environment and electronic properties of metal species throughout the sample.

Recently, Yu and coworkers investigated the coordination environment and the local structure of Ti species in a nano TS-1 zeolite sample (TS-1-AM).^{84,128} The intensity of the XANES pre-edge peak of the TS-1-AM sample is reduced, showing the presence of a deformed Ti structure with higher coordination states compared to the pure tetrahedrally coordinated TS-1 zeolite. The authors confirmed the octahedral coordination of the deformed Ti species by combining UV-Raman spectroscopy excited at 266 nm. The first shell coordination number is 4.3,

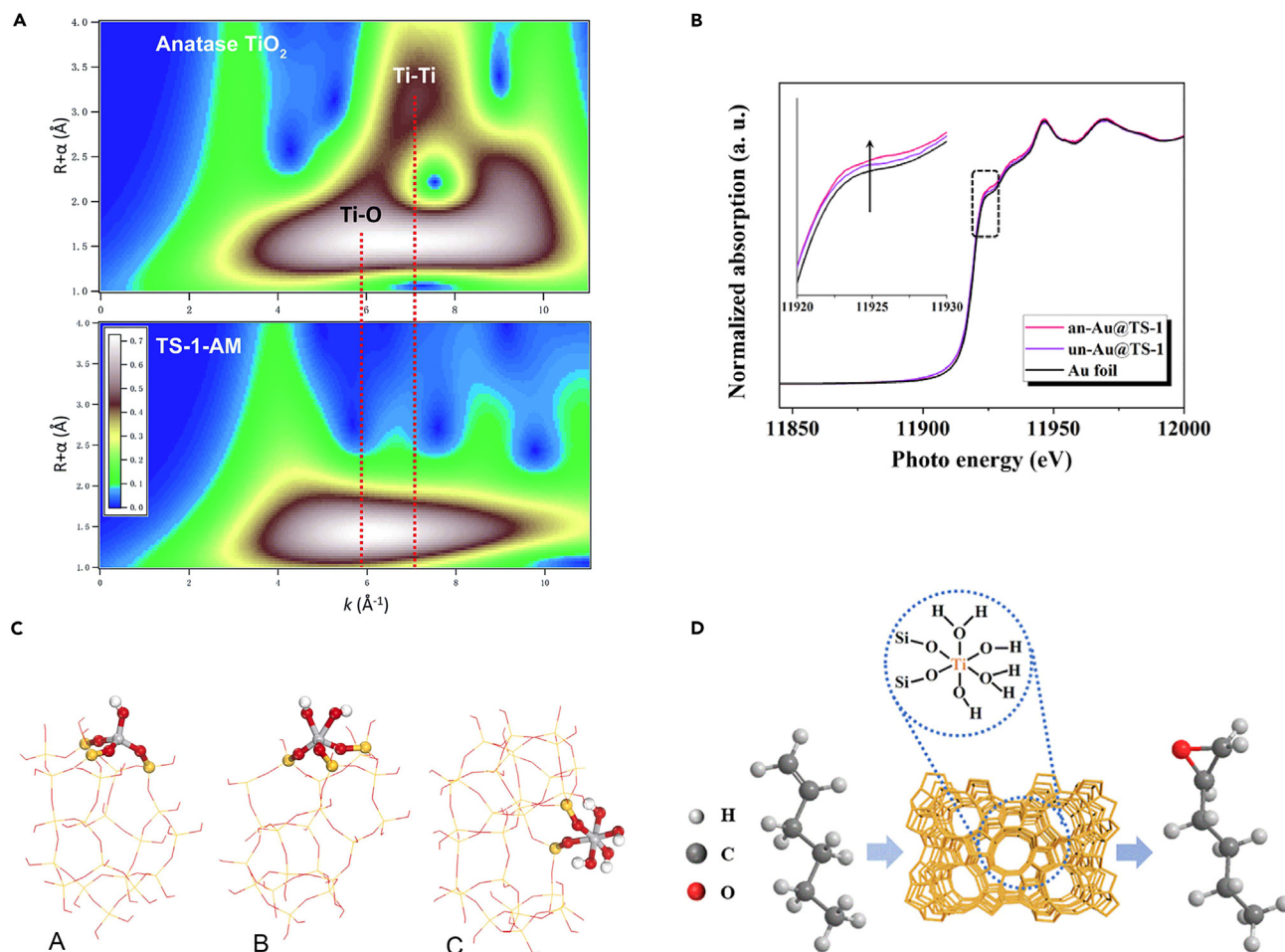


Figure 18. Characterization of catalysts and Ti active sites

(A) Wavelet transform (WT) of TS-1-AM and anatase TiO_2 . The WT contour plots are based on Morlet wavelets ($k = 6$, $\sigma = 0.8$). The vertical dashed lines point out the k -space position of the Ti-O and Ti-Ti contributions. Reproduced with permission.¹²⁸ Copyright 2020, The Royal Society of Chemistry.
 (B) Au LIII-edge XANES spectra of an-Au@TS-1 and un-Au@TS-1 (calibrated using Au foil standard sample).³³⁴ Copyright 2023, Elsevier B.V.
 (C) Proposed structures of the Ti-IV(A), Ti-V (B) and Ti-VI (C) by DFT.²²² Copyright 2023, Published by Elsevier B.V. The gray ball represents the Ti atom, yellow for Si, red for O, and white for H. They are the results after geometric optimization and frequency calculations.
 (D) Anatase-free TS-1 zeolites containing TiO_4 and TiO_6 .⁶⁸ Copyright 2022, American Chemical Society.

which is above that of the pure tetrahedrally coordinated TS-1 zeolite (4.0). This indicates that octahedrally coordinated Ti species are present in TS-1-AM. The absence of Ti-O-Ti bonding in EXAFS is an indication that all Ti in the TS-1-AM sample is in isolation. Wavelet Transform (WT)-EXAFS of TS-1-AM shows no Ti-Ti shell, indicating the lack of Ti-Ti coordination, and confirms the octahedral coordination of the mononuclear Ti species (Figure 18A). The Au foil has a lower LIII edge strength because of the fully occupied $5d^{10}$ orbit, as demonstrated by Wang et al. using XANES spectroscopy.³³⁴ An-Au@TS-1 exhibits higher LIII edge intensity, indicating the loss of more d-electrons (Figure 18B). The An-Au@TS-1 composite catalyst can better interact with the titanium surface because of the presence of bridging oxygen. Thus, the local environment of titanium is modulated and the Lewis acidity of the catalyst is increased.

Characterization of hierarchical structures

Pore size and partitioning, pore morphology and interconnectivity are intimately connected to mass transfer and active site accessibility and therefore affect zeolite catalytic performance. Several characterization techniques like physical and chemical sorption, mercury porosimetry, EM, synchrotron X-ray tomography, focused ion beam scanning electron tomography, nuclear magnetic resonance, quasi-elastic neutron, etc. have been applied to characterize the pore structures and mass transfer properties of hierarchical zeolites.^{156,335,336}

EM techniques, among them scanning electron microscopy (SEM), TEM, focused ion beam scanning electron microscopy (FIB-SEM), and electron chromatography imaging, utilize very short-wavelength electrons to visualize the atomic structure of zeolites at different resolution scales.^{336,337}

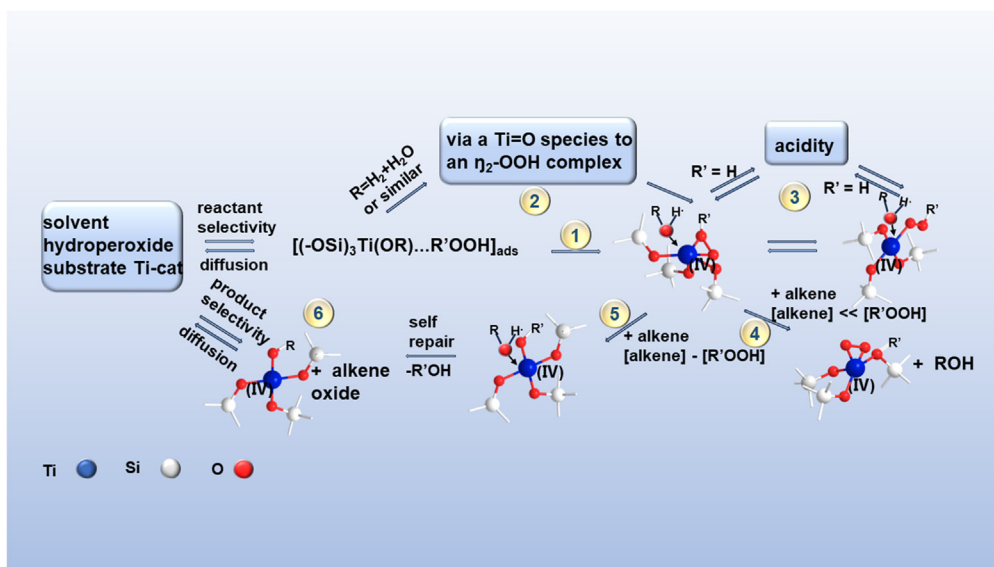


Figure 19. Mechanism of propylene epoxidation catalyzed by TS-1

The mechanism for alkene epoxidation at Ti-OR sites. R represents either $\equiv\text{SiO-}$, H or an organic function.³⁴¹ Copyright 1999, American Chemical Society.

Positron annihilation lifetime spectroscopy (PALS) has been shown to be an effective non-destructive technique for probing the porosity of hierarchical zeolites.³³⁸ The ortho-positronium (o-Ps) is generated by the implanted positron and has a lifetime that is long enough to allow it to diffuse through the porous media. But o-Ps lose energy upon collision with the channel surface and decay with a lifetime proportional to the aperture. PALS evaluates the degree of interconnection of the intermediary pore network of zeolite crystals in an indirect and effective way.

The above-mentioned advanced techniques provide revealing information about the pore structures in hierarchical zeolites, among them the shape, size and connectivity of the pores. The pore structures are of great importance for the comprehension of the role of the hierarchical structures in the outstanding catalytic performance of the TS-1 zeolites. However, developing operando techniques to determine the precise relationship between hierarchical structures and catalytic performance is still a challenging.

Density functional theory (DFT)

DFT is a technique used to investigate the electronic structure of multi-electron systems. The DFT calculations were performed with the Vienna ab initio simulation package (VASP). Projected augmented wave potentials were used to describe the interaction between the valence electrons and the nucleus. The exchange-correlation energy was calculated by means of the Generalized Gradient Approximation (GGA) approach according to the Perdew-Burke-Ernzerhof (PBE) function.

Recently, through a detailed and systematic UV-Raman resonance spectroscopy study coupled with DFT calculations, Wang et al. identified the new Penta-coordinated and hexacoordinated Ti sites for the first time (Figure 18C). In the epoxidation of propylene to produce PO, the new hexa-coordinated Ti site shows very high catalytic activity.²²² Further, Fan et al. using DR-UV-Vis, UV-Raman spectroscopy and DFT calculations, proposed for the first time a possible structure for a bipedal Ti center. The bipedal Ti center consists of an octahedral ligand sphere coordinated by two Ti-OH groups and two water molecules (Figure 18D).^{68,339}

REACTION PATHWAYS

Reaction mechanism

Previous studies have proposed three possible epoxidation pathways, namely the Sinclair and Catlow mechanism on tripodal site through Ti-OOH species, the Vayssilov and van Santen mechanism on tetrahedral Ti site without Ti-OOH formation, the Munakata et al. mechanism involving peroxy (Ti-O-O-Si) species.³⁴⁰ Next, we will provide a detailed introduction to the previously proposed mechanisms and the newly proposed mechanisms.

Sinclair and Catlow mechanism

A computational DFT investigation of the mechanism first reported by Bellussi et al. was performed by Sinclair and Catlow.³²⁸ The mechanism for epoxidizing propylene (ethylene in the original paper) with H_2O_2 using the TS-1 catalyst has two major steps: (1) the generation of the active hydroperoxide intermediate by H_2O_2 at the active Ti site in TS-1. (2) Propylene attacks the active hydroperoxide intermediate to produce PO and water. As shown in Figure 19, step 1 is likely to be faster than step 2 and probably represents the path to the active oxygen-donating species. Its formation will be dependent on the concentration of hydroperoxide at the Ti^{IV} site and on competitive adsorption

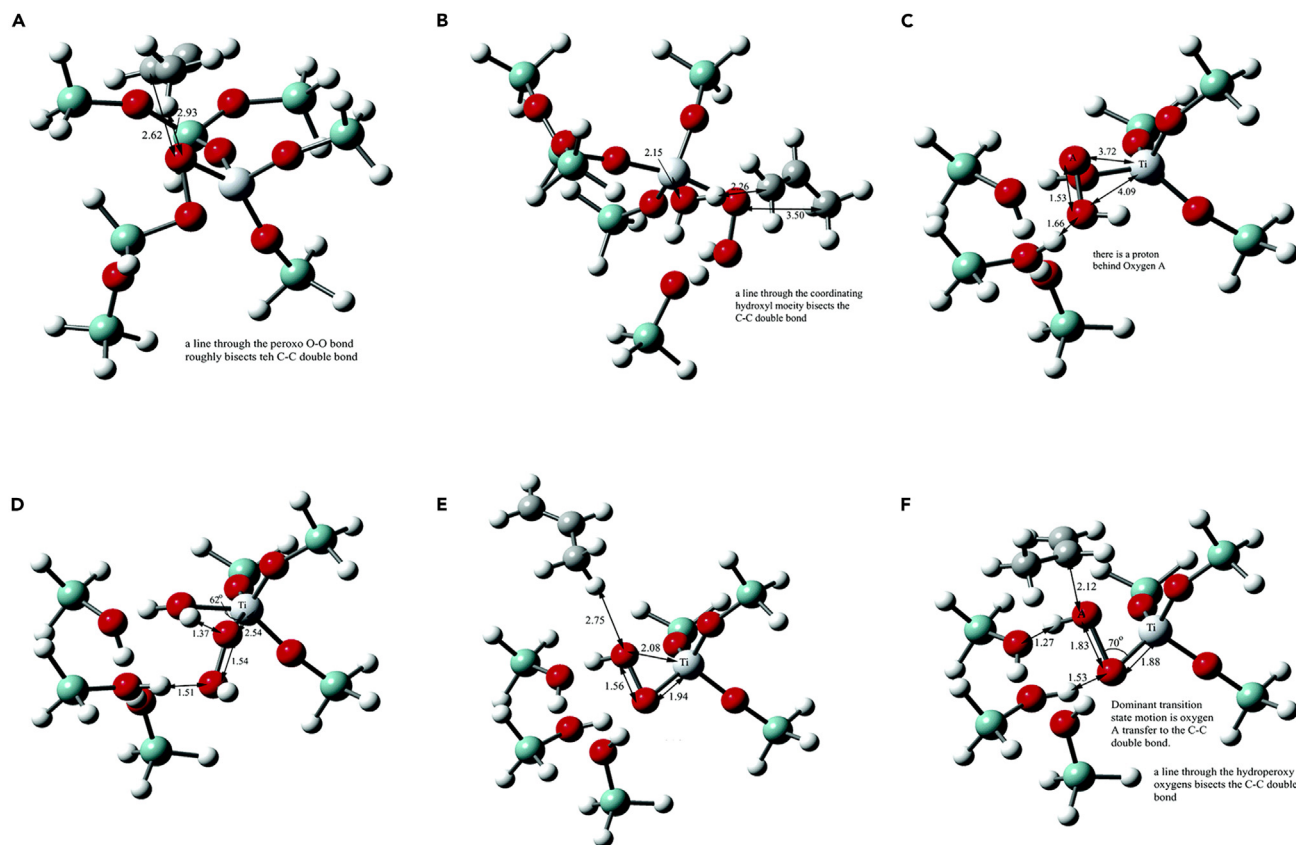


Figure 20. Mechanism of propylene epoxidation catalyzed by TS-1

Ti/defect mechanism for the partial silanol nest model: (A) transition-state geometry during epoxidation of propylene and (B) preadsorbed complex of propylene on the hydroperoxyl intermediate. Ti/defect mechanism for the full silanol nest model: (C) preadsorbed complex of H_2O_2 on the Ti site of TS-1 and (D) transition state geometry during the formation of the hydroperoxyl intermediate on the Ti site of TS-1.

(E) The preadsorbed complex of propylene on the hydroperoxyl intermediate.

(F) Transition-state geometry during epoxidation of propylene. All distances are in angstroms. ³⁴² Copyright 2006, American Chemical Society.

with solvent or base for the two coordination sites. Step 3 gives rise to acidity in the presence of hydrogen but not alkyl hydroperoxides. Steps 4 and 5 describe alkene epoxidation and catalyst deactivation, respectively. These two processes are likely to compete, but since the activation barrier is less for step 5 than for step 4, deactivation will only be significant when the concentration of alkene becomes smaller than the active oxygen-donating species. Finally, step 6, self-repair of the catalyst and diffusion of the products, close the catalytic cycle. An active intermediate ($\text{Ti}-\text{OOH}$) is generated by the adsorption of H_2O_2 on the Ti site. The $\text{Ti}-\text{OOH}$ species then reacts with the olefins through the oxygen atom of the $\text{Ti}-\text{OOH}$, oxidizing the olefins and forming the epoxidation products and H_2O_2 . However, the Sinclair and Catlow mechanism was not demonstrated for the closed internal Ti sites (tetrahedrally coordinated to four Si sites via lattice oxygens). In fact, this mechanism does not produce reaction intermediates at such sites.

Defect site mechanisms

The zeolite framework is free of defects if all Ti sites of the zeolite are linked tetrahedrally by $\text{Ti}-\text{O}-\text{Ti}$ bonds. However, it is also possible to discover a missing Ti atom (a defect in the zeolite) even in a well-prepared TS-1, leading to the generation of a local silanol nest. Reactivity at internal Ti sites could be explained by Ti/defect sites. The presence of neighboring defective sites provides a certain degree of steric freedom for reactions like the Sinclair and Catlow mechanisms to occur. ³⁴²

Partial silanol nest model. Discussion of the mechanism of epoxidation of hydrogen peroxide intermediates located at the internal Ti site is complicated because of the existence of nearby silanol groups. ³⁴² A Ti center with one defective neighbor would mean that there are a total of three adjacent hydroxyl groups within the reaction range of the molecules and groups attached to the active Ti center. Recently, Wells et al. reported a first approximation to this problem. Only the nearest nearby hydroxyl group was calculated and only one $\text{Si}-\text{OH}$ group (instead of

three) was modeled. The Si-OH neighborhood of the internal Ti/defect sites can be used as a rational model for the external Ti sites with a Si-OH neighbor. Figure 20A shows an example of the stable adsorption of H₂O₂ on the Ti/defect area with partial modeling of the defect. The hydroxyl groups on the Ti and Si can form hydrogen bonds with the H atoms of H₂O₂ at the ends of the molecule. The hydroperoxyl intermediate formation is an η -1 type instead of the η -2 type formerly observed in the Sinclair and Catlow mechanism. The stretched η -1 configuration results in a small energy gain through the formation of a hydrogen bond between the OOH and the adjacent silanol nest. Figure 20B shows the adsorption of propylene on the η -1 hydroperoxyl intermediate of the Ti/defect (partial) model. Compared to the mechanisms of Vayssilov and van Santen and Munakata et al., the partial silanol nesting mechanism is energetically more favorable. Nevertheless, the energy barrier in the epoxidation step is raised to 14.3 kcal/mol (Gibbs free energy at 298 K) by the η -1 to η -2 rearrangement. Compared to the Sinclair and Catlow mechanism (7.9 kcal/mol for the epoxidation step), this level makes this mechanism unattractive.

Full silanol nest model. Energy barriers for epoxidation closer to Sinclair and Catlow are obtained by considering a more complete silanol nest model.³⁴² Silanol nests with Si site defects in silicalite structures yield three hydroxyl groups, all at similar distances from adjacent Ti centers. This complexity can be handled with DFT theory, but the computational requirements increase significantly. With the three hydroxyls on the left side of the picture and the Ti midpoint close by, Figure 20C shows the geometry of this cluster model. H₂O₂ can easily bridge the gap between Ti and the hydroxyls of the silane network with hydrogen bonding. The energy barrier is 8.9 kcal/mol (Gibbs free energy at 298 K) for the generation of the hydroperoxyl intermediate by the transition geometry in Figure 20D. This energy barrier is lower than some of the silanol nests, partly because the hydroxyl groups displaced on the Ti center are able to search for hydrogen bonds in the neighboring silanol nests. But the energy barrier is higher than the Sinclair and Catlow mechanisms (7.9 kcal/mol). Significantly, propylene can be adsorbed in the geometry of Figure 20E prior to the reaction once water is removed from the active site. Hydrogen peroxide intermediates are in the η -2 configuration, with adjacent hydroxyl groups of the silanol nest being positioned to accommodate the fragments (i.e., OH groups) produced by OOH following the insertion of oxygen into the carbon-carbon double bond. The transition geometry in Figure 20F shows this accommodation. The transition energy barrier (Gibbs free energy at 298 K) is only 4.6 kcal/mol.

Binuclear catalytic mechanism

It is generally thought that the active site for selective oxidation is the isolated tetrahedrally coordinated framework Ti species [TiO₄] in the framework of TS-1 zeolites. Due to the transition metal nature of Ti, the Ti center can be coordinated with up to 6 linkers, and the local geometries of the Ti center can be altered to pentahedral or octahedral coordination. In a recent study, Gordon and his team used simulations and solid-state nuclear magnetic resonance techniques to determine that the active center of the catalytic oxidation may be composed of a pair of Ti atoms instead of a single active site in the framework structure. More advanced *in situ* characterization techniques and density functional theory calculations are needed to further investigate this mechanism. As shown in Figure 21, during the epoxidation, the hydroperoxo hydrogen atom is transferred to the adjacent Si-O group, generating a Ti-O-Ti moiety with a coordinated silanol Si-OH ligand (TS1-(OOH)(O)). The regeneration of the active bis-hydroperoxo species TS1-(OOH)₂+ propylene by reaction with propylene, H₂O₂ and release of water. The presence of bridging peroxy species at the binuclear Ti site makes propylene epoxidation a low-energy reaction pathway.³⁴³ Although it is challenging to synthesize TS-1, which has a single binuclear Ti active site, this new perspective on the active site structure can help to further optimize TS-1 and the industrial epoxidation process.²¹⁰

Qin et al. have studied the ring opening of by-products formed by PO on TS-1 with bipodal Ti sites using quantum mechanics (QM) and molecular mechanics (MM) calculations.³⁴⁰ Reactant adsorption, active intermediate formation, propylene epoxidation, and PO solvolysis are taken into account. Two types of mechanisms are studied for the epoxidation of propylene and the solvolysis of PO, the “one-step” mechanism and the “two-step” mechanism, as in Figure 22. The results show that the bipodal Ti active site promotes the epoxidation reaction, while at the same time decreasing the selectivity toward the epoxide products due to the Ti-OH group catalyzing the PO ring opening. The Ti- η ¹-OOH and Ti- η ²-OOH are considered the epoxidation intermediates, while the “two-step” mechanism is considered the operating mechanism for the epoxidation of propylene. The effective activation free energies of the total process for PO formation were determined to be 41.36 and 42.56 KJ/mol. These are smaller than the activation energies reported in the literature for epoxidation at the tripodal Ti site (99.56 KJ/mol) or at the Ti/defect site (56.48 KJ/mol). But bipodal Ti species show poorer selectivity for PO compared to tetrahedral sites.

Production process of propylene epoxidation

Commercial-scale plants based on the HPPO process have been installed. Most of them were built by Evonik (formerly Degussa), BASF, Dow and Uhde. The first commercial-scale plant for the production of PO based on HPPO technology was put into operation by Evonik in 2008. The following year, in a joint venture between BASF and Dow, a 300 kt/a PO industrial plant was built and commissioned.³⁴⁴ In addition to the processes that have been or are nearing commercialization, other pilot plants for propylene epoxidation process development are currently being designed and are in operation. For example, SINOPEC and Tianjin Dagu Chemical Co., Ltd. Successfully operated 1.0 and 1.5 kt/a HPPO process pilot plants, respectively, and Dalian University of Technology built a 100 t/a propylene epoxidation pilot plant.³⁴⁵ Fixed-bed reactors are suitable for the reaction from both an industrial application and economic point of view based on the requirements and characteristics of the HPPO process and engineering considerations (Figure 23A). Dow/BASF and Evonik/Uhde's industrialized HPPO processes use fixed-bed reactors.³⁴⁶

For industrial fixed bed applications, TS-1 powdered zeolites need to be formed into granular, spherical or extruded forms to reduce pressure drop and provide adequate mechanical strength. However, the difficulty of molding powder TS-1 is an obstacle to its application

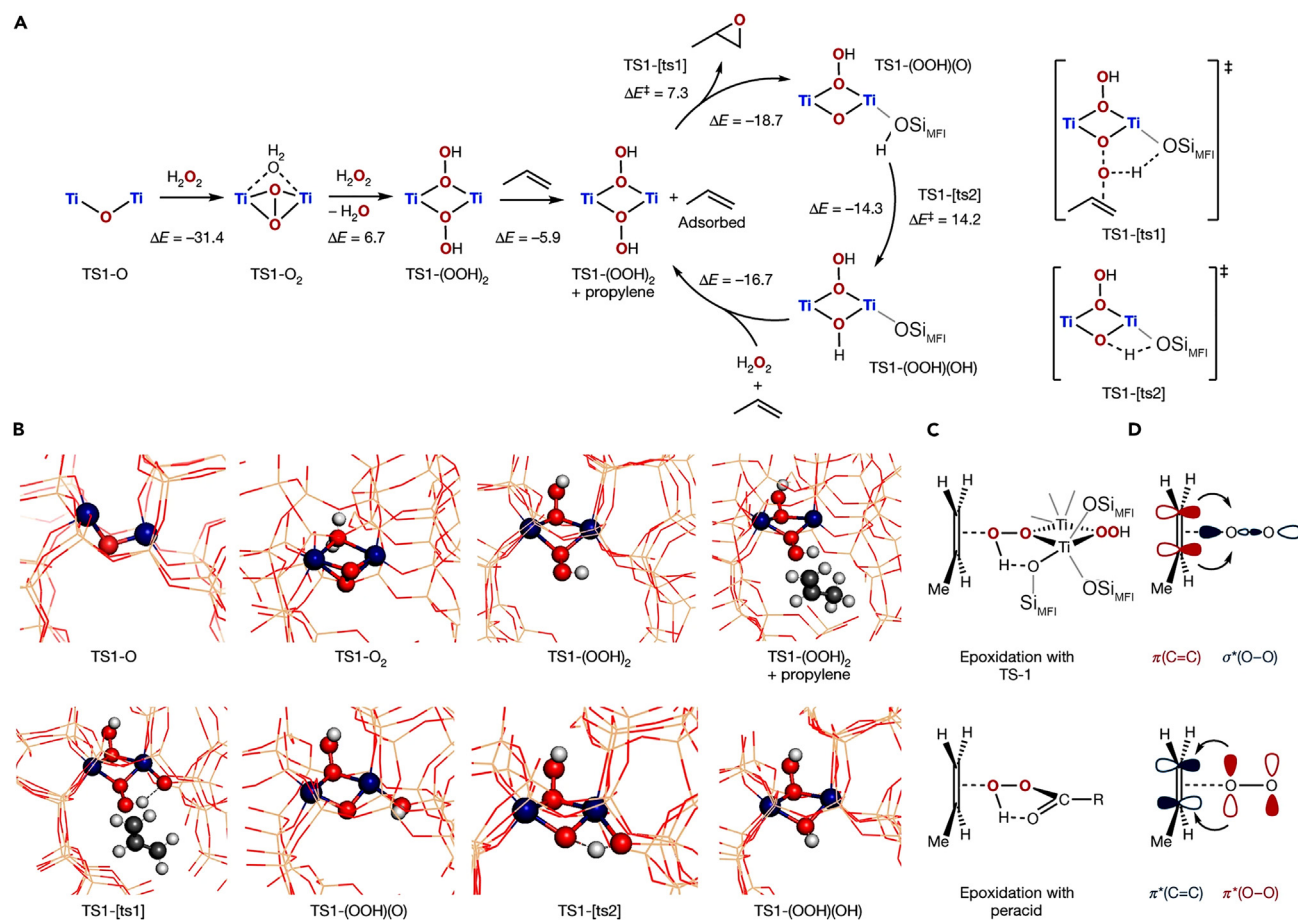


Figure 21. Mechanism of propylene epoxidation catalyzed by TS-1

(A) Propylene epoxidation at a binuclear Ti site.

(B) Calculated structures of selected stationary points of the mechanism. In this model, the two Ti atoms (blue spheres) are located at the adjacent T7 and T11 sites of the MFI structure.

(C) Key transition state of olefin epoxidation, which is assisted by a framework oxygen atom and related transition state of olefin epoxidation with peracids.

(D) Main orbital interactions involved in the epoxidation process with co-planar lone pairs on oxygen.³⁴³ Copyright 2020, Springer Nature Limited.

in fixed-bed reactors. Generally, extruded materials are made from slurries. The paste is obtained in advance by mixing the catalyst powder with the following components: (1) mechanical strength provided by an inorganic binder. (2) An organic binder is used to increase the viscosity of the paste to achieve adequate plasticity when extruded and molded. (3) A liquid phase provides effective lubrication during the extrusion process.³⁴⁷ The results show that the lamella TS-1 catalyst has better performance in propylene epoxidation than the strip TS-1 catalyst because of the shorter diffusion path for reaction heat, raw material and product.³⁴⁸

Lin et al. investigated the catalytic epoxidation of propylene in a fixed-bed reactor and under mild conditions at a pilot scale of 1.0 kt/a using hollow TS-1 zeolite as a catalyst. Figure 23B shows the corresponding schematic diagram. In a typical process, hollow TS-1 zeolites were ground into particles of about ϕ 1–3 mm and then they were added to a stainless-steel tube reactor. A mixture of methanol, hydrogen peroxide (30 wt %), water and propylene were injected into the bottom of the reactor at a reaction temperature of 30°C–70°C. Propylene is epoxidized with hydrogen peroxide. The mixture of solvents, products and reagents enters the C₃ separation tower. The mixture at the bottom of the C₃ separation tower enters the PO separation tower to separate crude PO from the aqueous CH₃OH solution. The crude PO is refined in the PO purification column, while the CH₃OH is purified in the H₂O/CH₃OH separation column. H₂O was removed from the process and the refined CH₃OH was recovered as a solvent for the reaction. The TS-1 zeolite with an abundance of intercrystalline mesopores and high Ti framework species exhibited a high catalytic activity and a long lifetime (more than 6000 h) in this procedure.²⁰⁵ Based on the results obtained in the 1.0kt/a pilot plant, a 100kt/a industrial demonstration unit for propylene epoxidation has already been installed at SINOPEC and has been operating smoothly for a long period.

The advantages of the fixed bed reactor are as follows: (1) the gas flow in the fixed bed is close to the push flow. The fluid and the catalyst can be contacted effectively, beneficial to achieve high conversion and selectivity. (2) the rate of chemical reaction is fast. A larger production capacity can be obtained with less catalyst and a smaller reactor volume. (3) the advantages of simple structure and low mechanical wear, so

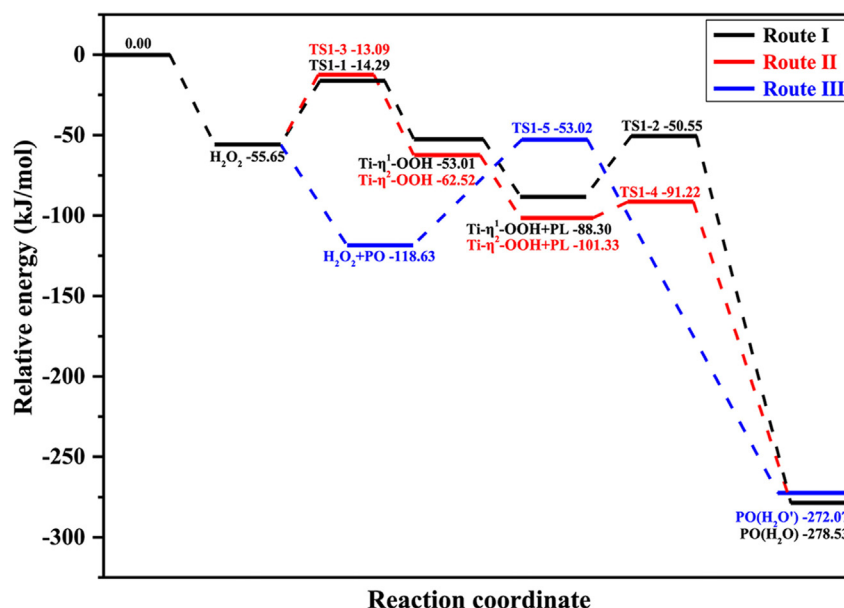


Figure 22. Mechanism of propylene epoxidation catalyzed by TS-1

Relative energy profiles for three routes of propylene epoxidation over TS-1 catalyst with bipodal Ti site at 313 K, together with the structures of reactant, transition state, intermediate, and product. Route I, the “two-step” mechanism via $\text{Ti-}\eta^1\text{-OOH}$ intermediate. Route II, the “two-step” mechanism via $\text{Ti-}\eta^2\text{-OOH}$ intermediate. Route III, the “one-step” mechanism. The energy unit is in KJ/mol.³⁴⁰ Copyright 2023, Elsevier B.V.

suitable for precious metal catalysts. (4) the operation is simple. Suitable for operation under high temperatures and high pressure. The current industrial process still faces a number of challenges. All of the installed HPPO processes operate in fixed-bed reactors. The TS-1 catalyst must be in the form of extrusion or immobilization on a support with an inorganic binder. First, the powdered catalyst is made into a solid body at the cost of reducing the effective specific surface area of the catalyst. Compared to a highly dispersed suspended catalyst, the catalytic activity of the catalyst is reduced.³⁴⁹ Second, the presence of aluminates and transition metal oxides in the inorganic binder can enhance H_2O_2 decomposition and solvent decomposition of PO. This reduces the reactant utilization and increases the risk of the process.³⁵⁰ In addition, fixed beds are typically operated at pressures of 3 Mpa to enable the propylene to act as a liquid and overcome the bed resistance. This leads to an increase in energy consumption.^{351,352}

Benefits of the slurry reactor (Figure 23C) include simplicity of design, good heat transfer performance, online catalyst addition and removal, and reasonable interphase mass transfer rate at lower energy input compared to the fixed bed reactor. The catalyst in the slurry reactor is highly dispersed and does not require a large amount of inorganic binder or catalyst support to maintain its shape. The catalytic efficiency and reactant utilization can be improved and side reactions can be reduced by using the slurry reactor in the catalytic reaction operation. In many chemical processes, there is a trend to move away from the fixed bed reactor to the slurry reactor. However, only a few detailed studies have been carried out on the H_2O_2 epoxidation of propylene using a TS-1 catalyst in a continuous slurry reactor. The average yield of PO was found to be quite low and the reported catalytic performance was found to be inconsistent.^{345,346}

Some articles use a continuous stirred tank reactor (CSTR) for experimental research. The CSTR facilitates the quantitative study of reaction orders, including product inhibition, by ensuring its concentration throughout the catalyst bed under all feed conditions and reactant conversions.^{353,354} Commonly used reactors also include stainless steel reactors,^{76,111,222} quartz tubular reactor^{5,228,226,355} and continuous flow fixed-bed reactor.^{334,356}

CONCLUSIONS AND PERSPECTIVES

Conclusions

We have comprehensively reviewed the latest progress of propylene epoxidation catalyzed by TS-1. In the past twenty years, substantial progress has been made in the green synthesis of TS-1, designing new, practical, and highly PO-selective TS-1 catalysts for propylene epoxidation, as well as determining the mechanism and reaction pathway of epoxidation. The cost of the TS-1 was reduced by using inexpensive raw materials, including various organic templates, Si sources and Ti sources. To reduce environmental pollution during the synthesis process, new synthesis methods such as post-processing, DGC, solvent-free method and microwave-assisted are used. Synthesis strategies to construct pore hierarchies with reduced mass transfer resistance can be categorized into “*in situ*” and “*post-synthesis*” approaches. Effective strategies to improve catalyst activity include post-treatment methods and the introduction of transition metals. Advances in the techniques for structural characterization of active metal centers have helped to gain insight into the reaction mechanism. Three prominent mechanisms have been proposed for propylene epoxidation, among which the bipodal Ti mechanism has been proposed in recent years, which has attracted

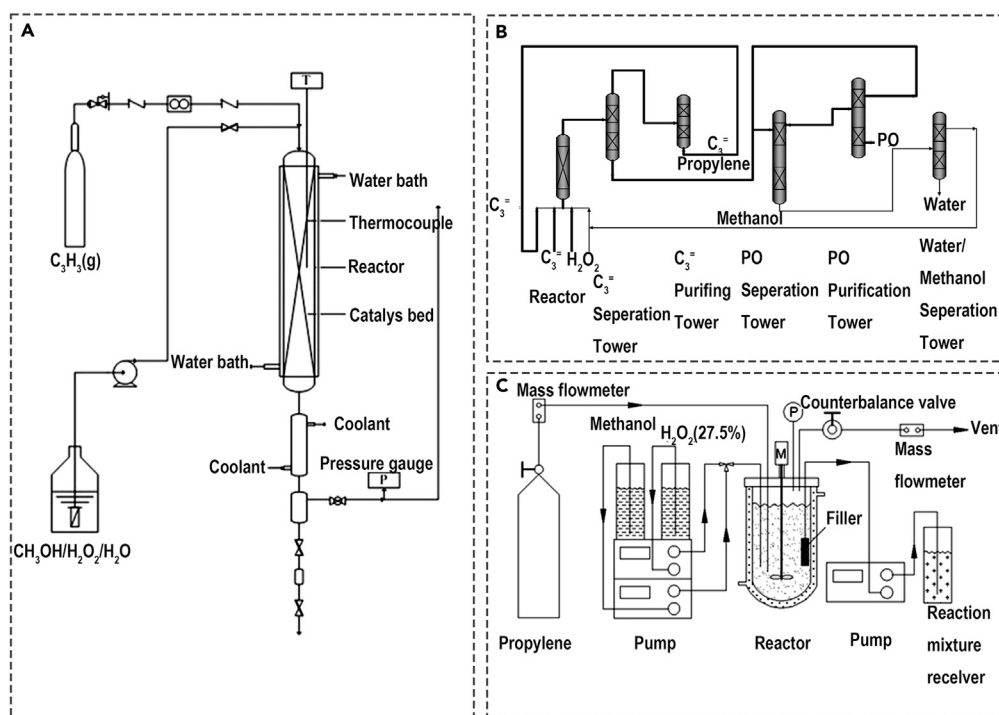


Figure 23. Schematic diagram of experimental apparatus

(A) Schematic diagram of experimental apparatus of the fixed-bed reactor.³⁴⁶ Copyright 2012, Elsevier B.V.

(B) Schematic diagram of experimental apparatus of the propylene epoxidation at 1.0 kt/a pilot scale.²⁰⁵ Copyright 2016, Elsevier B.V.

(C) Schematic diagram of experimental apparatus of the slurry reactor.³⁴⁵ Copyright 2015, American Chemical Society.

attention. Ti-containing zeolite catalysts can play an important role in the conversion of biomass, a sector that is of paramount importance in view of the growing demand for fuels and chemicals derived from renewable sources as a substitute for fossil ones. We believe that more progress will be made by continuing to accumulate synthetic knowledge, developing strong characterization and computational techniques, and exploring catalytic applications. It is expected the TS-1 catalyzed epoxidation of propylene will be more successful in the near future both in academia and in industry.

Perspectives

Despite the current strong position of zeolite in industrial catalytic applications. There are still many challenges in synthesis, application and mechanism (Figure 24) as follows:

Low cost and green synthesis of TS-1

Although much progress has been made in the preparation of TS-1, challenges still remain. At present, synthesizing TS-1 zeolite requires using an organic templating agent, and the cost is high. A template-free organic route for the synthesis of TS-1 zeolite is expected to be developed. The strong alkaline media are generally used in the industrial preparation of TS-1 zeolite. The mother liquor dissolves a large number of silica species. Synthesis of TS-1 zeolite under near-neutral conditions is necessary.

The ideal hierarchical pore architecture

Although the synthesis of hierarchical TS-1 by some mesoporous agents, non-mesoporous agents and demetallization processes has achieved great success. There are still many challenges in fine-tuning porosity, connectivity and secondary pore ordering. Finding the optimal balance between introduced mesopores, inherent microporosity, and optimal control of additional pore number, location, size distribution, and connectivity should be pursued to improve catalytic performance on zeolites. A new synthesis strategy should be developed to effectively construct an ideal hierarchical pore structure with low economic cost, low environmental impact and high versatility.

Improving the catalytic performance of TS-1

Conventional TS-1 molecular sieves need further improvement because of the spatial restriction of the internal pore structure and the restriction of acid centers in the framework. In the synthesizing procedure, inhibiting the formation of non-framework Ti species is more effective. The primary resolution is to add complexing agents, change the raw material type, and change the crystallization conditions to match the

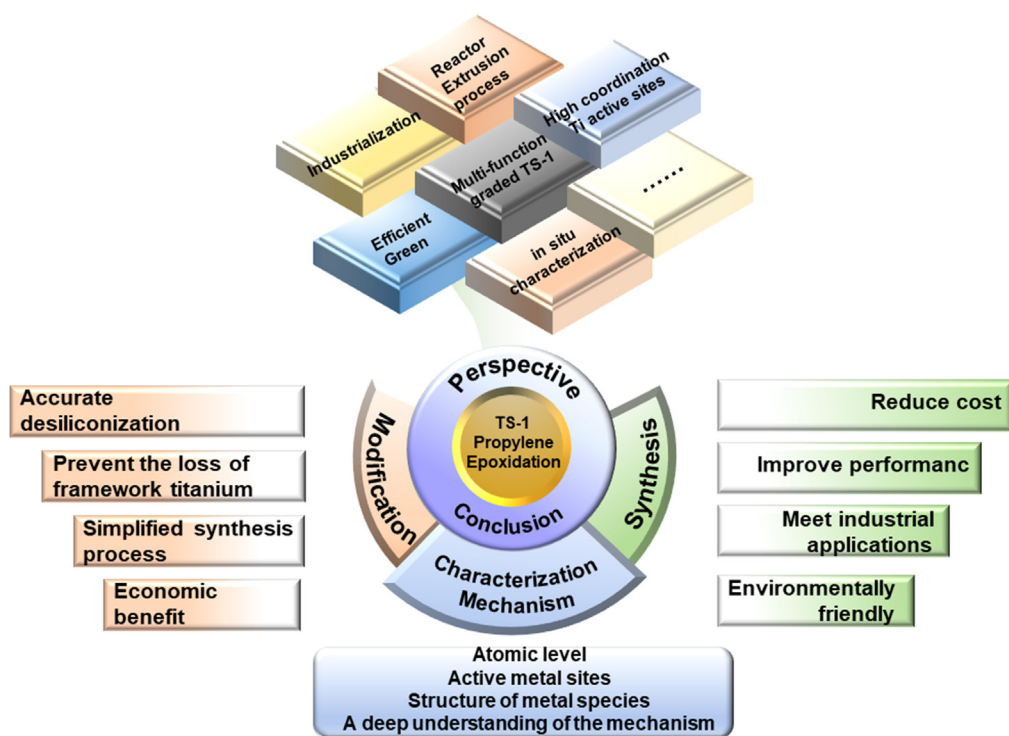


Figure 24. Conclusions and perspectives of TS-1 catalyzed propylene epoxidation

hydrolysis rate of the Si source and Ti source. There are three main methods for constructing highly active Ti sites. First, the positive charge property of the framework Ti species is enhanced through the introduction of fluorine, which has a strong ability to absorb electrons, or transition metals having empty orbitals. Second, highly coordinated Ti species can be constructed by modifying amino acids, constructing defect sites with organic amines, and microwave irradiation. Thirdly, Ti content can be increased and Ti distribution improved. Ti-rich molecular sieves are obtained through the addition of seeds, the addition of a crystallization modifier, and the modification of the crystallization mechanism. The organic template dissolution-recrystallization process can redistribute Ti. If non-framework Ti species are still present, post-treatment can passivate or remove them, but this will result in inaccurate desilication and removal of some framework Ti. Simple and convenient modification means and clear regulation mechanism still need to be developed and revealed.

Elucidation of reaction mechanism

Structural characterization of metal active centers and a thorough comprehension of the reaction mechanism are two critical prerequisites for establishing structure-property relationships and preparing more efficient zeolite metal catalysts. The catalytic performance of TS-1 is commonly ascribed to the existence of isolated Ti (IV) sites, Ti vacancies and Si vacancies within the zeolite framework. Despite nearly four decades of experimental and computational studies, the structure of these active Ti (IV) sites remains elusive because of the difficulties in fully characterizing TS-1. The bipedal Ti site has not yet been the subject of extensive theoretical investigation, and the structure of the bipedal Ti (IV) site has not yet been fully elucidated. It is necessary to develop techniques to directly visualize the pore systems, including the atomic Ti sites. Rational design of efficient zeolite catalysts requires a detailed understanding of the structure and dynamics of active metal sites. For this purpose, a combination of atomic-resolution spectroscopy and microscopy appears to be an effective way for obtaining information on the structure of active metal centers. To clarify the nature of real active metal centers in catalytic processes and to study catalytic reaction mechanisms, characterization techniques must be applied *in situ* or under operating conditions, especially at the atomic or molecular level. The conversion of the active site intermediates could still not be monitored during the reaction.

Ga phase propylene epoxidation

In the past decade, the gas phase epoxidation of propylene to PO on Au catalyst has been considered to be an ideal reaction because of its energy saving and sustainable characteristics. Au/TS-1 catalyst has good catalytic performance. Electrolysis from renewable electricity can produce both H₂ and O₂. The direct epoxidation of propylene over Au/Ti catalysts may eventually replace other indirect or multistep methods for the production of PO, but low H₂ utilization and low catalyst stability are two major obstacles. Additionally, the Au/TS-1 catalyst faces some problems such as serious deactivation and low PO selectivity. At present, the development of layered and structured TS-1 scaffolds to

improve the ability of mass transfer has become an effective strategy to restrain the problem of rapid inactivation. Ensuring that Au nanoparticles are highly dispersed, constructing hydrophobic scaffolds and improving their stability are essential for catalyst design. In addition, the design of new catalytic systems will contribute to the improvement of catalytic performance.

The future prospect of propylene epoxidation

Methanol is the optimum solvent and carrier for H₂O₂ in the commercial HPPO process. Methanol also has an important function in the activation of H₂O₂. Nevertheless, the use of methanol as a solvent accelerated the solvolysis of PO, which substantially decreased the selectivity. The complexity of the process would be further increased by the purification and recycling of the methanol solvent. Toxic contaminants from the solvent recycling process inhibit and deactivate the performance of the TS-1 catalyst. The use of multiple reactors and the need for a separate hydrogen peroxide production plant are the main disadvantages of HPPO. Thus, H₂O₂ epoxidation without solvent or carrier is highly desirable. Gas-phase epoxidation is a good approach for solvent-free epoxidation. Using the H₂/O₂ non-equilibrium plasma method, H₂O₂ vapor has been directly synthesized. However, the H₂O₂ utilization ratio in the gaseous epoxidation process is relatively less than the commercial requirement.

ACKNOWLEDGMENTS

Financial support from the National Natural Science Foundation of China (no. 22279118) is acknowledged.

AUTHOR CONTRIBUTIONS

J.Y.: investigation, visualization, writing – original draft, writing – review and editing, formal analysis. S.L.: writing – review and editing, formal analysis. Y.L.: investigation, writing – review and editing, visualization. L.Z.: formal analysis. Ha.W.: investigation, visualization. Hu.W.: investigation, visualization, formal analysis. R.S.: investigation, visualization. X.W.: formal analysis. J.J.: formal analysis. B.L.: visualization, formal analysis, supervision, funding acquisition, conceptualization.

DECLARATION OF INTERESTS

The authors declare no conflicts of interest.

REFERENCES

- Nijhuis, T.A., Huizinga, B.J., Makkee, M., and Moulijn, J.A. (1999). Direct Epoxidation of Propene Using Gold Dispersed on TS-1 and Other Titanium-Containing Supports. *Ind. Eng. Chem. Res.* 38, 884–891. <https://doi.org/10.1021/ie980494x>.
- Nijhuis, T.A., Makkee, M., Moulijn, J.A., and Weckhuysen, B.M. (2006). The Production of Propene Oxide: Catalytic Processes and Recent Developments. *Ind. Eng. Chem. Res.* 45, 3447–3459. <https://doi.org/10.1021/ie0513090>.
- Nijhuis, T.A., Makkee, M., Moulijn, J.A., and Weckhuysen, B.M. (2010). Reactivity of TiO₂ Rutile and Anatase Surfaces toward Nitroaromatics. *Ind. Eng. Chem. Res.* 45, 3447–3459. <https://doi.org/10.1021/ie0513090>.
- Feng, X., Lin, D., Chen, D., and Yang, C. (2021). Rationally constructed Ti sites of TS-1 for epoxidation reactions. *Sci. Bull.* 66, 1945–1949. <https://doi.org/10.1016/j.scib.2021.05.020>.
- Kapil, N., Weissenberger, T., Cardinale, F., Trogadas, P., Nijhuis, T.A., Nigra, M.M., and Coppens, M.O. (2021). Precisely Engineered Supported Gold Clusters as a Stable Catalyst for Propylene Epoxidation. *Angew. Chem. Int. Ed.* 60, 18185–18193. <https://doi.org/10.1002/anie.202104952>.
- Ghannadzadeh, A., and Tarighaleslami, A.H. (2022). Exergy-aided environmental life cycle assessment of propylene oxide production. *Int. J. Life Cycle Assess.* 27, 20–37. <https://doi.org/10.1007/s11367-021-01969-z>.
- Khatib, S.J., and Oyama, S.T. (2015). Direct Oxidation of Propylene to Propylene Oxide with Molecular Oxygen: A Review. *Catal. Rev.* 57, 306–344. <https://doi.org/10.1080/01614940.2015.1041849>.
- Huang, J., and Haruta, M. (2012). Gas-phase propene epoxidation over coinage metal catalysts. *Res. Chem. Intermed.* 38, 1–24. <https://doi.org/10.1007/s11164-011-0424-6>.
- Li, Z.M., and Linton, O. (2022). A ReMeDI for Microstructure Noise. *Econometrica* 90, 367–389. <https://doi.org/10.3982/ECTA17505>.
- Nguyen, V.-H., Nguyen, B.-S., Hu, C., Sharma, A., Vo, D.-V.N., Jin, Z., Shokouhimehr, M., Jang, H.W., Kim, S.Y., and Le, Q.V. (2020). Advances in Designing Au Nanoparticles for Catalytic Epoxidation of Propylene with H₂ and O₂. *Catalysts* 10, 442. <https://doi.org/10.3390/catal10040442>.
- Russo, V., Tesser, R., Santacesaria, E., and Di Serio, M. (2013). Chemical and Technical Aspects of Propene Oxide Production via Hydrogen Peroxide (HPPO Process). *Ind. Eng. Chem. Res.* 52, 1168–1178. <https://doi.org/10.1021/ie3023862>.
- Farinas, E.T., Alcalde, M., and Arnold, F. (2004). Alkene epoxidation catalyzed by cytochrome P450 BM-3 139-3. *Tetrahedron* 60, 525–528. <https://doi.org/10.1016/j.tet.2003.10.099>.
- Amano, F., and Tanaka, T. (2005). Modification of photocatalytic center for photo-epoxidation of propylene by rubidium ion addition to V₂O₅/SiO₂. *Catal. Commun.* 6, 269–273. <https://doi.org/10.1016/j.catcom.2005.01.007>.
- Nguyen, V.-H., Lin, S.D., and Wu, J.C.-S. (2015). Synergistic photo-epoxidation of propylene over V Ti/MCM-41 mesoporous photocatalysts. *J. Catal.* 331, 217–227. <https://doi.org/10.1016/j.jcat.2015.09.001>.
- Nguyen, V.-H., Lin, S.D., Wu, J.C.-S., and Bai, H. (2014). Artificial sunlight and ultraviolet light induced photo-epoxidation of propylene over V-Ti/MCM-41 photocatalyst. *Beilstein J. Nanotechnol.* 5, 566–576. <https://doi.org/10.3762/bjnano.5.67>.
- Nguyen, V.-H., Chan, H.-Y., and Wu, J.C.S. (2013). Synthesis, characterization and photo-epoxidation performance of Au-loaded photocatalysts. *J. Chem. Sci.* 125, 859–867. <https://doi.org/10.1007/s12039-013-0449-z>.
- Nguyen, V.-H., Wu, J.C., and Bai, H. (2013). Temperature effect on the photo-epoxidation of propylene over V-Ti/MCM-41 photocatalyst. *Catal. Commun.* 33, 57–60. <https://doi.org/10.1016/j.catcom.2012.12.024>.
- Nguyen, V.-H., Chan, H.-Y., Wu, J.C., and Bai, H. (2012). Direct gas-phase photocatalytic epoxidation of propylene with molecular oxygen by photocatalysts. *Chem. Eng. J.* 179, 285–294. <https://doi.org/10.1016/j.cej.2011.11.003>.
- Goodridge, F., Harrison, S., and Plimley, R.E. (1986). The electrochemical production of propylene oxide. *J. Electroanal. Chem. Interfacial Electrochem.* 214, 283–293. [https://doi.org/10.1016/0022-0728\(86\)80103-6](https://doi.org/10.1016/0022-0728(86)80103-6).
- Hayashi, T., Tanaka, K., and Haruta, M. (1998). Selective Vapor-Phase Epoxidation of Propylene over Au/TiO₂ Catalysts in the Presence of Oxygen and Hydrogen. *J. Catal.* 178, 566–575. <https://doi.org/10.1006/jcat.1998.2157>.
- Huybrechts, D.R.C., Bruycker, L.D., and Jacobs, P.A. (1990). Oxyfunctionalization of

- alkanes with hydrogen peroxide on titanium silicalite. *ChemInform* 345, 240–242. <https://doi.org/10.1002/chin.1990046113>.
22. Tatsumi, T., Nakamura, M., Negishi, S., and Tominaga, H.o. (1990). Shape-selective Oxidation of Alkanes with H₂O₂ catalysed by Titanosilicate. *J. Chem. Soc. Chem. Commun.* 2, 476. <https://doi.org/10.1039/c39900000476>.
23. Li, C., Xiong, G., Xin, Q., Liu, J., Ying, P., Feng, Z., Li, J., Yang, W., Wang, Y., Wang, G., et al. (1999). UV Resonance Raman Spectroscopic Identification of Titanium Atoms in the Framework of TS-1 Zeolite. *Angew. Chem. Int. Ed.* 38, 2220–2222. [https://doi.org/10.1002/\(SICI\)1521-3773\(19990802\)38:15<2220::AID-ANIE2220>3.0.CO;2-G](https://doi.org/10.1002/(SICI)1521-3773(19990802)38:15<2220::AID-ANIE2220>3.0.CO;2-G).
24. Taramasso, M., Perego, G., and Notari, B. (1983). Preparation of porous crystalline synthetic materials comprised of silicon and titanium oxides. US4410501 A.
25. Wang, X., Zhang, X., Wang, Y., Liu, H., Qiu, J., Wang, J., Han, W., and Yeung, K.L. (2011). Performance of TS-1-Coated Structured Packing Materials for Styrene Oxidation Reaction. *ACS Catal.* 1, 437–445. <https://doi.org/10.1021/cs1001509>.
26. Kuwahara, Y., Nishizawa, K., Nakajima, T., Kamegawa, T., Mori, K., and Yamashita, H. (2011). Enhanced Catalytic Activity on Titanosilicate Molecular Sieves Controlled by Cation- π Interactions. *J. Am. Chem. Soc.* 133, 12462–12465. <https://doi.org/10.1021/ja205699d>.
27. Hutchings, G.J., Lee, D.F., and Minihan, A.R. (1995). Epoxidation of allyl alcohol to glycidol using titanium silicalite TS-1: effect of the method of preparation. *Catal. Lett.* 33, 369–385. <https://doi.org/10.1007/BF00814239>.
28. Gallot, J.E., Kapoor, M.P., and Kaliaguine, S. (1998). Kinetics of 2-hexanol and 3-hexanol oxidation reaction over TS-1 catalysts. *AIChE J.* 44, 1438–1454. <https://doi.org/10.1002/aic.690440621>.
29. Shen, C., Wang, Y.J., Xu, J.H., and Luo, G.S. (2015). Synthesis of TS-1 on porous glass beads for catalytic oxidative desulfurization. *Chem. Eng. J.* 259, 552–561. <https://doi.org/10.1016/j.cej.2014.08.027>.
30. Shan, Z., Lu, Z., Wang, L., Zhou, C., Ren, L., Zhang, L., Meng, X., Ma, S., and Xiao, F.-S. (2010). Stable Bulky Particles Formed by TS-1 Zeolite Nanocrystals in the Presence of H₂O₂. *ChemCatChem* 2, 407–412. <https://doi.org/10.1002/cctc.200900312>.
31. Kerton, O.J., McMorn, P., Bethell, D., King, F., Hancock, F., Burrows, A., Kiely, C.J., Ellwood, S., and Hutchings, G. (2005). Effect of structure of the redox molecular sieve TS-1 on the oxidation of phenol, crotyl alcohol and norbornylene. *Phys. Chem. Chem. Phys.* 7, 2671–2678. <https://doi.org/10.1039/b503241e>.
32. Russo, V., Tesser, R., Santacesaria, E., and Di Serio, M. (2014). Kinetics of Propene Oxide Production via Hydrogen Peroxide with TS-1. *Ind. Eng. Chem. Res.* 53, 6274–6287. <https://doi.org/10.1021/ie404271k>.
33. Nemeth, L., and Bare, S.R. (2014). Science and Technology of Framework Metal-Containing Zeotype Catalysts. In *Advances in Catalysis* (Elsevier), pp. 1–97. <https://doi.org/10.1016/B978-0-12-800127-1.00001-1>.
34. Huybrechts, D.R.C., Buskens, P.L., and Jacobs, P.A. (1992). Physicochemical and catalytic properties of titanium silicalites. *J. Mol. Catal.* 71, 129–147. [https://doi.org/10.1016/0304-5102\(92\)80012-6](https://doi.org/10.1016/0304-5102(92)80012-6).
35. Bengoa, J.F., Gallegos, N.G., Marchetti, S.G., Alvarez, A.M., Cagnoli, M.V., and Yeramian, A. (1998). Influence of TS-1 structural properties and operation conditions on benzene catalytic oxidation with H₂O₂. *Microporous Mesoporous Mater.* 24, 163–172. [https://doi.org/10.1016/S1387-1811\(98\)00157-7](https://doi.org/10.1016/S1387-1811(98)00157-7).
36. Miyake, K., Ono, K., Nakai, M., Hirota, Y., Uchida, Y., Tanaka, S., Miyamoto, M., and Nishiyama, N. (2017). Solvent- and OSDA-Free Synthesis of ZSM-5 Assisted by Mechanochemical and Vapor Treatments. *ChemistrySelect* 2, 7651–7653. <https://doi.org/10.1002/slct.201701593>.
37. Notari, B. (1996). Microporous Crystalline Titanium Silicates. In *Advances in Catalysis* (Elsevier), pp. 253–334. [https://doi.org/10.1016/S0360-0564\(08\)60042-5](https://doi.org/10.1016/S0360-0564(08)60042-5).
38. Karge, H.G., Hunger, M., and Beyer, H.K. (1999). Characterization of zeolites e infrared and nuclear magnetic resonance spectroscopy and X-ray diffraction. *ChemInform* 30. <https://doi.org/10.1002/chin.199952243>.
39. Thangaraj, A., Eapen, M.J., Sivasanker, S., and Ratnasamy, P. (1992). Studies on the synthesis of titanium silicalite, TS-1. *Zeolites* 12, 943–950. [https://doi.org/10.1016/0144-2449\(92\)90159-M](https://doi.org/10.1016/0144-2449(92)90159-M).
40. Chu, C.T.W., and Chang, C.D. (1985). Isomorphous substitution in zeolite frameworks. 1. Acidity of surface hydroxyls in [B]-[Fe]-[Ga]- and [Al]-ZSM-5. *J. Phys. Chem.* 89, 1569–1571. <https://doi.org/10.1021/j100255a005>.
41. Prech, J. (2018). Catalytic performance of advanced titanosilicate selective oxidation catalysts – a review. *Catal. Rev.* 60, 71–131. <https://doi.org/10.1080/01614940.2017.1389111>.
42. Cheng, W., Jiang, Y., Xu, X., Wang, Y., Lin, K., and Pescarmona, P.P. (2016). Easily recoverable titanosilicate zeolite beads with hierarchical porosity: Preparation and application as oxidation catalysts. *J. Catal.* 333, 139–148. <https://doi.org/10.1016/j.jcat.2015.09.017>.
43. Wang, B., Lin, M., Zhu, B., Peng, X., Xu, G., and Shu, X. (2016). The synthesis, characterization and catalytic activity of the hierarchical TS-1 with the intracrystalline voids and grooves. *Catal. Commun.* 75, 69–73. <https://doi.org/10.1016/j.catcom.2015.12.007>.
44. Zhu, Q., Liang, M., Yan, W., and Ma, W. (2019). Effective hierarchization of TS-1 and its catalytic performance in propene epoxidation. *Microporous Mesoporous Mater.* 278, 307–313. <https://doi.org/10.1016/j.micromeso.2018.12.004>.
45. Wang, J., Xu, L., Zhang, K., Peng, H., Wu, H., Jiang, J.g., Liu, Y., and Wu, P. (2012). Multilayer structured MFI-type titanosilicate: Synthesis and catalytic properties in selective epoxidation of bulky molecules. *J. Catal.* 288, 16–23. <https://doi.org/10.1016/j.jcat.2011.12.023>.
46. Lin, J., Xin, F., Yang, L., and Zhuang, Z. (2014). Synthesis, characterization of hierarchical TS-1 and its catalytic performance for cyclohexanone ammoxidation. *Catal. Commun.* 45, 104–108. <https://doi.org/10.1016/j.catcom.2013.11.005>.
47. Lin, J., Yang, T., Lin, C., and Sun, J. (2018). Hierarchical MFI zeolite synthesized via regulating the kinetic of dissolution-recrystallization and their catalytic properties. *Catal. Commun.* 115, 82–86. <https://doi.org/10.1016/j.catcom.2018.07.006>.
48. Adedigba, A.-L., Sankar, G., Catlow, C.R.A., Du, Y., Xi, S., and Borgna, A. (2017). On the synthesis and performance of hierarchical nanoporous TS-1 catalysts. *Microporous Mesoporous Mater.* 244, 83–92. <https://doi.org/10.1016/j.micromeso.2017.02.048>.
49. Tosheva, L., and Valtchev, V.P. (2005). Nanozeolites: Synthesis, Crystallization Mechanism, and Applications. *Chem. Mater.* 17, 2494–2513. <https://doi.org/10.1021/cm047908z>.
50. Qin, Z., Cychosz, K.A., Melinte, G., El Siblani, H., Gilson, J.-P., Thommes, M., Fernandez, C., Mintova, S., Ersen, O., and Valtchev, V. (2017). Opening the Cages of Faujasite-Type Zeolite. *J. Am. Chem. Soc.* 139, 17273–17276. <https://doi.org/10.1021/jacs.7b10316>.
51. Awala, H., Gilson, J.-P., Retoux, R., Boullay, P., Goupil, J.-M., Valtchev, V., and Mintova, S. (2015). Template-free nanosized faujasite-type zeolites. *Nat. Mater.* 14, 447–451. <https://doi.org/10.1038/nmat4173>.
52. Zhou, H., Yi, X., Hui, Y., Wang, L., Chen, W., Qin, Y., Wang, M., Ma, J., Chu, X., Wang, Y., et al. (2021). Isolated boron in zeolite for oxidative dehydrogenation of propane. *Science* 372, 76–80. <https://doi.org/10.1126/science.abe7935>.
53. Thangaraj, A., and Sivasanker, S. (1992). An improved method for TS-1 synthesis: 29Si NMR studies. *J. Chem. Soc. Chem. Commun.* 123, 123. <https://doi.org/10.1039/c39920000123>.
54. Keshavaraja, A., Ramaswamy, V., Soni, H.S., Ramaswamy, A.V., Ratnasamy, P., and Catal, J. (1995). Synthesis, Characterization, and Catalytic Properties of Micro-Mesoporous. *J. Catal.* 157, 501–511.
55. Thangaraj, A. (1991). Catalytic properties of crystalline titanium silicalites II. Hydroxylation of phenol with hydrogen peroxide over TS-1 zeolites. *J. Catal.* 131, 294–297. [https://doi.org/10.1016/0021-9517\(91\)90347-7](https://doi.org/10.1016/0021-9517(91)90347-7).
56. Tuel, A., and Taa[^]rit, Y.B. (1994). Influence of the nature of silicon and titanium alkoxides on the incorporation of titanium in TS-1. *Appl. Catal. Gen.* 110, 137–151. [https://doi.org/10.1016/0926-860X\(94\)80112-6](https://doi.org/10.1016/0926-860X(94)80112-6).
57. Thangaraj, A., Kumar, R., and Ratnasamy, P. (1990). Direct catalytic hydroxylation of benzene with hydrogen peroxide over titanium-silicate zeolites. *Appl. Catal.* 57, L1–L3. [https://doi.org/10.1016/S0166-9834\(00\)80718-6](https://doi.org/10.1016/S0166-9834(00)80718-6).
58. Fan, W., Duan, R.-G., Yokoi, T., Wu, P., Kubota, Y., and Tatsumi, T. (2008). Synthesis, Crystallization Mechanism, and Catalytic Properties of Titanium-Rich TS-1 Free of Extraframework Titanium Species. *J. Am. Chem. Soc.* 130, 10150–10164. <https://doi.org/10.1021/ja7100399>.
59. Zhang, T., Zuo, Y., Liu, M., Song, C., and Guo, X. (2016). Synthesis of Titanium Silicalite-1 with High Catalytic Performance for 1-Butene Epoxidation by Eliminating the Extraframework Ti. *ACS Omega* 1, 1034–1040. <https://doi.org/10.1021/acsomega.6b00266>.
60. Wang, J., Wang, Y., Tatsumi, T., and Zhao, Y. (2016). Anionic polymer as a quasi-neutral medium for low-cost synthesis of

- titanosilicate molecular sieves in the presence of high-concentration alkali metal ions. *J. Catal.* 338, 321–328. <https://doi.org/10.1016/j.jcat.2016.03.027>.
61. Li, M., Zhai, Y., Zhang, X., Wang, F., Lv, G., Rosine, A., Li, M., Zhang, Q., and Liu, Y. (2022). $(\text{NH}_4)_2\text{SO}_4$ -assisted synthesis of thin-walled Ti-rich hollow titanium silicalite-1 zeolite for 1-hexene epoxidation. *Microporous Mesoporous Mater.* 331, 111655. <https://doi.org/10.1016/j.micromeso.2021.111655>.
 62. Zuo, Y., Chen, Y., Li, T., Yu, J., Yang, H., Liu, M., and Guo, X. (2022). Bulky macroporous titanium silicalite-1 free of extraframework titanium for phenol hydroxylation. *Microporous Mesoporous Mater.* 336, 111884. <https://doi.org/10.1016/j.micromeso.2022.111884>.
 63. Song, X., Yang, X., Zhang, T., Zhang, H., Zhang, Q., Hu, D., Chang, X., Li, Y., Chen, Z., Jia, M., et al. (2020). Controlling the Morphology and Titanium Coordination States of TS-1 Zeolites by Crystal Growth Modifier. *Inorg. Chem.* 59, 13201–13210. <https://doi.org/10.1021/acs.inorgchem.0c01518>.
 64. Zhang, J., Shi, H., Song, Y., Xu, W., Meng, X., and Li, J. (2021). High-efficiency synthesis of enhanced-titanium and anatase-free TS-1 zeolite by using a crystallization modifier. *Inorg. Chem. Front.* 8, 3077–3084. <https://doi.org/10.1039/D1QI00311A>.
 65. Zhang, J., Bai, R., Zhou, Y., Chen, Z., Zhang, P., Li, J., and Yu, J. (2022). Impact of a polymer modifier on directing the non-classical crystallization pathway of TS-1 zeolite: accelerating nucleation and enriching active sites. *Chem. Sci.* 13, 13006–13014. <https://doi.org/10.1039/D2SC04544C>.
 66. Li, M., Shen, X., Liu, M., and Lu, J. (2021). Synthesis TS-1 nanozelites via L-lysine assisted route for hydroxylation of Benzene. *Mol. Catal.* 513, 111779. <https://doi.org/10.1016/j.mcat.2021.111779>.
 67. Alba-Rubio, A.C., Fierro, J.L.G., León-Reina, L., Mariscal, R., Dumesic, J.A., and López Granados, M. (2017). Oxidation of furfural in aqueous H_2O_2 catalysed by titanium silicalite: Deactivation processes and role of extraframework Ti oxides. *Appl. Catal. B Environ.* 202, 269–280. <https://doi.org/10.1016/j.apcatb.2016.09.025>.
 68. Wang, Y., Li, L., Bai, R., Gao, S., Feng, Z., Zhang, Q., and Yu, J. (2021). Amino acid-assisted synthesis of TS-1 zeolites containing highly catalytically active TiO_6 species. *Chin. J. Catal.* 42, 2189–2196. [https://doi.org/10.1016/S1872-2067\(21\)63882-2](https://doi.org/10.1016/S1872-2067(21)63882-2).
 69. Xing, J., Yuan, D., Liu, H., Tong, Y., Xu, Y., and Liu, Z. (2021). Synthesis of TS-1 zeolites from a polymer containing titanium and silicon. *J. Mater. Chem. A* 9, 6205–6213. <https://doi.org/10.1039/D0TA11876A>.
 70. Wang, J., Zhao, Y., Yokoi, T., Kondo, J.N., and Tatsumi, T. (2014). High-Performance Titanosilicate Catalyst Obtained through Combination of Liquid-Phase and Solid-Phase Transformation Mechanisms. *ChemCatChem* 6, 2719–2726. <https://doi.org/10.1002/cctc.201402239>.
 71. Zhang, T., Chen, X., Chen, G., Chen, M., Bai, R., Jia, M., and Yu, J. (2018). Synthesis of anatase-free nano-sized hierarchical TS-1 zeolites and their excellent catalytic performance in alkene epoxidation. *J. Mater. Chem. A* 6, 9473–9479. <https://doi.org/10.1039/C8TA01439F>.
 72. Bai, R., Sun, Q., Song, Y., Wang, N., Zhang, T., Wang, F., Zou, Y., Feng, Z., Miao, S., and Yu, J. (2018). Intermediate-crystallization promoted catalytic activity of titanosilicate zeolites. *J. Mater. Chem. A* 6, 8757–8762. <https://doi.org/10.1039/C8TA01960F>.
 73. Lin, D., Zhang, Q., Qin, Z., Li, Q., Feng, X., Song, Z., Cai, Z., Liu, Y., Chen, X., Chen, D., et al. (2021). Reversing Titanium Oligomer Formation towards High-Efficiency and Green Synthesis of Titanium-Containing Molecular Sieves. *Angew. Chem. Int. Ed.* 60, 3443–3448. <https://doi.org/10.1002/anie.202011821>.
 74. Liu, C., Huang, J., Sun, D., Zhou, Y., Jing, X., Du, M., Wang, H., and Li, Q. (2013). Anatase type extra-framework titanium in TS-1: A vital factor influencing the catalytic activity toward styrene epoxidation. *Appl. Catal. Gen.* 459, 1–7. <https://doi.org/10.1016/j.apcata.2013.03.013>.
 75. Müller, U., and Steck, W. (1994). Ammonium-Based Alkaline-Free Synthesis of MFI-Type Boron- and Titanium Zeolites. In *Studies in Surface Science and Catalysis* (Elsevier), pp. 203–210. [https://doi.org/10.1016/S0167-2991\(08\)64115-4](https://doi.org/10.1016/S0167-2991(08)64115-4).
 76. Huang, M., Wen, Y., Wei, H., Zong, L., Gao, X., Wu, K., Wang, X., and Liu, M. (2021). The Clean Synthesis of Small-Particle TS-1 with High-Content Framework Ti by Using NH_4HCO_3 and Suspended Seeds as an Assistant. *ACS Omega* 6, 13015–13023. <https://doi.org/10.1021/acsomega.1c00412>.
 77. Zuo, Y., Wang, X., and Guo, X. (2011). Synthesis of Titanium Silicalite-1 with Small Crystal Size by Using Mother Liquid of Titanium Silicalite-1 As Seed. *Ind. Eng. Chem. Res.* 50, 8485–8491. <https://doi.org/10.1021/ie200281v>.
 78. Liu, M., Li, J., Chen, X., Song, J., Wei, W., Wen, Y., and Wang, X. (2021). Preparation of anatase-free hierarchical titanosilicalite-1 in favor of allyl chloride epoxidation. *Microporous Mesoporous Mater.* 326, 111388. <https://doi.org/10.1016/j.micromeso.2021.111388>.
 79. Yu, S., Sun, M.-H., Wang, Y.-Y., Liu, Z., Lyu, J.-M., Wang, Y.-L., Hu, Z.-Y., Li, Y., Chen, L.-H., and Su, B.-L. (2023). Hierarchical Titanium Silicalite-1 Zeolites Featuring an Ordered Macro-Meso-Microporosity for Efficient Epoxidations. *Cryst. Growth Des.* 23, 2818–2825. <https://doi.org/10.1021/acs.cgd.3c00014>.
 80. Tang, G., Li, Y., Yang, Z., Wang, Y., Li, G., Wang, Y., Chai, Y.-M., and Liu, C. (2023). Preparation of Micron-Sized TS-1 Spherical Membrane Catalysts and Their Performance in the Epoxidation of Chloropropene. *ACS Omega* 8, 19099–19108. <https://doi.org/10.1021/acsomega.3c02538>.
 81. Liu, Y., Zhao, C., Sun, B., Zhu, H., Shi, N., and Xu, W. (2023). TS-1 with Abundant Micropore Channel-Supported Au Catalysts toward Improved Performance in Gas-Phase Epoxidation of Propylene. *ACS Sustain. Chem. Eng.* 11, 7042–7052. <https://doi.org/10.1021/acssuschemeng.3c00018>.
 82. Xue, F., Qin, R., Zhu, R., and Zhou, X. (2022). Sn species modified mesoporous zeolite TS-1 with oxygen vacancy for enzyme-free electrochemical H_2O_2 detecting. *Dalton Trans.* 51, 18169–18175. <https://doi.org/10.1039/D2DT02926J>.
 83. Ji, Y., Zuo, Y., Liu, M., Wang, F., Song, C., and Guo, X. (2021). From nano aggregates to nano plates: The roles of gelatin in the crystallization of titanium silicate-1. *Microporous Mesoporous Mater.* 321, 111100. <https://doi.org/10.1016/j.micromeso.2021.111100>.
 84. Zhang, Q., Gao, S., and Yu, J. (2023). Metal Sites in Zeolites: Synthesis, Characterization, and Catalysis. *Chem. Rev.* 123, 6039–6106. <https://doi.org/10.1021/acs.chemrev.2c00315>.
 85. Wu, Q., Xu, C., Zhu, L., Meng, X., and Xiao, F.-S. (2022). Recent strategies for synthesis of metalloilicate zeolites. *Catal. Today* 390–391, 2–11. <https://doi.org/10.1016/j.cattod.2022.01.020>.
 86. Zhang, L., Zhu, X., Wang, X., and Shi, C. (2021). The synthesis of pure and uniform nanosized TS-1 crystals with a high titanium content and a high space-time yield. *Inorg. Chem. Front.* 8, 5260–5269. <https://doi.org/10.1039/D1QI01022K>.
 87. Kraushaar, B., and Van Hooff, J.H.C. (1988). A new method for the preparation of titanium-silicalite (TS-1). *Catal. Lett.* 1, 81–84. <https://doi.org/10.1007/BF00772769>.
 88. Wang, S., Yang, Q., Wu, Z., Li, M., Lu, J., Tan, Z., and Li, C. (2001). Epoxidation of cyclohexene on Ti/SiO_2 catalysts prepared by chemical grafting TiCl_4 on deboronated silica xerogel. *J. Mol. Catal. Chem.* 172, 219–225. [https://doi.org/10.1016/S1381-1169\(01\)00119-4](https://doi.org/10.1016/S1381-1169(01)00119-4).
 89. Bregante, D.T., and Flaherty, D.W. (2017). Periodic Trends in Olefin Epoxidation over Group IV and V Framework-Substituted Zeolite Catalysts: Akinetic and Spectroscopic Study. *J. Am. Chem. Soc.* 139, 6888–6898.
 90. Pang, T., Yang, X., Yuan, C., Elzatahy, A.A., Alghamdi, A., He, X., Cheng, X., and Deng, Y. (2021). Recent advance in synthesis and application of heteroatom zeolites. *Chin. Chem. Lett.* 32, 328–338. <https://doi.org/10.1016/j.ccl.2020.04.018>.
 91. Rigutto, M.S., de Ruiter, R., Niederer, J.P.M., and van Bekkum, H. (1994). Titanium-Containing Large Pore Molecular Sieves from Boron-Beta: Preparation, Characterization and Catalysis. In *Studies in Surface Science and Catalysis* (Elsevier), pp. 2245–2252. [https://doi.org/10.1016/S0167-2991\(08\)63787-8](https://doi.org/10.1016/S0167-2991(08)63787-8).
 92. Tang, B., Dai, W., Sun, X., Guan, N., Li, L., and Hunger, M. (2014). A procedure for the preparation of Ti-Beta zeolites for catalytic epoxidation with hydrogen peroxide. *Green Chem.* 16, 2281–2291. <https://doi.org/10.1039/C3GC42534G>.
 93. Gao, J., Liu, M., Wang, X., and Guo, X. (2010). Characterization of Ti-ZSM-5 Prepared by Isomorphous Substitution of B-ZSM-5 with TiCl_4 and Its Performance in the Hydroxylation of Phenol. *Ind. Eng. Chem. Res.* 49, 2194–2199. <https://doi.org/10.1021/ie901360y>.
 94. Yan, M., Jin, F., Ding, Y., Wu, G., Chen, R., Wang, L., and Yan, Y. (2019). Synthesis of Titanium-Incorporated MWW Zeolite by Sequential Deboronation and Atom-Planting Treatment of ERB-1 as an Epoxidation Catalyst. *Ind. Eng. Chem. Res.* 58, 4764–4773. <https://doi.org/10.1021/acs.iecr.8b05836>.
 95. Wang, T., Jin, F., Yi, X., Wu, G., and Zheng, A. (2021). Atom-planting synthesis of MCM-36 catalyst to investigate the influence of pore structure and titanium coordination

- state on epoxidation activity. *Microporous Mesoporous Mater.* 310, 110645. <https://doi.org/10.1016/j.micromeso.2020.110645>.
96. Xu, Y., Jin, F., Wu, G., Wang, T., Zhang, J., and Chen, Y. (2022). Effect of Surface Polarity of Titanium-Loaded ERB-1 Catalyst on Epoxidation and Ammoxidation. *Catal. Lett.* 153, 260–270. <https://doi.org/10.1007/s10562-022-03954-z>.
97. Matsukata, M., Ogura, M., Osaki, T., Nomura, M., and Kikuchi, E. (1999). Conversion of dry gel to microporous crystals in gas phase. *Topics in Catalysis* 9, 77–92. <https://doi.org/10.1023/A:1019106421183>.
98. Xu, W., Dong, J., Li, J., Li, J., and Wu, F. (1990). A novel method for the preparation of zeolite ZSM-5. *J. Chem. Soc. Chem. Commun.* 755, 755. <https://doi.org/10.1039/c39900000755>.
99. Kang, K.-K., and Rhee, H.-K. (2018). Synthesis and characterization of hierarchical titanium-containing mesoporous materials with MFI crystalline structure using the gas phase recrystallization for the improvement of olefins epoxidation activity. *Microporous Mesoporous Mater.* 257, 202–211. <https://doi.org/10.1016/j.micromeso.2017.08.040>.
100. Liu, X., Zeng, S., Wang, R., Zhang, Z., and Qiu, S. (2018). Sustainable Synthesis of Hierarchically Porous Silicalite-1 Zeolite by Steam-assisted Crystallization of Solid Raw Materials Without Secondary Templates. *Chem. Res. Chin. Univ.* 34, 350–357. <https://doi.org/10.1007/s40242-018-7400-2>.
101. Zhou, J., Hua, Z., Cui, X., Ye, Z., Cui, F., and Shi, J. (2010). Hierarchical mesoporous TS-1 zeolite: a highly active and extraordinarily stable catalyst for the selective oxidation of 2,3,6-trimethylphenol. *Chem. Commun.* 46, 4994–4996. <https://doi.org/10.1039/c0cc00499e>.
102. Wu, M., Liu, X., Wang, Y., Guo, Y., Guo, Y., and Lu, G. (2014). Synthesis and catalytic ammoxidation performance of hierarchical TS-1 prepared by steam-assisted dry gel conversion method: the effect of TPAOH amount. *J. Mater. Sci.* 49, 4341–4348. <https://doi.org/10.1007/s10853-014-8130-6>.
103. Feng, X., Sheng, N., Liu, Y., Chen, X., Chen, D., Yang, C., and Zhou, X. (2017). Simultaneously Enhanced Stability and Selectivity for Propene Epoxidation with H₂ and O₂ on Au Catalysts Supported on Nano-Crystalline Mesoporous TS-1. *ACS Catal.* 7, 2668–2675. <https://doi.org/10.1021/acscatal.6b03498>.
104. Wang, B., Zhu, Y., Han, H., Qin, Q., Zhang, Z., and Zhu, J. (2022). Preparation and Catalytic Performance in Propylene Epoxidation of Hydrophobic Hierarchical Porous TS-1 Zeolite. *Catal. Lett.* 152, 3076–3088. <https://doi.org/10.1007/s10562-021-03805-3>.
105. Du, C., Cui, N., Li, L., Hua, Z., and Shi, J. (2019). A large-surface-area TS-1 nanocatalyst: a combination of nanoscale particle sizes and hierarchical micro/mesoporous structures. *RSC Adv.* 9, 9694–9699. <https://doi.org/10.1039/C9RA00124G>.
106. Li, L., Wang, W., Huang, J., Dun, R., Yu, R., Liu, Y., and Hua, Z. (2022). Synthesis of hydrophobic nanosized hierarchical titanosilicate-1 zeolites by an alkali-etching protocol and their enhanced performance in catalytic oxidative desulfurization of fuels. *Appl. Catal. Gen.* 630, 118466. <https://doi.org/10.1016/j.apcata.2021.118466>.
107. Wang, H., Du, G., Chen, S., Su, Z., Sun, P., and Chen, T. (2022). Steam-assisted strategy to fabricate Anatase-free hierarchical titanium Silicalite-1 Single-Crystal for oxidative desulfurization. *J. Colloid Interface Sci.* 617, 32–43. <https://doi.org/10.1016/j.jcis.2022.02.121>.
108. Soekiman, C.N., Miyake, K., Hayashi, Y., Zhu, Y., Ota, M., Al-Jabri, H., Inoue, R., Hirota, Y., Uchida, Y., Tanaka, S., et al. (2020). Synthesis of titanium silicalite-1 (TS-1) zeolite with high content of Ti by a dry gel conversion method using amorphous TiO₂-SiO₂ composite with highly dispersed Ti species. *Mater. Today Chem.* 16, 100209. <https://doi.org/10.1016/j.mtchem.2019.100209>.
109. Zhang, M., Lin, Z., Huang, Q., Zhu, Y., Hu, H., and Chen, X. (2020). Green synthesis of submicron-sized Ti-rich MWW zeolite powders via a novel mechanochemical dry gel conversion in mixed steam environment. *Adv. Powder Technol.* 31, 2025–2034. <https://doi.org/10.1016/j.apt.2020.02.037>.
110. Du, Q., Guo, Y., Wu, P., Liu, H., and Chen, Y. (2019). Facile synthesis of hierarchical TS-1 zeolite without using mesopore templates and its application in deep oxidative desulfurization. *Microporous Mesoporous Mater.* 275, 61–68. <https://doi.org/10.1016/j.micromeso.2018.08.018>.
111. Li, Y., Li, Y., Zhu, G., Fan, J., Feng, X., Chai, Y., and Liu, C. (2020). Synthesis of Hierarchical TS-1 Nanocrystals with Controllable Grain Size and Mesoporosity: Enhanced Performance for Chloropropylene Epoxidation. *Ind. Eng. Chem. Res.* 59, 9364–9371. <https://doi.org/10.1021/acs.iecr.9b06490>.
112. Zhang, S., Zhang, X., Dong, L., Zhu, S., Yuan, Y., and Xu, L. (2022). *In situ* synthesis of Pt nanoparticles encapsulated in silicalite-1 zeolite via a steam-assisted dry-gel conversion method. *CrystEngComm* 24, 2697–2704. <https://doi.org/10.1039/D1CE01718G>.
113. Cho, H.J., Kim, D., Li, S., Su, D., Ma, D., and Xu, B. (2020). Molecular-Level Proximity of Metal and Acid Sites in Zeolite-Encapsulated Pt Nanoparticles for Selective Multistep Tandem Catalysis. *ACS Catal.* 10, 3340–3348. <https://doi.org/10.1021/acscatal.9b03842>.
114. Cho, H.J., Kim, D., Li, J., Su, D., and Xu, B. (2018). Zeolite-Encapsulated Pt Nanoparticles for Tandem Catalysis. *J. Am. Chem. Soc.* 140, 13514–13520. <https://doi.org/10.1021/jacs.8b09568>.
115. Cho, H.J., Kim, D., and Xu, B. (2020). Selectivity Control in Tandem Catalytic Furfural Upgrading on Zeolite-Encapsulated Pt Nanoparticles through Site and Solvent Engineering. *ACS Catal.* 10, 4770–4779. <https://doi.org/10.1021/acscatal.0c00472>.
116. Bai, R., Song, Y., Bai, R., and Yu, J. (2021). Creation of Hierarchical Titanosilicate TS-1 Zeolites. *Adv. Mater. Interfaces* 8, 2001095. <https://doi.org/10.1002/admi.202001095>.
117. Chu, P., Dwyer, F.G., and Vartuli, J.C. (1998). *Crystallization Method Employing Microwave Radiation (US Patents US4778666A)*.
118. Cundy, C.S., and Zhao, J.P. (1998). Remarkable synergy between microwave heating and the addition of seed crystals in zeolite synthesis—a suggestion verified. *Chem. Commun.* 14, 1465–1466. <https://doi.org/10.1039/a803324b>.
119. Tompsett, G.A., Conner, W.C., and Yngvesson, K.S. (2006). Microwave Synthesis of Nanoporous Materials. *Chemphyschem.* 7, 296–319. <https://doi.org/10.1002/cphc.200500449>.
120. Azzolina Jury, F., Polaert, I., Estel, L., and Pierella, L.B. (2014). Enhancement of synthesis of ZSM-11 zeolite by microwave irradiation. *Microporous Mesoporous Mater.* 198, 22–28. <https://doi.org/10.1016/j.micromeso.2014.07.006>.
121. Xu, C.-H., Jin, T., Jhung, S.H., Chang, J.-S., Hwang, J.-S., and Park, S.-E. (2006). Hydrophobicity and catalytic properties of Ti-MFI zeolites synthesized by microwave and conventional heating. *Catal. Today* 111, 366–372. <https://doi.org/10.1016/j.cattod.2005.10.063>.
122. Park, S.-E., Jiang, N., Park, S.-E., and Jiang, N. (2010). Morphological Synthesis of Zeolites. *Zeolites and Catalysis: Synthesis, Reactions and Applications*, 131. Chapter 5. <https://doi.org/10.1002/9783527630295>.
123. Hwang, Y.K., Chang, J.-S., Park, S.-E., Kim, D.S., Kwon, Y.-U., Jhung, S.H., Hwang, J.-S., and Park, M.S. (2005). Microwave Fabrication of MFI Zeolite Crystals with a Fibrous Morphology and Their Applications. *Angew. Chem. Int. Ed.* 44, 556–560. <https://doi.org/10.1002/anie.200461403>.
124. Pavel, C.C., and Schmidt, W. (2006). Generation of hierarchical pore systems in the titanosilicate ETS-10 by hydrogen peroxide treatment under microwave irradiation. *Chem. Commun.* 882, 882–884. <https://doi.org/10.1039/b515720j>.
125. Abelló, S., and Pérez-Ramírez, J. (2009). Accelerated generation of intracrystalline mesoporosity in zeolites by microwave-mediated desilication. *Phys. Chem. Chem. Phys.* 11, 2959–2963. <https://doi.org/10.1039/b819543a>.
126. Kim, S.-K., Reddy, B.M., and Park, S.-E. (2018). High-Performance Microwave Synthesized Mesoporous TS-1 Zeolite for Catalytic Oxidation of Cyclic Olefins. *Ind. Eng. Chem. Res.* 57, 3567–3574. <https://doi.org/10.1021/acs.iecr.7b04556>.
127. Cundy, C.S., Forrest, J.O., and Plaisted, R.J. (2003). Some observations on the preparation and properties of colloidal silicalites. Part I: synthesis of colloidal silicalite-1 and titanosilicalite-1 (TS-1). *Microporous Mesoporous Mater.* 66, 143–156. <https://doi.org/10.1016/j.micromeso.2003.08.021>.
128. Xu, W., Zhang, T., Bai, R., Zhang, P., and Yu, J. (2020). A one-step rapid synthesis of TS-1 zeolites with highly catalytically active mononuclear TiO₆ species. *J. Mater. Chem. A* 8, 9677–9683. <https://doi.org/10.1039/C9TA13851J>.
129. Zeng, X., Hu, X., Song, H., Xia, G., Shen, Z.-Y., Yu, R., and Moskovits, M. (2021). Microwave synthesis of zeolites and their related applications. *Microporous Mesoporous Mater.* 323, 111262. <https://doi.org/10.1016/j.micromeso.2021.111262>.
130. Pan, D., Kong, L., Zhang, H., Zhang, Y., and Tang, Y. (2023). TS-1 Synthesis via Subcrystal Aggregation: Construction of Highly Active Hydrogen-Bonded Titanium Species for Alkene Epoxidation. *ACS Appl. Mater. Interfaces* 15, 28125–28134. <https://doi.org/10.1021/acsmi.3c04487>.
131. Ren, L., Wu, Q., Yang, C., Zhu, L., Li, C., Zhang, P., Zhang, H., Meng, X., and Xiao, F.-S. (2012). Solvent-Free Synthesis of Zeolites from Solid Raw Materials. *J. Am. Chem. Soc.* 134, 15173–15176. <https://doi.org/10.1021/ja304495a>.

132. Wu, Q., Meng, X., Gao, X., and Xiao, F.-S. (2018). Solvent-Free Synthesis of Zeolites: Mechanism and Utility. *Acc. Chem. Res.* 51, 1396–1403. <https://doi.org/10.1021/acs.accounts.8b00057>.
133. Wu, Q., Liu, X., Zhu, L., Ding, L., Gao, P., Wang, X., Pan, S., Bian, C., Meng, X., Xu, J., et al. (2015). Solvent-Free Synthesis of Zeolites from Anhydrous Starting Raw Solids. *J. Am. Chem. Soc.* 137, 1052–1055. <https://doi.org/10.1021/ja5124013>.
134. Fu, T., Zhang, Y., Wu, D., Zhu, W., Gao, X., Han, C., Luo, Y., Ma, W., and Dionysiou, D.D. (2020). Solvent-free synthesis of MFI-type zeolites and their degradation properties of gas-phase styrene. *J. Hazard. Mater.* 397, 122630. <https://doi.org/10.1016/j.jhazmat.2020.122630>.
135. Jin, Y., Sun, Q., Qi, G., Yang, C., Xu, J., Chen, F., Meng, X., Deng, F., and Xiao, F.-S. (2013). Solvent-Free Synthesis of Silicoaluminophosphate Zeolites. *Angew. Chem. Int. Ed.* 52, 9172–9175. <https://doi.org/10.1002/anie.201302672>.
136. Zhu, L., Zhang, J., Wang, L., Wu, Q., Bian, C., Pan, S., Meng, X., and Xiao, F.-S. (2015). Solvent-free synthesis of titanosilicate zeolites. *J. Mater. Chem. A* 3, 14093–14095. <https://doi.org/10.1039/C5TA02680F>.
137. Zuo, X., Chang, K., Zhao, J., Xie, Z., Tang, H., Li, B., and Chang, Z. (2016). Bubble-template-assisted synthesis of hollow fullerene-like MoS₂ nanocages as a lithium ion battery anode material. *J. Mater. Chem. A* 4, 51–58. <https://doi.org/10.1039/C5TA06869J>.
138. Wang, L., Xu, Y., Zhai, G., Zheng, Y., Huang, J., Sun, D., and Li, Q. (2020). Biophenol-Mediated Solvent-Free Synthesis of Titanium Silicalite-1 to Improve the Acidity Character of Framework Ti toward Catalysis Application. *ACS Sustain. Chem. Eng.* 8, 12177–12186. <https://doi.org/10.1021/acssuschemeng.0c03685>.
139. Fan, Y., Gong, X., Si, X., Xia, C., Wu, P., and Ma, Y. (2022). Post-synthesis and structural evolution of hollow titanium silicalite-1 with solvent-free method. *Nano Res.* 16, 1740–1747. <https://doi.org/10.1007/s12274-022-4789-1>.
140. Wang, C., Wang, L., Zhang, J., Wang, H., Lewis, J.P., and Xiao, F.-S. (2016). Product Selectivity Controlled by Zeolite Crystals in Biomass Hydrogenation over a Palladium Catalyst. *J. Am. Chem. Soc.* 138, 7880–7883. <https://doi.org/10.1021/jacs.6b04951>.
141. Zhang, J., Wang, L., Zhu, L., Wu, Q., Chen, C., Wang, X., Ji, Y., Meng, X., and Xiao, F.-S. (2015). Solvent-Free Synthesis of Zeolite Crystals Encapsulating Gold-Palladium Nanoparticles for the Selective Oxidation of Bioethanol. *ChemSusChem* 8, 2867–2871. <https://doi.org/10.1002/cssc.201500261>.
142. Ma, R., Wang, L., Wang, S., Wang, C., and Xiao, F.-S. (2017). Eco-friendly photocatalysts achieved by zeolite fixing. *Appl. Catal. B Environ.* 212, 193–200. <https://doi.org/10.1016/j.apcatb.2017.04.071>.
143. Wang, C., Liu, Z., Wang, L., Dong, X., Zhang, J., Wang, G., Han, S., Meng, X., Zheng, A., and Xiao, F.-S. (2018). Importance of Zeolite Wettability for Selective Hydrogenation of Furfural over Pd@Zeolite Catalysts. *ACS Catal.* 8, 474–481. <https://doi.org/10.1021/acscatal.7b03443>.
144. Wang, L., Dai, J., Xu, Y., Hong, Y., Huang, J., Sun, D., and Li, Q. (2020). Titanium silicalite-1 zeolite encapsulating Au particles as a catalyst for vapor phase propylene epoxidation with H₂/O₂: a matter of Au–Ti synergic interaction. *J. Mater. Chem. A* 8, 4428–4436. <https://doi.org/10.1039/C9TA12470E>.
145. Wu, Q., Wang, X., Qi, G., Guo, Q., Pan, S., Meng, X., Xu, J., Deng, F., Fan, F., Feng, Z., et al. (2014). Sustainable Synthesis of Zeolites without Addition of Both Organotemplates and Solvents. *J. Am. Chem. Soc.* 136, 4019–4025. <https://doi.org/10.1021/ja500098j>.
146. Chen, X., Meng, X., and Xiao, F.S. (2015). Solvent-free synthesis of SAPO-5 zeolite with plate-like morphology in the presence of surfactants. *Chin. J. Catal.* 36, 797–800. [https://doi.org/10.1016/S1872-2067\(14\)60285-0](https://doi.org/10.1016/S1872-2067(14)60285-0).
147. Liu, H., Wang, Y., Ye, T., Wang, F., Ran, S., Xie, H., Liu, J., Li, Y., Li, B., Liu, Y., et al. (2022). Fully utilizing seeds solution for solvent-free synthesized nanosized TS-1 zeolites with efficient epoxidation of chloropropene. *J. Solid State Chem.* 307, 122844. <https://doi.org/10.1016/j.jssc.2021.122844>.
148. Xu, H., and Wu, P. (2022). New progress in zeolite synthesis and catalysis. *Natl. Sci. Rev.* 9, nwac045. <https://doi.org/10.1093/nsr/nwac045>.
149. Čejka, J., Centi, G., Perez-Pariente, J., and Roth, W.J. (2012). Zeolite-based materials for novel catalytic applications: Opportunities, perspectives and open problems. *Catal. Today* 179, 2–15. <https://doi.org/10.1016/j.cattod.2011.10.006>.
150. Hartmann, M., Machoke, A.G., and Schwieger, W. (2016). Catalytic test reactions for the evaluation of hierarchical zeolites. *Chem. Soc. Rev.* 45, 3313–3330. <https://doi.org/10.1039/C5CS00935A>.
151. Kärger, J., and Valiullin, R. (2013). Mass transfer in mesoporous materials: the benefit of microscopic diffusion measurement. *Chem. Soc. Rev.* 42, 4172–4197. <https://doi.org/10.1039/c3cs35326e>.
152. Schneider, D., Mehlhorn, D., Zeigermann, P., Kärger, J., and Valiullin, R. (2016). Transport properties of hierarchical microporous materials. *Chem. Soc. Rev.* 45, 3439–3467. <https://doi.org/10.1039/C5CS00715A>.
153. Wang, X., Ma, Y., Wu, Q., Wen, Y., and Xiao, F.-S. (2022). Zeolite nanosheets for catalysis. *Chem. Soc. Rev.* 51, 2431–2443. <https://doi.org/10.1039/D1CS00651G>.
154. Millini, R., Bellussi, G., Pollesel, P., Rizzo, C., and Perego, C. (2022). Beyond TS-1: Background and recent advances in the synthesis of Ti-containing zeolites. *Microporous Mesoporous Mater.* 346, 112286. <https://doi.org/10.1016/j.micromeso.2022.112286>.
155. Bai, R., Song, Y., Li, Y., and Yu, J. (2019). Creating Hierarchical Pores in Zeolite Catalysts. *Trends Chem.* 1, 601–611. <https://doi.org/10.1016/j.trechm.2019.05.010>.
156. Liu, Z., Hua, Y., Wang, J., Dong, X., Tian, Q., and Han, Y. (2017). Recent progress in the direct synthesis of hierarchical zeolites: synthetic strategies and characterization methods. *Mater. Chem. Front.* 1, 2195–2212. <https://doi.org/10.1039/C7QM00168A>.
157. Liu, X., Liu, H., Chen, L., Su, B., Lu, X., Xia, Q., and Zhou, D. (2022). Construction of Ti-containing zeolite with highly enhanced catalytic activity by active species surface implanting strategy. *Catal. Today* 405–406, 285–298. <https://doi.org/10.1016/j.cattod.2022.04.024>.
158. Verboekend, D., Nuttens, N., Locus, R., Van Aelst, J., Verolme, P., Groen, J.C., Pérez-Ramírez, J., and Sels, B.F. (2016). Synthesis, characterisation, and catalytic evaluation of hierarchical faujasite zeolites: milestones, challenges, and future directions. *Chem. Soc. Rev.* 45, 3331–3352. <https://doi.org/10.1039/C5CS00520E>.
159. Schwieger, W., Machoke, A.G., Weissenberger, T., Inayat, A., Selvam, T., Klumpp, M., and Inayat, A. (2016). Hierarchy concepts: classification and preparation strategies for zeolite containing materials with hierarchical porosity. *Chem. Soc. Rev.* 45, 3353–3376. <https://doi.org/10.1039/C5CS00599J>.
160. Sheng, N., Liu, Z., Song, Z., Lin, D., Feng, X., Liu, Y., Chen, X., Chen, D., Zhou, X., and Yang, C. (2019). Enhanced stability for propene epoxidation with H₂ and O₂ over wormhole-like hierarchical TS-1 supported Au nanocatalyst. *Chem. Eng. J.* 377, 119954. <https://doi.org/10.1016/j.cej.2018.09.115>.
161. Jie, Z., Yang, T., Wang, X., Ji, Y., Li, Y., Meng, B., Tan, X., and Liu, S. (2022). Insight into the effect of mass transfer channels and intrinsic reactivity in titanium silicalite catalyst for one-step epoxidation of propylene. *Surf. Interfaces* 29, 101741. <https://doi.org/10.1016/j.surfin.2022.101741>.
162. Chen, L.-H., Sun, M.-H., Wang, Z., Yang, W., Xie, Z., and Su, B.-L. (2020). Hierarchically Structured Zeolites: From Design to Application. *Chem. Rev.* 120, 11194–11294. <https://doi.org/10.1021/acs.chemrev.0c00016>.
163. Khatami Shal, Z., Goepel, M., Gläser, R., and Shakeri, M. (2022). Synthesis of TS-1 from supported embryonic to nano-/micro-metersized crystalline particles: The impact of accessibility of Ti species on the catalytic performance. *Microporous Mesoporous Mater.* 337, 111900. <https://doi.org/10.1016/j.micromeso.2022.111900>.
164. Fang, Y., and Hu, H. (2007). Mesoporous TS-1: Nanocasting synthesis with CMK-3 as template and its performance in catalytic oxidation of aromatic thiophene. *Catal. Commun.* 8, 817–820. <https://doi.org/10.1016/j.catcom.2006.09.018>.
165. Xin, H., Zhao, X., Xu, S., Li, J., Zhang, W., Guo, X., Hensen, E.J.M., Yang, Q., and Li, C. (2010). Enhanced Catalytic Oxidation by Hierarchically Structured TS-1 Zeolite. *J. Phys. Chem. C* 114, 6553–6559. <https://doi.org/10.1021/jp912112h>.
166. Wang, W., Li, G., Liu, L., and Chen, Y. (2013). Synthesis and catalytic performance of hierarchical TS-1 directly using agricultural products sucrose as meso/macropores template. *Microporous Mesoporous Mater.* 179, 165–171. <https://doi.org/10.1016/j.micromeso.2013.06.012>.
167. Chen, L.-H., Li, X.-Y., Tian, G., Li, Y., Rooke, J.C., Zhu, G.-S., Qiu, S.-L., Yang, X.-Y., and Su, B.-L. (2011). Highly Stable and Reusable Multimodal Zeolite TS-1 Based Catalysts with Hierarchically Interconnected Three-Level Micro-Meso-Macroporous Structure. *Angew. Chem. Int. Ed.* 50, 11156–11161. <https://doi.org/10.1002/anie.201105678>.
168. Liu, Y., Wang, F., Zhang, X., Zhang, Q., Zhai, Y., Lv, G., Li, M., and Li, M. (2022). One-step synthesis of anatase-free hollow titanium silicalite-1 by the solid-phase conversion method. *Microporous Mesoporous Mater.* 331, 111676. <https://doi.org/10.1016/j.micromeso.2021.111676>.

169. Zhu, H., Liu, Z., Wang, Y., Kong, D., Yuan, X., and Xie, Z. (2008). Nanosized CaCO₃ as Hard Template for Creation of Intracrystalline Pores within Silicalite-1 Crystal. *Chem. Mater.* 20, 1134–1139. <https://doi.org/10.1021/cm071385o>.
170. Lopez-Orozco, S., Inayat, A., Schwab, A., Selvam, T., and Schwieger, W. (2011). Zeolitic Materials with Hierarchical Porous Structures. *Adv. Mater.* 23, 2602–2615. <https://doi.org/10.1002/adma.201100462>.
171. Jacobsen, C.J.H., Madsen, C., Houzvicka, J., Schmidt, I., and Carlsson, A. (2000). Mesoporous Zeolite Single Crystals. *J. Am. Chem. Soc.* 122, 7116–7117. <https://doi.org/10.1021/ja000744c>.
172. Choi, M., Na, K., Kim, J., Sakamoto, Y., Terasaki, O., and Ryoo, R. (2009). Stable single-unit-cell nanosheets of zeolite MFI as active and long-lived catalysts. *Nature* 461, 246–249. <https://doi.org/10.1038/nature08288>.
173. Wang, M., Wang, X., You, Q., Wu, Y., Yang, X., Chen, H., Liu, B., Hao, Q., Zhang, J., and Ma, X. (2021). Dual-template synthesis of hierarchically layered titanosilicate-1 zeolites for catalytic epoxidation of cyclooctene. *Microporous Mesoporous Mater.* 323, 111207. <https://doi.org/10.1016/j.micromeso.2021.111207>.
174. Wang, J., Shen, X., Zhang, Y., Lu, J., Liu, M., Ling, L., Liao, J., Chang, L., and Xie, K. (2022). Synthesis of the Hierarchical TS-1 Using TritonX Homologues for Hydroxylation of Benzene. *Mol. Catal.* 532, 112744. <https://doi.org/10.1016/j.mcat.2022.112744>.
175. Liu, F., Willhammar, T., Wang, L., Zhu, L., Sun, Q., Meng, X., Carrillo-Cabrera, W., Zou, X., and Xiao, F.-S. (2012). ZSM-5 Zeolite Single Crystals with *b*-Axis-Aligned Mesoporous Channels as an Efficient Catalyst for Conversion of Bulky Organic Molecules. *J. Am. Chem. Soc.* 134, 4557–4560. <https://doi.org/10.1021/ja300078q>.
176. Liu, D., Li, G., Liu, J., Wei, Y., and Guo, H. (2018). Mesoporous Titanium-Silicalite Zeolite Containing Organic Templates as a Bifunctional Catalyst for Cycloaddition of CO₂ and Epoxides. *ACS Appl. Mater. Interfaces* 10, 22119–22129. <https://doi.org/10.1021/acsami.8b04759>.
177. Shen, X., Wang, J., Liu, M., Li, M., and Lu, J. (2019). Preparation of the Hierarchical Ti-Rich TS-1 via TritonX-100-Assisted Synthetic Strategy for the Direct Oxidation of Benzene. *Catal. Lett.* 149, 2586–2596. <https://doi.org/10.1007/s10562-019-02735-5>.
178. Xiao, F.-S., Wang, L., Yin, C., Lin, K., Di, Y., Li, J., Xu, R., Su, D.S., Schlögl, R., Yokoi, T., and Tatsumi, T. (2006). Catalytic Properties of Hierarchical Mesoporous Zeolites Templated with a Mixture of Small Organic Ammonium Salts and Mesoscale Cationic Polymers. *Angew. Chem. Int. Ed.* 45, 3090–3093. <https://doi.org/10.1002/anie.200600241>.
179. Zhu, J., Zhu, Y., Zhu, L., Rigutto, M., van der Made, A., Yang, C., Pan, S., Wang, L., Zhu, L., Jin, Y., et al. (2014). Highly Mesoporous Single-Crystalline Zeolite Beta Synthesized Using a Nonsurfactant Cationic Polymer as a Dual-Function Template. *J. Am. Chem. Soc.* 136, 2503–2510. <https://doi.org/10.1021/ja411117y>.
180. Du, S., Sun, Q., Wang, N., Chen, X., Jia, M., and Yu, J. (2017). Synthesis of hierarchical TS-1 zeolites with abundant and uniform intracrystalline mesopores and their highly efficient catalytic performance for oxidation desulfurization. *J. Mater. Chem. A* 5, 7992–7998. <https://doi.org/10.1039/C6TA10044A>.
181. Du, S., Chen, H.-M., Shen, H.-X., Chen, J., Li, C.-P., and Du, M. (2020). Hierarchically Nanoporous TS-1 Zeolites for Catalytic Oxidation Desulfurization of Liquid Fuels. *ACS Appl. Nano Mater.* 3, 9393–9400. <https://doi.org/10.1021/acsnano.0c02017>.
182. Zhang, M., Ren, S., Guo, Q., and Shen, B. (2021). Synthesis of hierarchically porous zeolite TS-1 with small crystal size and its performance of 1-hexene epoxidation reaction. *Microporous Mesoporous Mater.* 326, 111395. <https://doi.org/10.1016/j.micromeso.2021.111395>.
183. Du, Q., Guo, Y., Duan, H., Li, H., Chen, Y., and Liu, H. (2017). Synthesis of hierarchical TS-1 zeolite via a novel three-step crystallization method and its excellent catalytic performance in oxidative desulfurization. *Fuel* 188, 232–238. <https://doi.org/10.1016/j.fuel.2016.10.045>.
184. Cheneviere, Y., Chieux, F., Caps, V., and Tuel, A. (2010). Synthesis and catalytic properties of TS-1 with mesoporous/microporous hierarchical structures obtained in the presence of amphiphilic organosilanes. *J. Catal.* 269, 161–168. <https://doi.org/10.1016/j.jcat.2009.11.003>.
185. Serrano, D.P., Escola, J.M., and Pizarro, P. (2012). Synthesis strategies in the search for hierarchical zeolites. *Chem Soc Rev* 30. <https://doi.org/10.1039/c2cs35330j>.
186. Han, Z., Shen, Y., Wang, F., and Zhang, X. (2018). Synthesis of hierarchical titanium silicalite-1 in the presence of polyquaternium-7 and its application in the hydroxylation of phenol. *J. Mater. Sci.* 53, 12837–12849. <https://doi.org/10.1007/s10853-018-2582-z>.
187. Choi, M., Cho, H.S., Srivastava, R., Venkatesan, C., Choi, D.-H., and Ryoo, R. (2006). Amphiphilic organosilane-directed synthesis of crystalline zeolite with tunable mesoporosity. *Nat. Mater.* 5, 718–723. <https://doi.org/10.1038/nmat1705>.
188. Khomane, R.B., Kulkarni, B.D., and Ahedi, R.K. (2001). Synthesis and Characterization of Ferrierite-Type Zeolite in the Presence of Nonionic Surfactants. *J. Colloid Interface Sci.* 236, 208–213. <https://doi.org/10.1006/jcis.2000.7406>.
189. Khomane, R.B., Kulkarni, B.D., Paraskar, A., and Sainkar, S.R. (2002). Synthesis, characterization and catalytic performance of titanium silicalite-1 prepared in micellar media. *Mater. Chem. Phys.* 76, 99–103. [https://doi.org/10.1016/S0254-0584\(01\)00507-7](https://doi.org/10.1016/S0254-0584(01)00507-7).
190. Du, S., Li, F., Sun, Q., Wang, N., Jia, M., and Yu, J. (2016). A green surfactant-assisted synthesis of hierarchical TS-1 zeolites with excellent catalytic properties for oxidative desulfurization. *Chem. Commun.* 52, 3368–3371. <https://doi.org/10.1039/C5CC08441E>.
191. Su, Y., Li, F., Zhou, Z., Qin, J., Wang, X., Sun, P., and Wu, W. (2022). Acidic-treated TS-1 zeolites with high titanium for cyclohexanone efficient oximation. *Mol. Catal.* 533, 112752. <https://doi.org/10.1016/j.mcat.2022.112752>.
192. Chang, X., Yang, X., Song, X., Xu, L., Hu, D., Sun, Y., and Jia, M. (2022). Addition of polyethylene glycol for the synthesis of anatase-free TS-1 zeolites with excellent catalytic activity in 1-hexene epoxidation. *J. Porous Mater.* 29, 641–649. <https://doi.org/10.1007/s10934-021-01186-x>.
193. Wang, Y., Lin, M., and Tuel, A. (2007). Hollow TS-1 crystals formed via a dissolution–recrystallization process. *Microporous Mesoporous Mater.* 102, 80–85. <https://doi.org/10.1016/j.micromeso.2006.12.019>.
194. Yuan, J., Song, Z., Lin, D., Feng, X., Tuo, Y., Zhou, X., Yan, H., Jin, X., Liu, Y., Chen, X., et al. (2021). Mesopore-Free Strategy to Construct Hierarchical TS-1 in a Highly Concentrated System for Gas-Phase Propene Epoxidation with H₂ and O₂. *ACS Appl. Mater. Interfaces* 13, 26134–26142. <https://doi.org/10.1021/acsmi.1c06964>.
195. Sun, Q., Wang, N., Bai, R., Chen, G., Shi, Z., Zou, Y., and Yu, J. (2018). Mesopore-Free Synthesis of Nano-sized Hierarchical SAPO-34 Zeolite with Reduced Template Consumption and Excellent MTO Performance. *ChemSusChem* 11, 3812–3820. <https://doi.org/10.1002/cssc.201801486>.
196. Wang, C., An, G., Lin, J., Zhang, X., Liu, Z., Luo, Y., Liu, S., Cheng, Z., Guo, T., Gao, H., et al. (2023). Aromatic compounds-mediated synthesis of anatase-free hierarchical TS-1 zeolite: Exploring design strategies via machine learning and enhanced catalytic performance. *Aggregate* 4. <https://doi.org/10.1002/agt2.318>.
197. Tang, B., Li, S., Song, W.-C., Yang, E.-C., Zhao, X.-J., Guan, N., and Li, L. (2020). Fabrication of Hierarchical Sn-Beta Zeolite as Efficient Catalyst for Conversion of Cellulosic Sugar to Methyl Lactate. *ACS Sustain. Chem. Eng.* 8, 3796–3808.
198. Jiao, Y., Forster, L., Xu, S., Chen, H., Han, J., Liu, X., Zhou, Y., Liu, J., Zhang, J., Yu, J., et al. (2020). Creation of Al-Enriched Mesoporous ZSM-5 Nanoboxes with High Catalytic Activity: Converting Tetrahedral Extra-Framework Al into Framework Sites by Post Treatment. *Angew. Chem. Int. Ed.* 59, 19478–19486. <https://doi.org/10.1002/anie.202002416>.
199. He, Y.J., Nivarthi, G.S., Eder, F., Seshan, K., and Lercher, J.A. (1998). Synthesis, characterization and catalytic activity of the pillared molecular sieve MCM-36. *Microporous Mesoporous Mater.* 25, 207–224. [https://doi.org/10.1016/S1387-1811\(98\)00210-8](https://doi.org/10.1016/S1387-1811(98)00210-8).
200. Karwacki, L., de Winter, D.A.M., Aramburo, L.R., Lebbink, M.N., Post, J.A., Drury, M.R., and Weckhuyzen, B.M. (2011). Architecture-Dependent Distribution of Mesopores in Steamed Zeolite Crystals as Visualized by FIB-SEM Tomography. *Angew. Chem. Int. Ed.* 50, 1294–1298. <https://doi.org/10.1002/anie.201006031>.
201. Rezelorová, E., Zúkal, A., Čejka, J., Siperstein, F.R., Brennan, J.K., and Lísal, M. (2017). Adsorption and Diffusion of C₁ to C₄ Alkanes in Dual-Porosity Zeolites by Molecular Simulations. *Langmuir* 33, 11126–11137. <https://doi.org/10.1021/acs.langmuir.7b01772>.
202. Verboekend, D., Mitchell, S., Milina, M., Groen, J.C., and Pérez-Ramírez, J. (2011). Full Compositional Flexibility in the Preparation of Mesoporous MFI Zeolites by Desilication. *J. Phys. Chem. C* 115, 14193–14203. <https://doi.org/10.1021/jp201671s>.
203. Qin, Z., Lakiss, L., Gilson, J.-P., Thomas, K., Goupil, J.-M., Fernandez, C., and Valtchev, V. (2013). Chemical Equilibrium Controlled Etching of MFI-Type Zeolite and Its Influence on Zeolite Structure, Acidity, and Catalytic Activity. *Chem. Mater.* 25, 2759–2766. <https://doi.org/10.1021/cm400719z>.

204. Chlubná, P., Roth, W.J., Zukal, A., Kubů, M., and Pavlatová, J. (2012). Pillared MWW zeolites MCM-36 prepared by swelling MCM-22P in concentrated surfactant solutions. *Catal. Today* 179, 35–42. <https://doi.org/10.1016/j.cattod.2011.06.035>.
205. Lin, M., Xia, C., Zhu, B., Li, H., and Shu, X. (2016). Green and efficient epoxidation of propylene with hydrogen peroxide (H₂O₂) catalyzed by hollow TS-1 zeolite: A 1.0 kt/a pilot-scale study. *Chem. Eng. J.* 295, 370–375. <https://doi.org/10.1016/j.cej.2016.02.072>.
206. Li, Y., Zhang, R., Du, L., Zhang, Q., and Wang, W. (2016). Catalytic mechanism of C–F bond cleavage: insights from QM/MM analysis of fluoroacetate dehalogenase. *Catal. Sci. Technol.* 6, 73–80. <https://doi.org/10.1039/C5CY00777A>.
207. Wang, H., Chu, Q., Dong, Y., Zhang, S., Lu, D., Wang, P., Sun, Y., and Wang, M. (2022). Green Catalytic Epoxidation of Bulky Olefins via Hierarchical Cerium-Containing TS-1 Catalyst. *Catal. Lett.* 153, 2693–2705. <https://doi.org/10.1007/s10562-022-04146-5>.
208. Du, S., Chen, X., Sun, Q., Wang, N., Jia, M., Valtchev, V., and Yu, J. (2016). A non-chemically selective top-down approach towards the preparation of hierarchical TS-1 zeolites with improved oxidative desulfurization catalytic performance. *Chem. Commun.* 52, 3580–3583. <https://doi.org/10.1039/C5CC10232D>.
209. Akkal, T., Soualah, A., Morisset, S., Rousseau, J., Chaouati, N., and Sachse, A. (2022). Hierarchical TS-1 Through Ammonium Fluoride Etching. *ChemNanoMat* 8. <https://doi.org/10.1002/cnma.202200237>.
210. Wang, B., Guo, Y., Zhu, J., Ma, J., and Qin, Q. (2023). A review on titanosilicate-1 (TS-1) catalysts: Research progress of regulating titanium species. *Coord. Chem. Rev.* 476, 214931. <https://doi.org/10.1016/j.ccr.2022.214931>.
211. Liu, M., Wei, H., Li, B., Song, L., Zhao, S., Niu, C., Jia, C., Wang, X., and Wen, Y. (2018). Green and efficient preparation of hollow titanium silicalite-1 by using recycled mother liquid. *Chem. Eng. J.* 331, 194–202. <https://doi.org/10.1016/j.cej.2017.08.082>.
212. Vermeiren, W., and Gilson, J.-P. (2009). Impact of Zeolites on the Petroleum and Petrochemical Industry. *Top. Catal.* 52, 1131–1161. <https://doi.org/10.1007/s11244-009-9271-8>.
213. Walton, I.M., Cox, J.M., Benson, C.A., Patel, D.D.G., Chen, Y.S., Benedict, J.B., and Benedict, J.B. (2016). The role of atropisomers on the photo-reactivity and fatigue of diarylethene-based metal–organic frameworks. *New J. Chem.* 40, 101–106. <https://doi.org/10.1039/C5NJ01718A>.
214. Antonova, N.S., Carbo, J.J., Kortz, U., Kholdeeva, O.A., and Poblet, J.M. (2010). Mechanistic Insights into Alkene Epoxidation with H₂O₂ by Ti- and other TM-Containing Polyoxometalates: Role of the Metal Nature and Coordination Environment. *J. Am. Chem. Soc.* 132, 7488–7497. <https://doi.org/10.1021/ja1023157>.
215. Ye, J., Liu, C., Mei, D., and Ge, Q. (2013). Active Oxygen Vacancy Site for Methanol Synthesis from CO₂ Hydrogenation on In₂O₃ (110): A DFT Study. *ACS Catal.* 3, 1296–1306. <https://doi.org/10.1021/cs400132a>.
216. Tamura, M., Chaikitilp, W., Yokoi, T., and Okubo, T. (2008). Incorporation process of Ti species into the framework of MFI type zeolite. *Microporous Mesoporous Mater.* 112, 202–210. <https://doi.org/10.1016/j.micromeso.2007.09.044>.
217. Wilde, N., Pelz, M., Gebhardt, S.G., and Gläser, R. (2015). Highly efficient nano-sized TS-1 with micro-/mesoporosity from desilication and recrystallization for the epoxidation of biodesel with H₂O₂. *Green Chem.* 17, 3378–3389. <https://doi.org/10.1039/C5GC00406C>.
218. Bellussi, G. (1992). Reactions of titanium silicalite with protic molecules and hydrogen peroxide. *J. Catal.* 133, 220–230. [https://doi.org/10.1016/0021-9517\(92\)90199-R](https://doi.org/10.1016/0021-9517(92)90199-R).
219. Wu, P., Komatsu, T., and Yashima, T. (1998). Hydroxylation of Aromatics with Hydrogen Peroxide over Titanosilicates with MOR and MFI Structures: Effect of Ti Peroxo Species on the Diffusion and Hydroxylation Activity. *J. Phys. Chem. B* 102, 9297–9303. <https://doi.org/10.1021/jp982951t>.
220. Wilkenhöner, U., Langhendries, G., van Laar, F., Baron, G.V., Gammon, D.W., Jacobs, P.A., and van Steen, E. (2001). Influence of Pore and Crystal Size of Crystalline Titanosilicates on Phenol Hydroxylation in Different Solvents. *J. Catal.* 203, 201–212. <https://doi.org/10.1006/jcat.2001.3308>.
221. Wang, G., Du, W., Zhang, Z., Tang, Y., Xu, J., Cao, Y., Qian, G., Duan, X., Yuan, W., and Zhou, X. (2022). Combining trace Pt with surface silylation to boost Au/uncalcined TS-1 catalyzed propylene epoxidation with H₂ and O₂. *AIChE J.* 68. <https://doi.org/10.1002/aic.17416>.
222. Wang, Y., Yang, H., Zuo, Y., Tian, D., Hou, G., Su, Y., Feng, Z., Guo, X., and Li, C. (2023). New penta- and hexa-coordinated titanium sites in titanium silicalite-1 catalyst for propylene epoxidation. *Appl. Catal. B Environ.* 325, 122396. <https://doi.org/10.1016/j.apcatb.2023.122396>.
223. Miao, C., Zhu, Q., Yi, Y., Su, J., He, N., Liu, J., and Guo, H. (2019). Gas-Phase Epoxidation of Propylene with Hydrogen Peroxide Vapor: Effect of Modification with NaOH on TS-1 Titanosilicate Catalyst in the Presence of Tetra-propylammonium Bromide. *Ind. Eng. Chem. Res.* 58, 11739–11749. <https://doi.org/10.1021/acs.iecr.8b06481>.
224. Li, Y., Fan, Q., Li, Y., Feng, X., Chai, Y., and Liu, C. (2019). Seed-assisted synthesis of hierarchical nanosized TS-1 in a low-cost system for propylene epoxidation with H₂O₂. *Appl. Surf. Sci.* 483, 652–660. <https://doi.org/10.1016/j.apsusc.2019.03.334>.
225. Song, Z., Feng, X., Sheng, N., Lin, D., Li, Y., Liu, Y., Chen, X., Chen, D., Zhou, X., and Yang, C. (2019). Cost-Efficient Core-Shell TS-1/Silicalite-1 Supported Au Catalysts: Towards Enhanced Stability for Propene Epoxidation with H₂ and O₂. *Chem. Eng. J.* 377, 119927. <https://doi.org/10.1016/j.cej.2018.09.088>.
226. Zhang, Z., Tang, Y., Du, W., Xu, J., Wang, Q., Song, N., Qian, G., Duan, X., and Zhou, X. (2022). Engineering Gold Impregnated Uncalcined TS-1 to Boost Catalytic Formation of Propylene Oxide. *Appl. Catal. B Environ.* 319, 121837. <https://doi.org/10.1016/j.apcatb.2022.121837>.
227. Feng, X., Duan, X., Qian, G., Zhou, X., Chen, D., and Yuan, W. (2014). Au nanoparticles deposited on the external surfaces of TS-1: Enhanced stability and activity for direct propylene epoxidation with H₂ and O₂. *Appl. Catal. B Environ.* 151, 396–401. <https://doi.org/10.1016/j.apcatb.2013.12.041>.
228. Huang, J., Takei, T., Akita, T., Ohashi, H., and Haruta, M. (2010). Gold clusters supported on alkaline treated TS-1 for highly efficient propene epoxidation with O₂ and H₂. *Appl. Catal. B Environ.* 95, 430–438. <https://doi.org/10.1016/j.apcatb.2010.01.023>.
229. Sheng, N., Song, Z., Yuan, J., Liang, W., Zhao, J., Zhang, J., Xu, W., Sun, B., Feng, X., Yang, Z., and Yang, C. (2022). Effective Regulation of the Au Spatial Position in a Hierarchically Structured Au/HTS-1 Catalyst: To Boost the Catalytic Performance of Propene Epoxidation with H₂ and O₂. *ACS Sustain. Chem. Eng.* 10, 9515–9524. <https://doi.org/10.1021/acssuschemeng.2c02139>.
230. Lu, Z., Kunisch, J., Gan, Z., Bunian, M., Wu, T., and Lei, Y. (2020). Gold Catalysts Synthesized Using a Modified Incipient Wetness Impregnation Method for Propylene Epoxidation. *ChemCatChem* 12, 5993–5999. <https://doi.org/10.1002/cctc.202001053>.
231. Chen, Z., Zhang, L., Yu, Y., Liu, D., Fang, N., Lin, Y., Xu, D., Li, F., Liu, Y., and He, M. (2021). TS-1 zeolite with homogeneous distribution of Ti atoms in the framework: synthesis, crystallization mechanism and its catalytic performance. *J. Catal.* 404, 990–998. <https://doi.org/10.1016/j.jcat.2021.11.001>.
232. Yang, G., Han, J., Liu, Y., Qiu, Z., and Chen, X. (2020). The synthetic strategies of hierarchical TS-1 zeolites for the oxidative desulfurization reactions. *Chin. J. Chem. Eng.* 28, 2227–2234. <https://doi.org/10.1016/j.cjche.2020.06.026>.
233. Kong, L., Li, G., and Wang, X. (2004). Mild oxidation of thiophene over TS-1/H₂O₂. *Catal. Today* 93–95, 341–345. <https://doi.org/10.1016/j.cattod.2004.06.016>.
234. Liu, N., Guo, H., Wang, X., Chen, L., and Zoub, L. (2005). Increasing the propylene epoxidation activity of TS-1 catalysts by hydrothermal treatment of ammonia solution. *React. Kinet. Catal. Lett.* 87, 77–83. <https://doi.org/10.1007/s11144-006-0011-9>.
235. Liu, H., Lu, G., Guo, Y., Guo, Y., and Wang, J. (2004). Effect of pretreatment on properties of TS-1/diatomite catalyst for hydroxylation of phenol by H₂O₂ in fixed-bed reactor. *Catal. Today* 93–95, 353–357. <https://doi.org/10.1016/j.cattod.2004.06.083>.
236. Yu, Y., Tang, Z., Liu, W., Wang, J., Chen, Z., Shen, K., Wang, R., Liu, H., Huang, X., and Liu, Y. (2019). Enhanced catalytic oxidation performance of K⁺-modified Ti-MWW through selective breaking of interfacial hydrogen-bonding interactions of H₂O₂. *Appl. Catal. Gen.* 587, 117270. <https://doi.org/10.1016/j.apcata.2019.117270>.
237. Liu, B., Wattanaprayoon, C., Oh, S.C., Emdadi, L., and Liu, D. (2015). Synthesis of Organic Pillared MFI Zeolite as Bifunctional Acid-Base Catalyst. *Chem. Mater.* 27, 1479–1487. <https://doi.org/10.1021/cm5033833>.
238. Lin, Y., Xu, D., Chen, Z., Yu, Y., Li, F., Huang, X., Liu, Y., and He, M. (2022). P-modified deactivated TS-1: A benign catalyst for the MTP reaction. *Catal. Today* 405–406, 258–266. <https://doi.org/10.1016/j.cattod.2022.04.034>.
239. Wu, P., Tatsumi, T., Komatsu, T., and Yashima, T. (2001). A Novel Titanosilicate with MWW Structure. I. Hydrothermal Synthesis, Elimination of Extraframework Titanium, and Characterizations. *J. Phys.*

- Chem. B 105, 2897–2905. <https://doi.org/10.1021/jp002816s>.
240. Fan, W., Wu, P., Namba, S., and Tatsumi, T. (2004). A Titanosilicate That Is Structurally Analogous to an MWW-Type Lamellar Precursor. *Angew. Chem. Int. Ed.* 43, 236–240. <https://doi.org/10.1002/anie.200352723>.
241. Tatsumi, T., Koyano, K.A., and Shimizu, Y. (2000). Effect of potassium on the catalytic activity of TS-1. *Appl. Catal. Gen.* 200, 125–134. [https://doi.org/10.1016/S0926-860X\(00\)00630-X](https://doi.org/10.1016/S0926-860X(00)00630-X).
242. Li, G., Wang, X., Guo, X., Liu, S., Zhao, Q., Bao, X., and Lin, L. (2001). Titanium species in titanium silicalite TS-1 prepared by hydrothermal method. *Mater. Chem. Phys.* 71, 195–201. [https://doi.org/10.1016/S0254-0584\(01\)00281-4](https://doi.org/10.1016/S0254-0584(01)00281-4).
243. Morin, S., Ayrault, P., and Gnep, N.S. (1998). Influence of the framework composition of commercial HFAU zeolites on their activity and selectivity in m-xylene transformation. *Appl. Catal. A Gen.* 166, 281–292. [https://doi.org/10.1016/S0926-860X\(97\)00263-9](https://doi.org/10.1016/S0926-860X(97)00263-9).
244. Groen, J.C., Moulijn, J.A., and Pérez-Ramírez, J. (2006). Desilication: on the controlled generation of mesoporosity in MFI zeolites. *J. Mater. Chem.* 16, 2121–2131. <https://doi.org/10.1039/B517510K>.
245. Hua, Z.L., Zhou, J., and Shi, J.L. (2011). Recent advances in hierarchically structured zeolites: synthesis and material performances. *Chem. Commun.* 47, 10536–10547. <https://doi.org/10.1039/c1cc10261c>.
246. Patil, C.R., Niphadkar, P., Kamble, S.P., and Rode, C.V. (2022). Enhanced anisole hydroxylation over a hierarchical micro/mesoporous TS-1 catalyst. *New J. Chem.* 46, 14667–14675. <https://doi.org/10.1039/D2NJ01556K>.
247. Pérez-Ramírez, J., Verboekend, D., Bonilla, A., and Abelló, S. (2009). Zeolite Catalysts with Tunable Hierarchy Factor by Pore-Growth Moderators. *Adv. Funct. Mater.* 19, 3972–3979. <https://doi.org/10.1002/adfm.200901394>.
248. Zhang, M., Wen, Y., Zong, L., Wei, H., and Wang, X. (2020). Improved Ti species distribution and hierarchical pores in TS-1: towards regeneration of TS-1 deactivated due to alkali corrosion. *New J. Chem.* 44, 6394–6401. <https://doi.org/10.1039/D0NJ00960A>.
249. Jin, X., Peng, R., Tong, W., Yin, J., Xu, H., and Wu, P. (2022). Investigation of the active centers and structural modifications for TS-1 in catalyzing the Beckmann rearrangement. *Catal. Today* 405–406, 193–202. <https://doi.org/10.1016/j.cattod.2022.05.033>.
250. Zhao, P., Li, Z., Zhang, Y., Cui, D., Guo, Q., Dong, Z., Qi, G., Xu, J., and Deng, F. (2022). Tuning Lewis acid sites in TS-1 zeolites for hydroxylation of anisole with hydrogen peroxide. *Microporous Mesoporous Mater.* 335, 111840. <https://doi.org/10.1016/j.micromeso.2022.111840>.
251. Li, X., Hernandez Gaitan, J.A., Kokuryo, S., Sumi, T., Kitamura, H., Miyake, K., Uchida, Y., and Nishiyama, N. (2022). Hierarchical zeolites with high hydrothermal stability prepared via desilication of OSDA-occluded zeolites. *Microporous Mesoporous Mater.* 344, 112096. <https://doi.org/10.1016/j.micromeso.2022.112096>.
252. Wang, B., Lin, M., Peng, X., Zhu, B., and Shu, X. (2016). Hierarchical TS-1 synthesized effectively by post-modification with TPAOH and ammonium hydroxide. *RSC Adv.* 6, 44963–44971. <https://doi.org/10.1039/C6RA06657G>.
253. Wang, J., Chen, Z., Yu, Y., Tang, Z., Shen, K., Wang, R., Liu, H., Huang, X., and Liu, Y. (2019). Hollow core-shell structured TS-1@S-1 as an efficient catalyst for alkene epoxidation. *RSC Adv.* 9, 37801–37808. <https://doi.org/10.1039/C9RA07893B>.
254. Zhang, J., Chen, C., Chen, S., Hu, Q., Gao, Z., Li, Y., and Qin, Y. (2017). Highly dispersed Pt nanoparticles supported on carbon nanotubes produced by atomic layer deposition for hydrogen generation from hydrolysis of ammonia borane. *Catal. Sci. Technol.* 7, 322–329. <https://doi.org/10.1039/C6CY01960A>.
255. Wu, G., Lin, Z., Li, L., Zhang, L., Hong, Y., Wang, W., Chen, C., Jiang, Y., and Yan, X. (2017). Experiments and kinetics of the epoxidation of allyl chloride with H₂O₂ over organic base treated TS-1 catalysts. *Chem. Eng. J.* 320, 1–10. <https://doi.org/10.1016/j.cej.2017.03.030>.
256. Liu, M., Huang, Z., Wei, W., Wang, X., and Wen, Y. (2021). Synthesis of Low Cost Titanium Silicalite-1 Zeolite for Highly Efficient Propylene Epoxidation. *Front. Chem.* 9, 682404. <https://doi.org/10.3389/fchem.2021.682404>.
257. Malola, S., Svelle, S., Bleken, F.L., and Swang, O. (2012). Detailed Reaction Paths for Zeolite Dealumination and Desilication From Density Functional Calculations. *Angew. Chem. Int. Ed.* 51, 652–655. <https://doi.org/10.1002/anie.201104462>.
258. Silaghi, M.-C., Chizallet, C., and Raybaud, P. (2014). Challenges on molecular aspects of dealumination and desilication of zeolites. *Microporous Mesoporous Mater.* 191, 82–96. <https://doi.org/10.1016/j.micromeso.2014.02.040>.
259. Verboekend, D., and Pérez-Ramírez, J. (2011). Desilication Mechanism Revisited: Highly Mesoporous Al-Silica Zeolites Enabled Through Pore-Directing Agents. *Chem. - Eur. J.* 17, 1137–1147. <https://doi.org/10.1002/chem.201002589>.
260. Ghosh, A. (1987). Acidity and activity of fluorinated mordenites. *J. Catal.* 103, 399–406. [https://doi.org/10.1016/0021-9517\(87\)90131-X](https://doi.org/10.1016/0021-9517(87)90131-X).
261. Sánchez, N.A., Saniger, J.M., d'Espinose de la Caillerie, J.-B., Blumenfeld, A.L., and Fripiat, J.J. (2001). Reaction of HY Zeolite with Molecular Fluorine. *J. Catal.* 201, 80–88. <https://doi.org/10.1006/jcat.2001.3226>.
262. Mao, R., Le, T.S., Fairbairn, M., Muntasar, A., and Denes, G. (1999). Zsm-5 zeolite with enhanced acidic properties. *Applied Catalysis A General* 185, 41–52. [https://doi.org/10.1016/S0926-860X\(99\)00132-5](https://doi.org/10.1016/S0926-860X(99)00132-5).
263. Nikolopoulos, A.A., Kogelbauer, A., Goodwin, J.G., and Marcelin, G. (1996). Gas phase synthesis of MTBE on fluoride-modified zeolites. *Catal. Lett.* 39, 173–178. <https://doi.org/10.1007/BF00805579>.
264. Hammond, C., and Tarantino, G. (2015). Switching off H₂O₂ Decomposition during TS-1 Catalysed Epoxidation via Post-Synthetic Active Site Modification. *Catalysts* 5, 2309–2323. <https://doi.org/10.3390/catal5042309>.
265. Qin, Z., Melinte, G., Gilson, J.-P., Jaber, M., Bozhilov, K., Boullay, P., Mintova, S., Ersen, O., and Valtchev, V. (2016). The Mosaic Structure of Zeolite Crystals. *Angew. Chem.* 128, 15273–15276. <https://doi.org/10.1002/ange.201608417>.
266. Qin, Z., Pinard, L., Benghalem, M.A., Daou, T.J., Melinte, G., Ersen, O., Asahina, S., Gilson, J.-P., and Valtchev, V. (2019). Preparation of Single-Crystal “House-of-Cards”-like ZSM-5 and Their Performance in Ethanol-to-Hydrocarbon Conversion. *Chem. Mater.* 31, 4639–4648. <https://doi.org/10.1021/acs.chemmater.8b04970>.
267. Chang, X.-Y., Sun, Y.-T., Song, X.-J., Yang, X.-T., Wu, Y.-Q., and Jia, M.-J. (2022). Hydrothermal Modification of TS-1 Zeolites with Organic Amines and Salts to Construct Highly Selective Catalysts for Cyclopentene Epoxidation. *Catalysts* 12, 1241. <https://doi.org/10.3390/catal12101241>.
268. Cerón, M.R., Izquierdo, M., Alegret, N., Valdez, J.A., Rodríguez-Fortea, A., Olmstead, M.M., Balch, A.L., Poblet, J.M., and Echevoyen, L. (2016). Reactivity differences of Sc₃N@C_{2n} (2n = 68 and 80). Synthesis of the first methanofullerene derivatives of Sc₃N@D_{5h}-C₈₀. *Chem. Commun.* 52, 64–67. <https://doi.org/10.1039/C5CC07416A>.
269. Delannoy, L., El Hassan, N., Musi, A., Le To, N.N., Krafft, J.-M., and Louis, C. (2006). Preparation of Supported Gold Nanoparticles by a Modified Incipient Wetness Impregnation Method. *J. Phys. Chem. B* 110, 22471–22478. <https://doi.org/10.1021/jp062130l>.
270. Somodi, F., Borbáth, I., Hegedűs, M., Tompos, A., Sajó, I.E., Szegedi, Á., Rojas, S., Fierro, J.L.G., Margitfalvi, J.L., and Margitfalvi, J.L. (2008). Modified preparation method for highly active Au/SiO₂ catalysts used in CO oxidation. *Appl. Catal. A* 347, 216–222. <https://doi.org/10.1016/j.apcata.2008.06.017>.
271. Zhang, Z., Shi, S., Tang, Y., Xu, J., Du, W., Wang, Q., Yu, D., Liao, Y., Song, N., Duan, X., and Zhou, X. (2022). Using ammonia solution to fabricate highly active Au/uncalcined TS-1 catalyst for gas-phase epoxidation of propylene. *J. Catal.* 416, 410–422. <https://doi.org/10.1016/j.jcat.2022.11.019>.
272. Clerici, M.G. (2015). The activity of titanium silicalite-1 (TS-1): Some considerations on its origin. *Kinet. Catal.* 56, 450–455. <https://doi.org/10.1134/S0023158415040059>.
273. Fraile, J.M., García, J.I., Mayoral, J.A., and Vispe, E. (2004). Comparison of hydrophilic and hydrophobic silicas as supports for titanium catalysts. *Appl. Catal. Gen.* 276, 113–122. <https://doi.org/10.1016/j.apcata.2004.07.048>.
274. Sonoda, J., Kamegawa, T., Kuwahara, Y., Mori, K., and Yamashita, H. (2010). Hydrophobic Modification of Ti-Containing Zeolite (TS-1) and Their Applications in Liquid-Phase Selective Catalytic Reactions. *Bull. Chem. Soc. Jpn.* 83, 592–594. <https://doi.org/10.1246/bcsj.20090265>.
275. Corrigenda. (1996). *Angew. Chem. Int. Ed. Engl.* 35, 2881. <https://doi.org/10.1002/anie.199628811>.
276. Lv, Q., Li, G., and Sun, H. (2014). Synthesis of hierarchical TS-1 with convenient separation and the application for the oxidative desulfurization of bulky and small reactants. *Fuel* 130, 70–75. <https://doi.org/10.1016/j.fuel.2014.04.042>.
277. Wang, B., Han, H., Ge, B., Ma, J., Zhu, J., and Chen, S. (2019). An efficient hydrophobic modification of TS-1 and its application in the epoxidation of propylene. *New J. Chem.* 43, 10390–10397. <https://doi.org/10.1039/C9NJ01937E>.

278. Ramakrishna Prasad, M., Hamdy, M.S., Mul, G., Bouwman, E., and Drent, E. (2008). Efficient catalytic epoxidation of olefins with silylated Ti-TUD-1 catalysts. *J. Catal.* **260**, 288–294. <https://doi.org/10.1016/j.jcat.2008.09.021>.
279. Almeida, A.R., Carneiro, J.T., Moulijn, J.A., and Mul, G. (2010). Improved performance of TiO₂ in the selective photo-catalytic oxidation of cyclohexane by increasing the rate of desorption through surface silylation. *J. Catal.* **273**, 116–124. <https://doi.org/10.1016/j.jcat.2010.05.006>.
280. Lee, S.-U., Lee, Y.-J., Kim, J.-R., and Jeong, S.-Y. (2017). Rational synthesis of silylated Beta zeolites and selective ring opening of 1-methylnaphthalene over the NiW-supported catalysts. *Appl. Catal. B Environ.* **219**, 1–9. <https://doi.org/10.1016/j.apcatb.2017.07.047>.
281. Lin, K., Wang, L., Meng, F., Sun, Z., Yang, Q., Cui, Y., Jiang, D., and Xiao, F. (2005). Formation of better catalytically active titanium species in Ti-MCM-41 by vapor-phase silylation. *J. Catal.* **235**, 423–427. <https://doi.org/10.1016/j.jcat.2005.08.003>.
282. Capel-Sanchez, M.C., Campos-Martin, J.M., and Fierro, J.L.G. (2010). Silylation of titanium-containing amorphous silica catalyst: Effect on the alkenes epoxidation with H₂O₂. *Catal. Today* **158**, 103–108. <https://doi.org/10.1016/j.cattod.2010.07.022>.
283. Qi, C., Akita, T., Okumura, M., Kuraoka, K., and Haruta, M. (2003). Effect of surface chemical properties and texture of mesoporous titanates on direct vapor-phase epoxidation of propylene over Au catalysts at high reaction temperature. *Appl. Catal. Gen.* **253**, 75–89. [https://doi.org/10.1016/S0926-860X\(03\)00526-X](https://doi.org/10.1016/S0926-860X(03)00526-X).
284. Chowdhury, B., Bando, K.K., Bravo-Suárez, J., Tsubota, S., and Haruta, M. (2012). Activity of silylated titanate supported gold nanoparticles towards direct propylene epoxidation reaction in the presence of trimethylamine. *J. Mol. Catal. Chem.* **359**, 21–27. <https://doi.org/10.1016/j.molcata.2012.03.016>.
285. Tatsumi, T., Koyano, K.A., and Igarashi, N. (1998). Remarkable activity enhancement by trimethylsilylation in oxidation of alkenes and alkanes with H₂O₂ catalyzed by titanium-containing mesoporous molecular sieves. *Chem. Commun.* **3**, 325–326. <https://doi.org/10.1039/a706175g>.
286. Sun, J., Ma, D., Zhang, H., Liu, X., Han, X., Bao, X., Weinberg, G., Pfänder, N., and Su, D. (2006). Toward Monodispersed Silver Nanoparticles with Unusual Thermal Stability. *J. Am. Chem. Soc.* **128**, 15756–15764. <https://doi.org/10.1021/ja064884j>.
287. Kosinov, N., Sripathi, V.G., and Hensen, E.J. (2014). Improving separation performance of high-silica zeolite membranes by surface modification with triethoxyfluorosilane. *Microporous Mesoporous Mater.* **194**, 24–30. <https://doi.org/10.1016/j.micromeso.2014.03.034>.
288. Uphade, B.S., Akita, T., Nakamura, T., and Haruta, M. (2002). Vapor-Phase Epoxidation of Propene Using H₂ and O₂ over Au/Ti-MCM-48. *J. Catal.* **209**, 331–340. <https://doi.org/10.1006/jcat.2002.3642>.
289. Kanungo, S., Keshri, K.S., van Hoof, A.J.F., d'Angelo, M.N., Schouten, J.C., Nijhuis, T.A., Hensen, E.J.M., and Chowdhury, B. (2016). Silylation enhances the performance of Au/Ti-SiO₂ catalysts in direct epoxidation of propene using H₂ and O₂. *J. Catal.* **344**, 434–444. <https://doi.org/10.1016/j.jcat.2016.10.004>.
290. Kanungo, S., Keshri, K.S., Hensen, E.J.M., Chowdhury, B., Schouten, J.C., and Neira d'Angelo, M.F. (2018). Direct epoxidation of propene on silylated Au-Ti catalysts: a study on silylation procedures and the effect on propane formation. *Catal. Sci. Technol.* **8**, 3052–3059. <https://doi.org/10.1039/C8CY00439K>.
291. Bravo-Suárez, J.J., Lu Dallos, C.G., Dallos, C.G., Fujitani, T., and Oyama, S.T. (2007). Kinetic Study of Propylene Epoxidation with H₂ and O₂ over a Gold/Mesoporous Titanosilicate Catalyst. *J. Phys. Chem. C* **111**, 17427–17436. <https://doi.org/10.1021/jp075098j>.
292. Wang, Q., Zhang, Z., Sang, K., Chen, W., Qian, G., Zhang, J., Zhou, X., and Duan, X. (2022). Kinetics and mechanistic insights into the active sites of Au catalysts for selective propylene oxidation. *Nano Res.* **16**, 6220–6227. <https://doi.org/10.1007/s12274-022-5283-5>.
293. Lee, W.-S., Lai, L.-C., Cem Akatay, M., Stach, E.A., Ribeiro, F.H., and Delgass, W.N. (2012). Probing the gold active sites in Au/TS-1 for gas-phase epoxidation of propylene in the presence of hydrogen and oxygen. *J. Catal.* **296**, 31–42. <https://doi.org/10.1016/j.jcat.2012.08.021>.
294. Feng, X., Chen, D., and Zhou, X.G. (2016). Thermal stability of TPA template and size-dependent selectivity of uncalcined TS-1 supported Au catalyst for propene epoxidation with H₂ and O₂. *RSC Adv.* **6**, 44050–44056. <https://doi.org/10.1039/C6RA05772A>.
295. Qi, C., Huang, J., Bao, S., Su, H., Akita, T., and Haruta, M. (2011). Switching of reactions between hydrogenation and epoxidation of propene over Au/Ti-based oxides in the presence of H₂ and O₂. *J. Catal.* **281**, 12–20. <https://doi.org/10.1016/j.jcat.2011.03.028>.
296. Yang, H., Tang, D., Lu, X., and Yuan, Y. (2009). Superior Performance of Gold Supported on Titanium-Containing Hexagonal Mesoporous Molecular Sieves for Gas-Phase Epoxidation of Propylene with Use of H₂ and O₂. *J. Phys. Chem. C* **113**, 8186–8193. <https://doi.org/10.1021/jp810187f>.
297. Ruiz, A., Van Der Linden, B., Makkee, M., and Mul, G. (2009). Acrylate and propoxy-groups: Contributors to deactivation of Au/TiO₂ in the epoxidation of propene. *J. Catal.* **266**, 286–290. <https://doi.org/10.1016/j.jcat.2009.06.019>.
298. Wang, H., and Pinnavaia, T.J. (2006). MFI Zeolite with Small and Uniform Intracrystal Mesopores. *Angew. Chem. Int. Ed.* **45**, 7603–7606. <https://doi.org/10.1002/anie.200602595>.
299. Wang, Y., Zheng, J.-M., Fan, K., and Dai, W.-L. (2011). One-pot solvent-free synthesis of sodium benzoate from the oxidation of benzyl alcohol over novel efficient AuAg/TiO₂ catalysts. *Green Chem.* **13**, 1644. <https://doi.org/10.1039/c1gc15311k>.
300. Venezia, A. (2003). Activity of SiO₂ supported gold-palladium catalysts in CO oxidation. *Appl. Catal. Gen.* **251**, 359–368. [https://doi.org/10.1016/S0926-860X\(03\)00343-0](https://doi.org/10.1016/S0926-860X(03)00343-0).
301. Doherty, R.P., Krafft, J.-M., Méthivier, C., Casale, S., Remita, H., Louis, C., and Thomas, C. (2012). On the promoting effect of Au on CO oxidation kinetics of Au–Pt bimetallic nanoparticles supported on SiO₂: An electronic effect? *J. Catal.* **287**, 102–113. <https://doi.org/10.1016/j.jcat.2011.12.011>.
302. Bracey, C.L., Ellis, P.R., and Hutchings, G.J. (2009). Application of copper–gold alloys in catalysis: current status and future perspectives. *Chem. Soc. Rev.* **38**, 2231–2243. <https://doi.org/10.1039/b817729p>.
303. Li, N., Yang, B., Liu, M., Chen, Y., and Zhou, J. (2017). Synergetic photo-epoxidation of propylene with molecular oxygen over bimetallic Au–Ag/TS-1 photocatalysts. *Chin. J. Catal.* **38**, 831–843. [https://doi.org/10.1016/S1872-2067\(17\)62832-8](https://doi.org/10.1016/S1872-2067(17)62832-8).
304. Feng, X., Yang, J., Duan, X., Cao, Y., Chen, B., Chen, W., Lin, D., Qian, G., Chen, D., Yang, C., and Zhou, X. (2018). Enhanced Catalytic Performance for Propene Epoxidation with H₂ and O₂ over Bimetallic Au–Ag/Uncalcined Titanium Silicate-1 Catalysts. *ACS Catal.* **8**, 7799–7808. <https://doi.org/10.1021/acscatal.8b01324>.
305. Lee, W.-S., Cem Akatay, M., Stach, E.A., Ribeiro, F.H., and Nicholas Delgass, W. (2013). Enhanced reaction rate for gas-phase epoxidation of propylene using H₂ and O₂ by Cs promotion of Au/TS-1. *J. Catal.* **308**, 98–113. <https://doi.org/10.1016/j.jcat.2013.05.023>.
306. Bravo-Suárez, J.J., Bando, K.K., Lu, J., Haruta, M., Fujitani, T., and Oyama, T. (2008). Transient Technique for Identification of True Reaction Intermediates: Hydroperoxide Species in Propylene Epoxidation on Gold/Titanosilicate Catalysts by X-ray Absorption Fine Structure Spectroscopy. *J. Phys. Chem. C* **112**, 1115–1123. <https://doi.org/10.1021/jp077501s>.
307. Sandoval, A., Aguilar, A., Louis, C., Traverse, A., and Zanella, R. (2011). Bimetallic Au–Ag/TiO₂ catalyst prepared by deposition–precipitation: High activity and stability in CO oxidation. *J. Catal.* **281**, 40–49. <https://doi.org/10.1016/j.jcat.2011.04.003>.
308. Solé-Daura, A., Zhang, T., Fouilloux, H., Robert, C., Thomas, C.M., Chamoreau, L.-M., Carbo, J.J., Proust, A., Guillemot, G., and Poblet, J.M. (2020). Catalyst Design for Alkene Epoxidation by Molecular Analogues of Heterogeneous Titanium-Silicalite Catalysts. *ACS Catal.* **10**, 4737–4750. <https://doi.org/10.1021/acscatal.9b05147>.
309. Zhang, B., Wu, Q., Zhang, C., Su, X., Shi, R., Lin, W., Li, Y., and Zhao, F. (2017). A Robust Ru/ZSM-5 Hydrogenation Catalyst: Insights into the Resistances to Ruthenium Aggregation and Carbon Deposition. *ChemCatChem* **9**, 3646–3654. <https://doi.org/10.1002/cctc.201700664>.
310. Wang, N., Sun, Q., Bai, R., Li, X., Guo, G., and Yu, J. (2016). In Situ Confinement of Ultrasmall Pd Clusters within Nanosized Silicalite-1 Zeolite for Highly Efficient Catalysis of Hydrogen Generation. *J. Am. Chem. Soc.* **138**, 7484–7487. <https://doi.org/10.1021/jacs.6b03518>.
311. Sun, Q., Wang, N., Zhang, T., Bai, R., Mayoral, A., Zhang, P., Zhang, Q., Terasaki, O., and Yu, J. (2019). Zeolite-Encaged Single-Atom Rhodium Catalysts: Highly-Efficient Hydrogen Generation and Shape-Selective Tandem Hydrogenation of Nitroarenes. *Angew. Chem. Int. Ed.* **58**, 18570–18576. <https://doi.org/10.1002/anie.201912367>.
312. Zhang, X., He, N., Liu, C., and Guo, H. (2019). Pt–Cu Alloy Nanoparticles Encapsulated in

- Silicalite-1 Molecular Sieve: Coke-Resistant Catalyst for Alkane Dehydrogenation. *Catal. Lett.* 149, 974–984. <https://doi.org/10.1007/s10562-019-02671-4>.
313. Yang, D., Xu, P., Browning, N.D., and Gates, B.C. (2016). Tracking Rh Atoms in Zeolite HY: First Steps of Metal Cluster Formation and Influence of Metal Nuclearity on Catalysis of Ethylene Hydrogenation and Ethylene Dimerization. *J. Phys. Chem. Lett.* 7, 2537–2543. <https://doi.org/10.1021/acs.jpcclett.6b01153>.
314. Liu, C., Wang, J., Zhu, P., Liu, H., and Zhang, X. (2022). Relating the performances of selective phenol hydrogenation with encapsulated palladium nanoparticles and surrounding distinct LTL-zeolite microenvironments. *Chem. Eng. J.* 430, 132589. <https://doi.org/10.1016/j.cej.2021.132589>.
315. Rasmussen, K.H., Mielby, J., and Kegnæs, S. (2018). Towards Encapsulation of Nanoparticles in Chabazite Through Interzeolite Transformation. *ChemCatChem* 10, 4380–4385. <https://doi.org/10.1002/cctc.201800914>.
316. Dai, C., Zhang, A., Liu, M., Gu, L., Guo, X., and Song, C. (2016). Hollow Alveolus-Like Nanovesicle Assembly with Metal-Encapsulated Hollow Zeolite Nanocrystals. *ACS Nano* 10, 7401–7408. <https://doi.org/10.1021/acsnano.6b00888>.
317. Ma, L., Ding, C., Wang, J., Li, Y., Xue, Y., Guo, J., Zhang, K., Liu, P., and Gao, X. (2019). Highly dispersed Pt nanoparticles confined within hierarchical pores of silicalite-1 zeolite via crystal transformation of supported Pt/S-1 catalyst for partial oxidation of methane to syngas. *Int. J. Hydrogen Energy* 44, 21847–21857. <https://doi.org/10.1016/j.ijhydene.2019.06.051>.
318. Feng, X., Song, Z., Liu, Y., Chen, X., Jin, X., Yan, W., Yang, C., Luo, J., Zhou, X., and Chen, D. (2018). Manipulating Gold Spatial Location on Titanium Silicalite-1 To Enhance the Catalytic Performance for Direct Propene Epoxidation with H₂ and O₂. *ACS Catal.* 8, 10649–10657. <https://doi.org/10.1021/acscatal.8b02836>.
319. Murayama, H., Hasegawa, T., Yamamoto, Y., Tone, M., Kimura, M., Ishida, T., Honma, T., Okumura, M., Isogai, A., Fujii, T., and Tokunaga, M. (2017). Chloride-free and water-soluble Au complex for preparation of supported small nanoparticles by impregnation method. *J. Catal.* 353, 74–80. <https://doi.org/10.1016/j.jcat.2017.07.002>.
320. Cheng, F., Cheng, J., Nan, Y., Xie, Y., Yang, T., Cheng, D., Zhu, J., and Xu, H. (2022). Enhancing oxidative hydration of ethylene towards ethylene glycol over metal-modified titanosilicate catalysts. *Appl. Catal. Gen.* 643, 118752. <https://doi.org/10.1016/j.apcata.2022.118752>.
321. Ishida, T., Kinoshita, N., Okatsu, H., Akita, T., Takei, T., and Haruta, M. (2008). Influence of the Support and the Size of Gold Clusters on Catalytic Activity for Glucose Oxidation. *Angew. Chem. Int. Ed.* 47, 9265–9268. <https://doi.org/10.1002/anie.200802845>.
322. Gu, J., Zhang, Z., Ding, L., Huang, K., Xue, N., Peng, L., Guo, X., and Ding, W. (2017). Platinum nanoparticles encapsulated in HZSM-5 crystals as an efficient catalyst for green production of p-aminophenol. *Catal. Commun.* 97, 98–101. <https://doi.org/10.1016/j.catcom.2017.04.028>.
323. Chen, H., Zhang, R., Wang, H., Bao, W., and Wei, Y. (2020). Encapsulating uniform Pd nanoparticles in TS-1 zeolite as efficient catalyst for catalytic abatement of indoor formaldehyde at room temperature. *Appl. Catal. B Environ.* 278, 119311. <https://doi.org/10.1016/j.apcatb.2020.119311>.
324. Qiu, L., Ying, F., Jinyu, Z., Nangu, H., Lijun, L., Xuzhi, G., Mudi, X., Yibin, L., Yanqiang, S., and Guangtong, X. (2017). Investigation on the cation location, structure and performances of rare earth-exchanged Y zeolite. *J. Rare Earths* 35, 658–666. [https://doi.org/10.1016/S1002-0721\(17\)60960-8](https://doi.org/10.1016/S1002-0721(17)60960-8).
325. Chen, Z., Zhang, L., Yu, Y., Liu, D., Fang, N., Liu, Y., and He, M. (2022). Molecular traffic control for catalytic oxidation reaction in TS-1 zeolite. *Microporous Mesoporous Mater.* 332, 111715. <https://doi.org/10.1016/j.micromeso.2022.111715>.
326. Li, S., Lafon, O., Wang, W., Wang, Q., Wang, X., Li, Y., Xu, J., and Deng, F. (2020). Recent Advances of Solid-State NMR Spectroscopy for Microporous Materials. *Adv. Mater.* 32, 2002879. <https://doi.org/10.1002/adma.202002879>.
327. Paul, G., Bisio, C., Braschi, I., Cossi, M., Gatti, G., Gianotti, E., and Marchese, L. (2018). Combined solid-state NMR, FT-IR and computational studies on layered and porous materials. *Chem. Soc. Rev.* 47, 5684–5739. <https://doi.org/10.1039/C7CS00358G>.
328. Bai, R., Song, Y., Lätsch, L., Zou, Y., Feng, Z., Copéret, C., Corma, A., and Yu, J. (2022). Switching between classical/nonclassical crystallization pathways of TS-1 zeolite: implication on titanium distribution and catalysis. *Chem. Sci.* 13, 10868–10877. <https://doi.org/10.1039/D2SC02679A>.
329. Dong, J., Zhu, H., Xiang, Y., Wang, Y., An, P., Gong, Y., Liang, Y., Qiu, L., Zheng, A., Peng, X., et al. (2016). Toward a Unified Identification of Ti Location in the MFI Framework of High-Ti-Loaded TS-1: Combined EXAFS, XANES, and DFT Study. *J. Phys. Chem. C* 120, 20114–20124. <https://doi.org/10.1021/acs.jpcc.6b05087>.
330. Xu, J., Zhang, Z., Yu, D., Du, W., Song, N., Duan, X., and Zhou, X. (2023). Au/TS-1 catalyst for propylene epoxidation with H₂ and O₂: Effect of surface property and morphology of TS-1 zeolite. *Nano Res.* 16, 6278–6289. <https://doi.org/10.1007/s12274-023-5440-5>.
331. Zhang, T., Chen, Z., Walsh, A.G., Li, Y., and Zhang, P. (2020). Single-Atom Catalysts Supported by Crystalline Porous Materials: Views from the Inside. *Adv. Mater.* 32, 2002910. <https://doi.org/10.1002/adma.202002910>.
332. Zhang, P. (2014). X-ray Spectroscopy of Gold-Thiolate Nanoclusters. *J. Phys. Chem. C* 118, 25291–25299. <https://doi.org/10.1021/jp507739u>.
333. Meitzner, G., Via, G.H., Lytle, F.W., and Sinfelt, J.H. (1992). Analysis of x-ray absorption edge data on metal catalysts. *J. Phys. Chem.* 96, 4960–4964. <https://doi.org/10.1021/j100191a043>.
334. Wang, L., Xu, W., Yuan, Z., Xu, Y., Sun, D., and Li, Q. (2023). Tannic Acid Assisted Construction of Au-Ti Integrated Catalyst Regulating the Local Environment of Framework Ti toward Propylene Epoxidation under H₂/O₂. *Mol. Catal.* 545, 113206. <https://doi.org/10.1016/j.mcat.2023.113206>.
335. Wei, Y., Parmentier, T.E., De Jong, K.P., and Zečević, J. (2015). Tailoring and visualizing the pore architecture of hierarchical zeolites. *Chem. Soc. Rev.* 44, 7234–7261. <https://doi.org/10.1039/C5CS00155B>.
336. Milina, M., Mitchell, S., Crivelli, P., Cooke, D., and Pérez-Ramírez, J. (2014). Mesopore quality determines the lifetime of hierarchically structured zeolite catalysts. *Nat. Commun.* 5, 3922. <https://doi.org/10.1038/ncomms4922>.
337. Suga, M., Asahina, S., Sakuda, Y., Kazumori, H., Nishiyama, H., Nokuo, T., Alfredsson, V., Kjellman, T., Stevens, S.M., Cho, H.S., et al. (2014). Recent progress in scanning electron microscopy for the characterization of fine structural details of nano materials. *Prog. Solid State Chem.* 42, 1–21. <https://doi.org/10.1016/j.progsolidstchem.2014.02.001>.
338. Warringham, R., Gerchow, L., Zubiaga, A., Cooke, D., Crivelli, P., Mitchell, S., and Pérez-Ramírez, J. (2016). Insights into the Mechanism of Zeolite Detemplation by Positron Annihilation Lifetime Spectroscopy. *J. Phys. Chem. C* 120, 25451–25461. <https://doi.org/10.1021/acs.jpcc.6b08931>.
339. Guo, Q., Sun, K., Feng, Z., Li, G., Guo, M., Fan, F., and Li, C. (2012). A Thorough Investigation of the Active Titanium Species in TS-1 Zeolite by In Situ UV Resonance Raman Spectroscopy. *Chem. - Eur. J.* 18, 13854–13860. <https://doi.org/10.1002/chem.201201319>.
340. Qin, Q., Guo, Y., Liu, H., Ma, J., Zhu, J., and Wang, B. (2023). Effect of the bipodal Ti species on activity and selectivity of propylene epoxidation with H₂O₂ over TS-1: A theoretical study. *Mol. Catal.* 543, 113147. <https://doi.org/10.1016/j.mcat.2023.113147>.
341. Sinclair, P.E., and Catlow, C.R.A. (1999). Quantum Chemical Study of the Mechanism of Partial Oxidation Reactivity in Titanosilicate Catalysts: Active Site Formation, Oxygen Transfer, and Catalyst Deactivation. *J. Phys. Chem. B* 103, 1084–1095. <https://doi.org/10.1021/jp9821679>.
342. Wells, D.H., Joshi, A.M., Delgass, W.N., and Thomson, K.T. (2006). A Quantum Chemical Study of Comparison of Various Propylene Epoxidation Mechanisms Using H₂O₂ and TS-1 Catalyst. *J. Phys. Chem. B* 110, 14627–14639. <https://doi.org/10.1021/jp062368f>.
343. Gordon, C.P., Engler, H., Traigl, A.S., Plodinec, M., Lunkenbein, T., Berkessel, A., Teles, J.H., Parvulescu, A.-N., and Copéret, C. (2020). Efficient epoxidation over dinuclear sites in titanium silicalite-1. *Nature* 586, 708–713. <https://doi.org/10.1038/s41586-020-2826-3>.
344. Bassler, P., Weidenbach, M., and Goebbel, H. (2010). The new hppo process for propylene oxide: from joint development to world scale production. *Chem. Eng. Trans.* 21, 571–576. <https://doi.org/10.3303/CET1021096>.
345. Liu, M., Ye, X., Liu, Y., Wang, X., Wen, Y., Sun, H., and Li, B. (2015). Highly Selective Epoxidation of Propylene in a Low-Pressure Continuous Slurry Reactor and the Regeneration of Catalyst. *Ind. Eng. Chem. Res.* 54, 5416–5426. <https://doi.org/10.1021/acs.iecr.5b00410>.
346. Wu, G., Wang, Y., Wang, L., Feng, W., Shi, H., Lin, Y., Zhang, T., Jin, X., Wang, S., Wu, X., and Yao, P. (2013). Epoxidation of propylene with H₂O₂ catalyzed by supported TS-1 catalyst in a fixed-bed reactor: Experiments and kinetics. *Chem. Eng. J.* 215–216, 306–314. <https://doi.org/10.1016/j.cej.2012.11.055>.

347. Serrano, D.P., Sanz, R., Pizarro, P., Moreno, I., de Frutos, P., and Blázquez, S. (2009). Preparation of extruded catalysts based on TS-1 zeolite for their application in propylene epoxidation. *Catal. Today* 143, 151–157. <https://doi.org/10.1016/j.cattod.2008.09.039>.
348. Li, G., Wang, X., Yan, H., Liu, Y., and Liu, X. (2002). Epoxidation of propylene using supported titanium silicalite catalysts. *Appl. Catal. Gen.* 236, 1–7. [https://doi.org/10.1016/S0926-860X\(02\)00288-0](https://doi.org/10.1016/S0926-860X(02)00288-0).
349. Meng, Y., Huang, X., Yanga, Q., Qiana, Y., Kubotab, N., and Fukunagab, S. (2005). Treatment of polluted river water with a photocatalytic slurry reactor using low-pressure mercury lamps coupled with a membrane. *Desalination* 181, 121–133.
350. Yi-chuan, L., Ben-xian, S., and Ji-gang, Z. (2013). Effect of propylene glycol monomethyl ether and rust impurities on TS-1 deactivation in propylene epoxidation. *Catal. Today* 212, 169–174. <https://doi.org/10.1016/j.cattod.2012.09.039>.
351. Song, W., Zuo, Y., Xiong, G., Zhang, X., Jin, F., Liu, L., and Wang, X. (2014). Transformation of SiO₂ in Titanium Silicalite-1/SiO₂ extrudates during tetrapropylammonium hydroxide treatment and improvement of catalytic properties for propylene epoxidation. *Chem. Eng. J.* 253, 464–471. <https://doi.org/10.1016/j.cej.2014.05.075>.
352. Zuo, Y., Wang, M., Song, W., Wang, X., and Guo, X. (2012). Characterization and Catalytic Performance of Deactivated and Regenerated TS-1 Extrudates in a Pilot Plant of Propene Epoxidation. *Ind. Eng. Chem. Res.* 51, 10586–10594. <https://doi.org/10.1021/ie300581z>.
353. Arvay, J.W., Hong, W., Li, C., Delgass, W.N., Ribeiro, F.H., and Harris, J.W. (2022). Kinetics of Propylene Epoxidation over Extracrystalline Gold Active Sites on AU/TS-1 Catalysts. *ACS Catal.* 12, 10147–10160. <https://doi.org/10.1021/acscatal.2c02213>.
354. Harris, J.W., Arvay, J., Mitchell, G., Delgass, W.N., and Ribeiro, F.H. (2018). Propylene oxide inhibits propylene epoxidation over Au/TS-1. *J. Catal.* 365, 105–114. <https://doi.org/10.1016/j.jcat.2018.06.015>.
355. Otto, T., Zhou, X., Zones, S.I., and Iglesia, E. (2022). Synthesis, characterization, and function of Au nanoparticles within TS-1 zeotypes as catalysts for alkene epoxidation using O₂/H₂O reactants. *J. Catal.* 410, 206–220. <https://doi.org/10.1016/j.jcat.2022.04.002>.
356. Alvear, M., Eränen, K., Murzin, D.Y., and Salmi, T. (2021). Study of the Product Distribution in the Epoxidation of Propylene over TS-1 Catalyst in a Trickle-Bed Reactor. *Ind. Eng. Chem. Res.* 60, 2430–2438. <https://doi.org/10.1021/acs.iecr.0c06150>.